

Adaptation in changing environments

A Thesis

Submitted for the Degree of
DOCTOR OF PHILOSOPHY

by

ARCHANA DEVI



THEORETICAL SCIENCES UNIT
JAWAHARLAL NEHRU CENTRE FOR ADVANCED SCIENTIFIC
RESEARCH
(A Deemed University)
Bangalore – 560 064

October 2021

To my family

DECLARATION

I hereby declare that the matter embodied in the thesis entitled “**Adaptation in changing environments**” is the result of investigations carried out by me at the Theoretical Sciences Unit, Jawaharlal Nehru Centre for Advanced Scientific Research, Bangalore, India under the supervision of **Prof. Kavita Jain**, and that it has not been submitted elsewhere for the award of any degree or diploma.


In keeping with the general practice in reporting scientific observations, due acknowledgment has been made whenever the work described is based on the findings of other investigators.

Archana Devi

Archana Devi

CERTIFICATE

I hereby certify that the matter embodied in this thesis entitled “**Adaptation in changing environments**” has been carried out by **Ms. Archana Devi** at the Theoretical Sciences Unit, Jawaharlal Nehru Centre for Advanced Scientific Research, Bangalore, India under my supervision and that it has not been submitted elsewhere for the award of any degree or diploma.



Prof. Kavita Jain

(Research Supervisor)

Acknowledgments

First of all, I express my deepest gratitude to my Ph.D. supervisor Prof. Kavita Jain for her constant support, guidance, and encouragement. Her enthusiasm and dedication towards science were always a source of inspiration. Her help and valuable suggestions enabled me to finish my Ph.D. on time. She has also guided me in overcoming all the difficult situations of my life during this Ph.D. journey. I am grateful to her for her understanding and friendly nature, and it was an enjoyable experience to work with her.

I acknowledge the financial support and excellent research facilities of JNCASR. I would like to express my sincere gratitude to Prof. Swapan K. Pati, Dr. Meher K. Prakash, and Prof. Amitabh Joshi for the wonderful courses they provided. I am thankful to all the faculty members of TSU for their support in various ways. I would also like to thank my GSAC members Prof. Vishwesh Guttal and Dr. Meher K. Prakash for their support and valuable discussions.

I am grateful to all my teachers. I acknowledge my school teachers Ms. Asima Pradhan and Ms. Kabita Rani Behere, who always encourage me to fulfill my dreams. I would also like to acknowledge Prof. Rabindranath Mishra, who motivated me to pursue interdisciplinary research. I am so grateful to Mr. Tapan K. Manna, who is an amazing teacher in mathematics, and his teaching style and encouragement made me fall in love with mathematics. I express my deep gratitude to my dance teacher Ms. Devjani Sen and music teacher Ms. Paromita Ghosh for whom I could live a joyful life in Bangalore.

I thank all my past and present labmates Sarada, Sona, Priyanka, Ananthu, Jyoti, Sayani, Sachin, and Iyyappan for their help and support. I express my special thanks to Sayani and Sachin for being supportive and caring. I am thankful to my friend Nalina and ex-roommate Geetika for their help whenever I needed it. I am deeply thankful to Anjan, Aparna, Sushree, Sanskruti, Ranjan, and Pranay for being there for me in my good and bad times. I extend my special thanks to Smarak, Supriti, Saswati, and Satya for their support during my emotional low points. I really appreciate the help I got from Nalina and Ranjan to get rid of the technical issues I faced during the thesis compilation, and they were always approachable and ready to help.

I would like to express my endless gratitude to my family members for their unconditional love and support. My parents always encourage me to rise from one height to the other, and my mother's constant motivations to pursue higher studies in science led me to what I am today. I am lucky to have three loving and caring siblings Anjana, Abhik, and Bharati. Their affections make me forget all my sorrows and pains.

Last but not least, I appreciate the help and support I have received from all the academic and non-academic staff in JNCASR.

Synopsis

Adaptation is a ubiquitous phenomenon that enables a population to survive in its environment. As natural environments change with time, it is crucial to understand the dynamics of adaptation in varying environments. When the time scales of the environmental and evolutionary changes are very different, the fluctuations in the environment can be neglected for the evolutionary process. However, these time scales can overlap, and then the effect of the time-varying environment plays a major role in determining the evolutionary fate of the population. This is a less studied problem due to its complexity, but its importance and intriguing features motivated us to understand the effect of changing environments on the adaptation of a population.

Evolution occurs via evolutionary forces, namely, natural selection, mutation, recombination, and random genetic drift. To understand the evolutionary process, we use the theoretical population genetics approach to incorporate these forces in a mathematical model. This thesis considers the adaptation of a single trait with free recombination and neglects the pleiotropic effects due to other traits. A trait is said to be monogenic when a single gene controls it, such as sickle cell anemia and albinism, and polygenic, when many genes influence the trait, for example, quantitative traits such as human height and weight. We study the adaptation of both the monogenic and polygenic traits in different environmental conditions that are modeled as a sudden-change in the environment and linearly-changing and periodically-varying selection. The primary focus of the thesis is to understand the effect of changing environments on the survivability of a population. The thesis is divided into five chapters, and a brief description of each chapter is given below.

In Chapter 1, we first provide an introduction to the relevant evolutionary forces and a brief description of the deterministic and stochastic models pertinent to the discussion in this thesis. Specifically, we discuss two theoretical models: birth-death process and infinitesimal model that are classical models in population genetics and quantitative genetics, respectively [1]. Some useful frameworks (branching process and diffusion theory) used to obtain our results are also described in this chapter [2, 3].

In Chapter 2, we focus on the evolution of a monogenic trait due to a periodically changing environment. Seasonality and antibiotic cycling are well-known examples of periodic environmental change which have a significant impact on the survival probability of a mutant [4]. This motivated us to study a model where the selection pressure changes its sign with time, and the mutant, which is favorable for certain times, can become unfavorable at other times [5]. We studied the mutant's fixation probability (the

probability that ultimately all the individuals in the population become the mutant type) in a finite diploid population and found that it depends on the rate of environmental change, its time of appearance, and its dominance parameter. The interesting results we found in this study are, (i) an initially beneficial (deleterious) mutant can have a fixation probability lower (higher) than that for a neutral mutant depending on its time of appearance and rate of environmental change, and (ii) Haldane's sieve (fixation probability of a dominant beneficial mutant in a static environment is higher than when it is recessive) [6] does not always hold in a time-varying environment. These results were obtained using a combination of analytical work based on branching process and diffusion theory, and numerical simulations.

In Chapter 3, we investigate the adaptation of a polygenic trait where selection acts on a large number of genes to maintain an optimum phenotype. The Fokker-Planck equation for a polygenic trait is high dimensional, and in general, a mathematically intractable problem [7]. Therefore, we study an infinitely large population where we can neglect stochasticity and solve the deterministic equations to understand the evolution of a polygenic trait due to a linearly changing environment (for example, as a result of global warming) [8]. Previous work based on an infinitesimal model that neglects recurrent mutations has shown that the mean trait moves with the speed of the optimum and there is a constant lag between them [9]. In contrast, our work showed that the mean trait evolves with a speed lower than that of the phenotypic optimum. This is an important result that can have a potential application in conservation biology.

The bulk of the thesis describes the evolution of a trait in a changing environment. However, the stochastic dynamics of adaptation, even under constant selection, are not well-studied [10]. To get an insight into the problem, we study the relevant Fokker-Planck equation in Chapter 4, using an eigenfunction expansion method [11]. We found that (i) the eigenfunctions obey a confluent Heun equation which is a generalization of the hypergeometric equation [12], and (ii) the first eigenvalue that determines the dynamics shows a sharp transition: for mutation rate below one, the eigenvalue increases linearly with increasing mutation rate and then remains a constant.

In Chapter 5, we conclude our main results. We also discuss some interesting open questions that can be addressed by extending our work.

Bibliography

- [1] B. Charlesworth and D. Charlesworth. *Elements of Evolutionary Genetics*. Ben Roberts, Colorado, 2010.
- [2] L. J. S. Allen. *An Introduction to Stochastic Processes with Applications to Biology*. CRC Press, Boca Raton, 2010.
- [3] W. J. Ewens. *Mathematical Population Genetics*. Springer, Berlin, 2004.
- [4] C. M. Williams, G. J. Ragland, G. Betini, L. B. Buckley, Z. A. Cheviron, K. Donohue, J. Hereford, M. M. Humphries, S. Lisovski, K. E. Marshall, P. S. Schmidt, K. S. Sheldon, Ø. Varpe, and M. E. Visser. Understanding evolutionary impacts of seasonality: an introduction to the symposium. *Integr. Comp. Biol.*, **57**: 921-933, 2017
- [5] A. Devi and K. Jain. The impact of dominance on adaptation in changing environments. *Genetics*, **216**: 227-240, 2020
- [6] J. B. S. Haldane. A mathematical theory of natural and artificial selection, part v: selection and mutation. *Proc. Camb. Philos. Soc.*, **23**: 838-844, 1927
- [7] W. Martens and U. von Wagner. On the solution of high dimensional Fokker Planck equations using orthogonal polynomial expansion. *Proc. Appl. Math. Mech.*, **10**: 257-258, 2010.
- [8] K. Jain and A. Devi. Polygenic adaptation in changing environments. *EPL*, **123**: 48002, 2018.
- [9] R. Bürger and M. Lynch. Evolution and extinction in a changing environment: a quantitative-genetic analysis. *Evolution*, **49**:151-163, 1995.
- [10] M. Kimura. Diffusion models in population genetics. *J. Appl. Probab.*, **1**: 177-232, 1964.
- [11] K. Jain and A. Devi. Evolutionary dynamics and eigenspectrum of confluent Heun equation. *J. Phys. A: Math. Theor.*, **53**: 395602, 2020.
- [12] P. P. Fiziev and D. Staicova. The Heun project: Heun functions, their generalizations and applications. <https://theheunproject.org>, 2012.

List of publications

- K. Jain and A. Devi. Polygenic adaptation in changing environments. *EPL*, **123**: 48002, 2018.
- A. Devi and K. Jain. The impact of dominance on adaptation in changing environments. *Genetics*, **216**: 227-240, 2020.
- K. Jain and A. Devi. Evolutionary dynamics and eigenspectrum of confluent Heun equation. *J. Phys. A: Math. Theor.*, **53**: 395602, 2020.

Table of contents

List of figures	xix
1 Introduction	1
1.1 Evolutionary Forces	1
1.1.1 Natural selection	1
1.1.2 Mutation	3
1.1.3 Recombination	3
1.1.4 Random genetic drift	3
1.2 Mathematical Models	4
1.2.1 Deterministic models	4
1.2.2 Stochastic models	5
1.3 Mathematical Frameworks	6
1.3.1 Branching process	6
1.3.2 Diffusion theory	7
1.4 Quantities of interest	8
1.4.1 Fixation Probability	8
1.4.2 Allele frequency distribution	9
1.5 Overview of the thesis	10
Bibliography	13
2 The impact of dominance on adaptation in changing environments	15
2.1 Introduction	15
2.2 Model	16
2.3 Fixation probability of a rare mutant	17
2.3.1 Qualitative features	18
2.3.2 On average beneficial mutant in a large population	19

2.3.3	On average neutral mutant in a finite population	22
2.3.4	On average deleterious mutant in a finite population	25
2.4	Average allele frequency and population fitness	29
2.5	Discussion	31
Bibliography		35
3	Polygenic adaptation in changing environments	39
3.1	Introduction	39
3.2	Models	40
3.3	Results	43
3.3.1	When most effects are small ($\bar{\gamma} \ll \hat{\gamma}$)	43
3.3.2	When most effects are large ($\bar{\gamma} \gg \hat{\gamma}$)	46
3.4	Summary and open questions	50
Bibliography		53
4	Evolutionary dynamics and eigenspectrum of confluent Heun equation	57
4.1	Introduction	57
4.2	Model	58
4.3	Confluent Heun equation for the eigenfunctions	60
4.4	Eigenvalue problem: numerical analysis	62
4.4.1	Eigenvalues	64
4.4.2	Eigenfunctions	64
4.5	Weak selection limit	64
4.6	Strong selection limit	66
4.6.1	Scaling form for the expansion coefficients	66
4.6.2	Expansion coefficients for infinite selection	69
4.7	Discussion	70
Bibliography		73
5	Conclusions and open questions	77
Appendix A		81
A.1	Discrete and continuous time models for diploids	81
A.2	Fixation probability of a mutant that is beneficial at all times	82

A.3	Fixation probability of an on average neutral mutant	83
A.4	Fixation probability of a mutant in transiently varying selection	83
Appendix Bibliography		85
Appendix B		87
B.1	Branching process approximation	87
B.2	Diffusion approximation for small cycling frequencies	88
B.3	Diffusion approximation for large cycling frequencies	90
B.4	Allele frequency distribution for strong mutation	91
Appendix Bibliography		93
Appendix C		95
C.1	Frobenius series expansion	95
C.2	Orthogonal polynomial expansion	96
C.3	Stationary state	97
C.4	Generating function for strong selection	97
Appendix Bibliography		101

List of figures

1.1	Schematic diagram of different types of selection that affects the population frequency (adapted from [1]). The red color line represents the original population, whereas the blue line shows the population after selection acts on it.	2
1.2	Schematic diagram of a birth-death process (adapted from [15]).	6
1.3	Schematic diagram of a discrete-time branching process starting with a single individual at $t = 0$ (adapted from [15]). The mutant becomes extinct after $t = 5$ generations.	7
1.4	The figure shows the fixation probability (1.6) of a <i>de novo</i> , codominant ($h = 1/2$) mutant with population size. The black dotted line shows the fixation probability of a beneficial mutant for large population size.	9
2.1	Fixation probability (2.5) obtained using branching process approximation for a mutant that is beneficial on average ($\bar{s} = 0.005, \sigma = 2\bar{s}$) for $\theta_a = \pi/4, 7\pi/8, 5\pi/4, 7\pi/4$ (clockwise from top left as shown in insets) for $h = 0.3$ (dotted), 0.5 (dashed), 0.7 (solid). Note that the h -dependence of the fixation probability is different at small and large cycling frequencies when the mutant is deleterious at the time of appearance.	20
2.2	Fixation probability as a function of cycling frequency for a mutation that is neutral on average and arises in a large population of size $N \gg \sigma^{-1}$ for $h = 0.1(\nabla)$ and $0.9(\Delta)$, and $\theta_a = \pi/4, 3\pi/4, 5\pi/4, 7\pi/4$ (clockwise from top left). The other parameters are $N = 100$ and $\sigma = 0.1$. The simulation data are obtained by averaging over 10^7 independent runs. A dominant (recessive) mutant that is beneficial (deleterious) when it appears in the population can be disfavored at large cycling frequencies.	23

- 2.3 Fixation probability of a mutant which is deleterious on average for $\bar{s} = -0.04$, $\sigma = 0.06$, and $\theta_a = \pi/8$ (left panel) and $3\pi/4$ (right panel). The simulation data are averaged over 10^7 runs. The other parameters are $N = 50$, $h = 0.1(\nabla)$, $0.9(\Delta)$. In the left panel, the data for $h = 0.1$, $N = 100$ (\blacktriangledown) is shown to support the claim that the resonance frequency scales as N^{-1} . Note that the recessive mutant that is beneficial when it appears in the population is favored at large cycling frequencies. 25
- 2.4 Stochastic trajectories of allele frequency for an on average neutral mutant, starting with a single mutant for $N = 200$, $\bar{s} = 0$, $\sigma = 0.1$, $h = 0.5$, $\theta_a = \pi/4$ for $\omega = 0.005$ (top) and 0.1 (bottom). The successful mutant passes through several cycles of selection before fixing in a rapidly changing environment. 26
- 2.5 Effect of a changing environment on the fixation probability of a mutant that is neutral on average and arises in a small population ($N \ll \sigma^{-1}$, top) and large population ($N \gg \sigma^{-1}$, bottom). The points show the simulation data obtained by averaging over 10^7 independent runs. The analytical results obtained using the diffusion theory are shown by lines; the solid lines show the expression (2.8a) for small cycling frequencies and the dashed lines represent (2.8b) for large cycling frequencies. Here $N = 100$, $\sigma = 0.005$ (top) and $N = 1000$, $\sigma = 0.01$ (bottom), $\theta_a = 0$, and $h = 0.1(\nabla)$, $0.5(\circ)$, $0.9(\Delta)$. The value $P_{\text{fix}}(\omega = 0)$ subtracted on the y -axis was obtained numerically. 27
- 2.6 Main: Average log fitness (2.16) in a periodically changing environment as a function of scaled mutation rate $U = 4N\mu$ for scaled selection $S = 4N\sigma = 20$, scaled cycling frequency $\Omega = 2N\omega = 0.1$ (dashed lines), 10 (solid lines) and dominance parameter $h = 0.1$ (blue), 0.5 (red). The effect of dominance is apparent only for small cycling frequency in the weak mutation regime. Inset: Dynamics of population-averaged allele frequency (2.14) for $U = 6$ (dashed), 40 (solid). The mutations decrease the phase lag between the average allele frequency and selection (dotted). Note that $\langle x(t) \rangle$ is independent of dominance coefficient. In the inset plots, $N = 100$, $\sigma = 0.01$, and $\omega = 0.05$ 28

- 3.1 Evolution of mean trait (main) in the full model when most effects are small ($\bar{\gamma} = 0.05 \ll \hat{\gamma} \approx 0.89$) and the phenotypic optimum moves with a constant speed $v = 10^{-4}$ for various ℓ . Here $s = 10^{-2}, \mu = 10^{-3}, z_0 = 0$ and $z_\tau = 0.8\ell\bar{\gamma}$. The phenotypic optimum $z_f(t)/z_\tau$ is also shown for comparison. The inset shows the evolution of genetic variance for $\ell = 200$. 44
- 3.2 Lag in mean when most effects are small (main). While the lag is constant in the directional selection model, it increases in the full model. This is because the mean trait moves slower than the phenotypic optimum (inset). Here $\ell = 200$ and rest of the parameters are the same as in Fig. 3.1. . . . 45
- 3.3 Evolution of mean (main) and genetic variance (inset) when most effects are large ($\bar{\gamma} = 0.1 \gg \hat{\gamma} \approx 0.0028$) and the phenotypic optimum moves with a constant speed $v = 10^{-4}$. Here $\ell = 200, s = 10^{-2}, \mu = 10^{-8}, z_0 = 0$ and $z_\tau = 18$ 46
- 3.4 Lag in mean (main) and allele frequency dynamics (inset) when most effects are large. All the parameters are the same as in Fig. 3.3. 47
- 3.5 Evolution of mean (main), lag in mean (top left inset) and genetic variance (bottom right inset) when equal number of effects are small and large ($\bar{\gamma} = 0.05, \hat{\gamma} \approx 0.028$) and the phenotypic optimum moves with a constant speed $v = 10^{-4}$. Here $\ell = 200, s = 10^{-2}, \mu = 10^{-6}, z_0 = 0$ and $z_\tau = 8$. The dotted line in the inset is the minimum lag $v(s\ell\bar{\gamma}^2)^{-1}$ 50
- 4.1 Variation of eigenvalue λ_1 with mutation rate μ for various values of selection parameter σ and $K = 1000$. The points are obtained numerically using (4.10), and the solid and dotted lines show the conjecture (4.17) for strong selection and analytical expression (4.19) for weak selection, respectively. 63
- 4.2 Eigenvalue spectrum for strong selection obtained numerically using (4.10) for $\sigma = 50$ and $K = 1000$ 63
- 4.3 First two excited states, $\phi_1(p)$ (main) and $\phi_2(p)$ (inset) obtained numerically using (4.8) and (4.10) for $\mu = 1/2$ (top panel) and $3/2$ (bottom panel), and $K = 1000$ for various selection strengths. 65
- 4.4 Main: Expansion coefficient $|c_n^{(1)}|$ obtained numerically (points) for various σ and analytical expression (4.23) in scaling limit for $\mu = 1/2$ (top) and $3/2$ (bottom), and $K = 1000$. The inset shows the expansion coefficient for small n and is compared with (4.26). 67

- 4.5 First two excited states, $\phi_1(p)$ (main) and $\phi_2(p)$ (inset) obtained numerically when the orthogonal expansion series (4.8) is terminated at $n = K+1$ for strong selection ($\sigma = 100$) and mutation rate, $\mu = 1/2$ (top panel) and $3/2$ (bottom panel). 68
- A.2 The inset shows the fixation probability $P_{\text{fix}}(\omega)$ given by (2.5) for a mutant that is beneficial on average for dominance coefficient $h = 0.4, 0.5, 0.6$ (bottom to top). In the main figure, the effect of a changing environment is shown by subtracting the fixation probability $P_{\text{fix}}(\omega = 0) = hs(t_a)/[1 + hs(t_a)]$ with $s(t_a) = \bar{s} + \sigma \sin(\theta_a)$ for $h = 0.1, 0.5, 0.9$ (bottom to top). In both plots, $\bar{s} = 0.05, \sigma = 0.2\bar{s}, \theta_a = 0$ 82
- A.3 Fixation probability of a mutant that is neutral on average for $N\sigma \gg 1$ when the mutant appeared at $\theta_a = \pi/4$ (left panel) and $5\pi/4$ (right panel). The solid line shows the expression (2.11b) (left panel) and (2.11c) (right panel) for small cycling frequencies and the dashed lines represent (2.8b) for large cycling frequencies. Here $N = 100, \sigma = 0.1$ and $h = 0.3(\nabla), 0.5(\circ), 0.7(\Delta)$. The numerically obtained value $P_{\text{fix}}(\omega = 0) = 2.53 \times 10^{-2}, 3.40 \times 10^{-2}, 4.38 \times 10^{-2}$ for $h = 0.3, 0.5, 0.7$, respectively, for the left panel. For the right panel, $P_{\text{fix}}(\omega = 0) = 3.55 \times 10^{-5}, 2.58 \times 10^{-5}, 1.98 \times 10^{-5}$ for $h = 0.3, 0.5, 0.7$, respectively. The simulation results are averaged over 10^7 runs. 83
- A.4 Fixation probability of a mutant in transiently varying environments defined by (A.4.1) and (A.4.2) and illustrated in the inset. The lines show the expression (A.4.4) and the points show the simulation data obtained by averaging over 10^7 independent runs for $\theta_a = 3\pi/4, T_e = 2\pi/\omega$ (left panel) and $\theta_a = \pi/2, T_e = \pi/\omega$ (right panel). In all the plots, $N = 100, \sigma = 0.1$ and $h = 0.1(\nabla), 0.9(\Delta)$ 84

Chapter 1

Introduction

Evolution is a heritable change in the characteristics of the population over time, and adaptation is the evolutionary process by which a population survives in its environment. Theoretical population genetics aims to understand the adaptation process and mechanisms of evolution, incorporating evolutionary forces such as natural selection, mutation, recombination, and random genetic drift in mathematical models. As real biological evolution is very complex, it is hard to make theoretical progress in models that include all the complexities of the real population, and therefore, we require simple models that do not significantly alter the essential properties of the evolutionary process but are tractable. This Chapter introduces various terms and mathematical techniques relevant to the thesis and explains how we model the adaptation process.

1.1 Evolutionary Forces

The basic evolutionary processes pertinent to the discussion in this thesis are described below in some detail.

1.1.1 Natural selection

Natural selection is the cause of adaptation that favors individuals who are better suited to its environment and gives a comparative advantage in the reproduction or survival ability of the individuals. A large body of experimental and theoretical work assumes a constant environment; however, natural environments are seldom static (e.g., climate change), and it is important to understand the dynamics of adaptation in changing environments. In this thesis, we study the evolution of a population in both constant

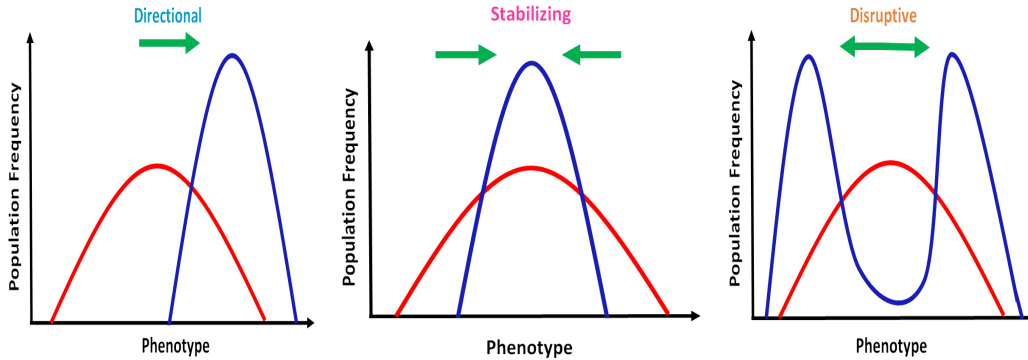


Fig. 1.1 Schematic diagram of different types of selection that affects the population frequency (adapted from [1]). The red color line represents the original population, whereas the blue line shows the population after selection acts on it.

and changing environments; however, our main focus is on the adaptation of a population in continually changing environments.

Although selection acts on the phenotype (such as the color of a flower) of the population, it alters the allele (different versions of the same gene) frequencies through the genotypes associated with the phenotypes. Some categories of selection depending on its effect on the allele frequency, as shown in Fig. 1.1, are described below:

(i) Directional selection: A single extreme phenotype is favored due to this selection. A classic example of a trait under this selection is the industrial melanism where the dark peppered moth, which was rare initially, became common in the population in about 50 years of evolution [2, 3]. In a single biallelic locus model in which a single gene with two types of allele is assumed to be under selection, the fitness of the advantageous allele can be written as $w_1 = 1 + s$ where $s > 0$ is the selection coefficient and the wild-type allele is assigned the fitness $w_0 = 1$. We study the dynamics of allele frequency when the population is under directional selection in Chapter 2 when the selection coefficient is time-dependent and in Chapter 4 for constant selection.

(ii) Stabilizing selection: It acts against the deleterious alleles and maintains a phenotypic optimum in several quantitative traits such as human height and weight [4, 5]. In quantitative genetics, the stabilizing selection is modeled by a Gaussian function, $w(z) = \exp[-s(z - z_0)^2]$ where z denotes the trait value of an individual, z_0 is the phenotypic optimum, and s is the strength of selection [6]. In Chapter 3, we study the evolution of a quantitative trait under stabilizing selection when the phenotypic opti-

mum moves in time to model a changing environment.

(iii) Disruptive selection: This favors the extreme phenotypes and acts against intermediate phenotypes [7]. We will encounter this selection in Chapter 3 when the average trait value of the population reaches the phenotypic optimum.

1.1.2 Mutation

A mutation is a change in the genetic sequence due to errors during replication or due to an external environment such as radiation [8]. Mutation creates variation in the population, and therefore, it is an important evolutionary force required for the evolution of the population. The mutation, based on its effect on the fitness of the individual, can be beneficial, neutral, or deleterious for the individual. The change in the genetic sequence due to a beneficial mutation produces a favorable phenotype, and it is essential for a population to adapt to its environment; however, biological observations predict that the beneficial mutations are rare in nature [9]. The neutral mutation alters the genetic sequence without affecting the phenotype, whereas the deleterious mutation decreases the fitness of the individual and becomes unfavorable by selection.

1.1.3 Recombination

Recombination is a process by which two strands of DNA recombine to produce a new combination of alleles that increases the genetic diversity in a population. In a fully recombining population, the frequency of a genotype can be expressed as the product of the allele frequency at each locus; however, linkage disequilibrium (nonrandom assortment of alleles at two or more loci) needs to be considered when the recombination rate is low where the allele frequencies are not sufficient to describe the genotype frequencies [6]. For this reason, in this thesis, we consider a fully recombining population.

1.1.4 Random genetic drift

Random genetic drift refers to stochastic fluctuations in the allele frequencies of a finite population due to chance events (for example, an individual can die by chance due to the finite carrying capacity of the population, even when it is as fit as the other individuals in the population). Although all populations are subject to random genetic drift, the fluctuations accumulate slowly and are small in a large population [8]. For this reason, it

plays a major role in deciding the fate of a new mutant due to its small initial frequency in the population. Whereas selection tries to fix a beneficial mutant (the frequency of the mutant becomes one), genetic drift can remove it from the population; similarly, a deleterious mutant can be fixed in a finite population due to stochastic fluctuations. We study stochastic models of evolution that include the effect of genetic drift in Chapter 2 and Chapter 4.

1.2 Mathematical Models

In this section, we discuss how we construct mathematical models to incorporate the above-mentioned evolutionary forces. We assume a biallelic, fully recombining population throughout the thesis.

1.2.1 Deterministic models

In an infinitely large population, stochastic fluctuations can be ignored, and the evolutionary dynamics can be described deterministically. Although natural populations evolve stochastically, deterministic models [10] are useful in developing stochastic theories, as we shall see below in Sect. 1.3.2.

We first describe some simple deterministic models commonly used in population genetics. In linkage equilibrium, the mutant's allele frequency x at a locus evolves due to selection according to the Wright's equation as [6],

$$\dot{x} = \frac{x(1-x)}{2\bar{w}} \frac{\partial \bar{w}}{\partial x}, \quad (1.1)$$

where \bar{w} represents the average fitness of the population. In Chapter 2, we consider a diploid population with a single locus under directional selection whose average fitness $\bar{w} = \exp[sx(x + 2h(1-x))]$, where h is the dominance parameter; the special case of $h = 1/2$ is studied in Chapter 4. In Chapter 3, we study the evolution of a polygenic trait that is under stabilizing selection where the average fitness is a function of the allele frequencies of all loci and given by $\bar{w} = \exp[-s\{c_2 + (c_1 - z_0)^2\}]$ with $c_1 = \sum_{i=1}^{\ell} \gamma_i(2x_i - 1)$ and $c_2 = 2 \sum_{i=1}^{\ell} \gamma_i^2 x_i(1 - x_i)$ are the mean and variance of the trait with effect sizes $\gamma_i/2$ at the i th locus with ℓ number of loci [11].

The alleles can mutate to each other, and the evolution equation of the allele frequency due to mutation is given by,

$$\dot{x} = \mu(1 - x) - \nu x, \quad (1.2)$$

where the mutant allele changes to the wild type allele with a rate ν and the wild type becomes the mutant with mutation rate μ . We have considered an equal mutation rate between the alleles in all the Chapters of the thesis.

We now describe the infinitesimal model, which is a widely used deterministic model in quantitative genetics to understand the adaptation of a quantitative trait without taking the genetic details into account. In this model, a trait is assumed to be affected by selection at infinitely many loci, each of which contributes an infinitesimally small amount of genetic variance to the trait [12]. To maintain a finite genetic variance V_A , that does not vary with time, if the trait consists of ℓ loci, then the effect on the trait by a single locus is of order $\sqrt{V_A/\ell}$ [13]. Therefore, for an infinitely large number of loci, each locus has an infinitesimally small effect on the trait, and the allele frequencies also change infinitesimally, which keeps the genetic variance constant over time.

However, in reality, the number of loci affecting a trait is finite and genetic variance can also change with time. Therefore, in Chapter 3, we consider a finite-loci model where the effect size of a locus can be small or large relative to a threshold effect size which depends on the mutation rate and selection coefficient, but not on the number of loci [14]. We find that the results obtained in the finite-loci model differ significantly from those obtained using the infinitesimal model.

1.2.2 Stochastic models

Stochastic models are required to understand the evolution of a finite population which is subjected to random genetic drift. One such model is a birth-death process which is a classical continuous-time Markov process (a random process whose transition probabilities for next generation depend only on the present generation and are independent of the past) where the number i of an allele increases or decreases by at most one in a small time interval with the birth rate b_i and death rate d_i , respectively, as depicted in Fig. 1.2. This process deals with the discrete number of individuals and useful to find the extinction probability of a rare mutant. The probability of the mutant population

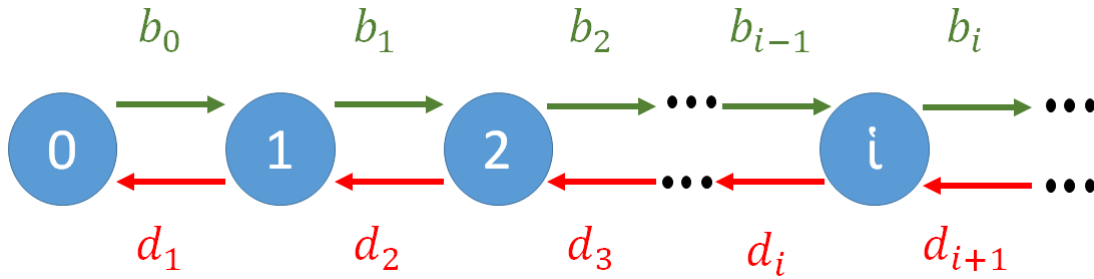


Fig. 1.2 Schematic diagram of a birth-death process (adapted from [15]).

with size i at time t for an absorbing state at zero evolves as [15],

$$\dot{P}_i(t) = b_{i-1}P_{i-1}(t) - (b_i + d_i)P_i(t) + d_{i+1}P_{i+1}(t), \quad (1.3)$$

with boundary condition $P_i(t) = 0$ for $i < 0$ and $b_0 = d_0 = 0$. When the birth and death rates are linear in i , the above equation can be solved using the generating function method, and the extinction probability $P_0(t)$ can be obtained from the generating function. The birth and death rates may or may not be functions of time. In Chapter 2, we use this process in a changing environment where the birth and death rates are time-dependent.

1.3 Mathematical Frameworks

To understand the adaptation process, we study the mathematical models analytically using appropriate mathematical frameworks that are described below.

1.3.1 Branching process

The branching process is a widely used framework to understand various problems ranging from the propagation of neutrons in a nuclear reactor to the extinction probability of a mutant in a population [16]. In this process, each individual produces a random number of offspring each generation, independently from other individuals [15]. Figure 1.3 shows a discrete-time branching process where a newly produced mutant gets lost from the population after $t = 5$ generations. Since the branching process ignores interaction between lineages, the birth and death rates in a birth-death process can be linearised, and the resulting model can be easily solved. We use this framework in Chapter 2 to find the fixation probability of a mutant (the probability that ultimately all the individuals

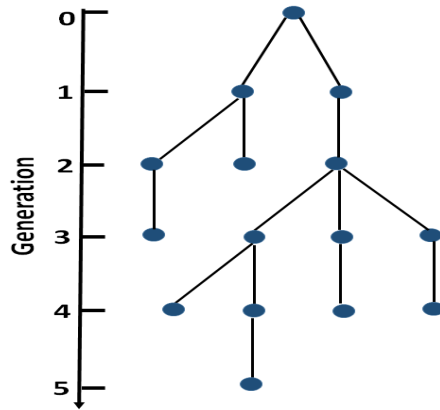


Fig. 1.3 Schematic diagram of a discrete-time branching process starting with a single individual at $t = 0$ (adapted from [15]). The mutant becomes extinct after $t = 5$ generations.

in the population become the mutant type) when the mutant remains beneficial at all times in a changing environment. The branching process works for a growing population whose average number of offspring is larger than one, otherwise the population certainly gets extinct in this process, and therefore, gives the fixation probability to be zero for a neutral or deleterious mutant. We use diffusion theory described in the next subsection to compute the fixation probability of neutral and deleterious mutants.

1.3.2 Diffusion theory

The diffusion theory is a general approach to describe a stochastic process defined in continuous space and time. It can be derived from the discrete Markov chain by scaling the space and time appropriately by the system size and taking the system size to be infinite. In population genetics, we require a large population size $N \rightarrow \infty$ with weak selection, weak mutation ($s, \mu \rightarrow 0$) that keeps $Ns, N\mu$ finite. In this limit, one can derive a forward Kolmogorov (Fokker-Planck) equation and a backward Kolmogorov equation for the probability distribution of allele frequency. The forward Kolmogorov equation is mainly used to find the stationary state probability distribution of an allele, whereas the backward Kolmogorov equation is mostly used to obtain the fixation probability of a mutant. The Kolmogorov equations are [17],

$$\frac{\partial f(x, t)}{\partial t} = -\frac{\partial}{\partial x}(M_{\delta x} f(x, t)) + \frac{1}{2} \frac{\partial^2}{\partial x^2}(V_{\delta x} f(x, t)) \quad (1.4)$$

$$\frac{\partial f(x, t)}{\partial t} = M_{\delta x} \frac{\partial}{\partial x} f(x, t) + \frac{1}{2} V_{\delta x} \frac{\partial^2}{\partial x^2} f(x, t) \quad (1.5)$$

where (1.4) represents forward Kolmogorov equation and (1.5) is a backward Kolmogorov equation. The function $f(x, t)$ represents the probability density function, and $M_{\delta x}$ and $V_{\delta x}$ are the mean and variance of the process over a small time interval, respectively.

In Chapter 2, along with the perturbation theory, we use the forward Kolmogorov equation to find the allele frequency distribution and the backward Kolmogorov equation to find the fixation probability of a mutant in a periodically changing environment where the mutant can be beneficial and deleterious during the part of the selection cycle. In Chapter 4, we carry out the eigenfunction expansion [18] of the allele frequency distribution when the environment is constant. This method results in recursion equations for certain coefficients that can be easily solved numerically and thereby allowing one to construct the eigenfunctions.

1.4 Quantities of interest

We will be mainly concerned with the following two quantities in this thesis.

1.4.1 Fixation Probability

When the mutation rate is low, a newly arisen mutant can either fix or get lost from the population before a new mutant arises. The diffusion theory discussed in Sect. 1.3.2 shows that the fixation probability of a mutant when a single biallelic locus is under selection, depends on both the selection coefficient and the size of the population as [19],

$$P_{fix} = \frac{\int_0^p \exp \left\{ - \int^x \frac{2M_{\delta x'}}{V_{\delta x'}} dx' \right\} dx}{\int_0^1 \exp \left\{ - \int^x \frac{2M_{\delta x'}}{V_{\delta x'}} dx' \right\} dx}, \quad (1.6)$$

where $M_{\delta x} = sx(1-x)(x+h(1-2x))$ and $V_{\delta x} = \frac{x(1-x)}{N}$ are the mean and variance of the change in allele frequency x per generation with an initial frequency p in a birth-death process of a diploid population with intermediate dominance. The fixation probability of a beneficial mutant approaches hs for large populations and can also be obtained using the branching process described in Sec. 1.3.1, which shows that the allele is more favorable if it is dominant (Haldane's sieve) [20]. But the dominant mutant has a lower chance of fixation if it is deleterious. The fixation probability of a neutral mutant depends on its initial frequency p in the population. As the population size increases, the fixation probability goes towards zero for the deleterious and neutral mutants that shows the strength of genetic drift decreases with the population size, as shown in Fig.

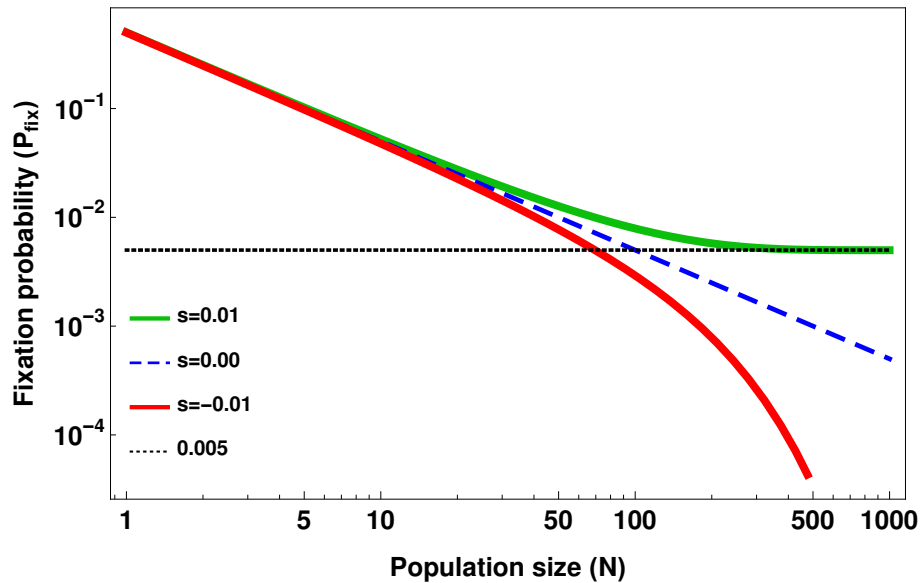


Fig. 1.4 The figure shows the fixation probability (1.6) of a *de novo*, codominant ($h = 1/2$) mutant with population size. The black dotted line shows the fixation probability of a beneficial mutant for large population size.

1.4. We generalize the above result (1.6) obtained in the static environment to changing environment in Chapter 2.

1.4.2 Allele frequency distribution

Due to stochasticity, the allele frequency is distributed according to a distribution whose variance depends on the size of the population. To find this distribution, we can use the forward Kolmogorov equation and solve it using the eigenfunction expansion method. When selection, mutation, and population size are time-independent, we can separate the time and space part of (1.4) and get a first-order and second-order ordinary differential equations for the time and space parts, respectively. When selection is absent, the space part of the diffusion equation obeys the Gegenbauer equation and Gauss hypergeometric equation in the absence and presence of mutation, respectively [19]. But in the presence of selection, the second-order differential equation obeys an oblate spheroidal equation in the absence of mutation, and neither the eigenvalues nor the eigenfunctions are explicitly known, and the eigenspectrum was not studied in the presence of mutation. In Chapter 2, we, therefore, use the perturbation method to find the allele frequency distribution and fixation probability taking the time-dependent selection coefficient as the perturbation parameter. In Chapter 4, we study the dynamics of adaptation when selection, mutation,

and drift are present and find that the eigenfunctions obey a confluent Heun equation in which the Frobenius series or other orthogonal polynomial expansions lead to three-term recurrence relations for the expansion coefficients that are nontrivial to solve. We use scaling ideas to find the expressions for the expansion coefficients, and obtain eigenvalues using a perturbation theory for weak selection and numerically for strong selection.

1.5 Overview of the thesis

In this thesis, we want to understand how a population adapts to its environment under the action of evolutionary forces described in Sect. 1.1. Whereas the bulk of the thesis considers the evolution in a continually changing environment, we have also studied the evolutionary dynamics of a trait due to a single sudden change in the environment.

In Chapter 2, we study the evolution of a monogenic trait in a periodically changing environment (for example, due to seasonality and drug cycling) [21]. We calculate the fixation probability of a mutant in a finite, diploid population with intermediate dominance and find that depending on the rate of environmental change and the time of appearance of the mutant, an initially beneficial (deleterious) mutant can have a fixation probability lower (higher) than that for a neutral mutant. We also find an interesting result that Haldane's sieve [20] does not always hold in a time-varying environment.

We also investigate the adaptation of a polygenic trait where selection acts on a large number of genes to maintain an optimum phenotype. However, the incorporation of genetic drift in the evolution equation of the polygenic trait makes it a high-dimensional diffusion equation which is a complex problem to be solved mathematically. Therefore, in Chapter 3, we study a deterministic model to understand the evolution of a polygenic trait due to a linearly changing environment (for example, as a result of global warming) [22]. In contrast to the previous work, our results show that the mean trait evolves with a speed lower than that of the phenotypic optimum.

Although our main focus is on the evolution of a trait in a changing environment, as the dynamics of adaptation under constant selection are not well-understood [19], we study the relevant forward Kolmogorov equation in Chapter 4, using an eigenfunction expansion method [23]. We find that the eigenfunctions obey a confluent Heun equation which is a generalization of the hypergeometric equation [24], and the first eigenvalue that determines the dynamics shows a sharp transition from a linearly increasing function of mutation rate to a constant when mutation rate crosses one.

Our main results are summarized in Chapter 5. Some interesting open problems related to this thesis are also discussed in this Chapter.

Bibliography

- [1] Wikipedia contributors. Natural selection. Wikipedia, The Free Encyclopedia, 2021.
- [2] H. B. D. Kettlewell. Selection experiments on industrial melanism in the Lepidoptera. *Heredity*, **9**: 323–342, 1955.
- [3] L. M. Cook and I. J. Saccheri. The peppered moth and industrial melanism: evolution of a natural selection case study. *Heredity*, **110**: 207-212, 2013.
- [4] J. S. Sanjak, J. Sidorenko, M. R. Robinson, K. R. Thornton, and P. M. Visscher. Evidence of directional and stabilizing selection in contemporary humans. *Proc. Natl. Acad. Sci. USA*, **115**: 151-156, 2018.
- [5] J. A. Endler. *Natural Selection in the Wild*. Princeton, N.J.:University Press, 1986.
- [6] R. Bürger. *The Mathematical Theory of Selection, Recombination, and Mutation*. Wiley, Chichester, 2000.
- [7] C. Rueffler, T. J. M. Van Dooren, O. Leimar, and P. A. Abrams. Disruptive selection and then what? *Trends Ecol. Evol.*, **21**: 238-245, 2006.
- [8] N. H. Barton, D. E. G. Briggs, J. A. Eisen, D. B. Goldstein, and N. H. Patel. *Evolution*. Cold Spring Harbor Laboratory Press, New York, 2007.
- [9] A. Eyre-Walker and P. D. Keightley. The distribution of fitness effects of new mutations. *Nat. Rev. Genet.*, **8**: 610-618, 2007.
- [10] K. Jain and S. Seetharaman. Nonlinear deterministic equations in biological evolution. *J. Nonlinear Math. Phys.*, **18**: 321-338, 2011.
- [11] K. Jain and W. Stephan. Rapid adaptation of a polygenic trait after a sudden environmental shift. *Genetics*, **206**: 389-406, 2017.

-
- [12] B. Walsh and M. Lynch. *Evolution and Selection of Quantitative Traits*. Oxford University Press, New York, 2018.
- [13] B. Charlesworth and D. Charlesworth. *Elements of Evolutionary Genetics*. Ben Roberts, Colorado, 2010.
- [14] N. H. Barton. The maintenance of polygenic variation through a balance between mutation and stabilizing selection. *Genet. Res.*, **47**: 209-216, 1986.
- [15] L. J. S. Allen. *An Introduction to Stochastic Processes with Applications to Biology*. CRC Press, Boca Raton, 2010.
- [16] T. E. Harris. *The Theory of Branching Processes*. Springer-Verlag, Berlin, 1964.
- [17] W. J. Ewens. *Mathematical Population Genetics*. Springer, Berlin, 2004.
- [18] H. Risken. *The Fokker-Planck Equation, Methods of Solution and Applications*. Springer-Verlag, Berlin, 1996.
- [19] M. Kimura. Diffusion models in population genetics. *J. Appl. Probab.*, **1**: 177-232, 1964.
- [20] J. B. S. Haldane. A mathematical theory of natural and artificial selection, part v: selection and mutation. *Proc. Camb. Philos. Soc.*, **23**: 838-844, 1927.
- [21] A. Devi and K. Jain. The impact of dominance on adaptation in changing environments. *Genetics*, **216**: 227-240, 2020.
- [22] K. Jain and A. Devi. Polygenic adaptation in changing environments. *EPL*, **123**: 48002, 2018.
- [23] K. Jain and A. Devi. Evolutionary dynamics and eigenspectrum of confluent Heun equation. *J. Phys. A: Math. Theor.*, **53**: 395602, 2020.
- [24] P. P. Fiziev and D. Staicova. The Heun project: Heun functions, their generalizations and applications. <https://theheunproject.org>, 2012.

Chapter 2

The impact of dominance on adaptation in changing environments

2.1 Introduction

In this Chapter, we study the evolution of a monogenic trait in a finite, diploid population due to a periodically changing environment. Our primary purpose in this Chapter is to understand how the fixation probability of a rare mutant depends on its dominance coefficient and the rate of environmental change.

Natural environments change with time and a population must continually adapt to keep up with the varying environment [1–3]. It is therefore important to understand the adaptation dynamics of a finite population subject to both random genetic drift and environmental fluctuations. This is, in general, a hard problem but some understanding of such dynamics has been obtained in previous investigations. For example, when the environment changes very rapidly, on the time scale of a generation, the dynamics of adaptation are simply determined by the time-averaged environment [1].

Environments can, of course, vary slowly and recent experiments have shown the impact of rate of change in the environment on the population fitness [4, 5]. The fixation probability, fixation time, and adaptation rate in changing environments have also been studied in a number of theoretical studies [6–14], and it has been found that when the environment changes at a finite rate, population dynamics are strongly determined by the environment in which the mutant arose.

In diploid populations, the degree of dominance also affects the evolutionary dynamics; in particular, in a static environment, the fixation probability of a dominant beneficial mutant is known to be higher than when it is recessive (*Haldane's sieve*) [15], while the opposite trend holds if the mutant is deleterious [16]. How these results are affected in changing environments is, however, not completely understood.

To understand the adaptive process in variable environments, Uecker and Hermisson (2011) developed a framework for general time-dependent selection schemes; however, their analysis was limited to very large populations and did not explicitly address how dominance affects the fixation process. In this article, we employ their formalism to study the dynamics of adaptation of a finite, diploid population evolving in an environment that changes periodically due to, for example, seasonal changes or drug cycling with a particular focus on the impact of dominance. We find that, in time-dependent environments, the magnitude of the fixation probability of a rare mutant differs substantially from the corresponding results in the time-averaged environment. Furthermore, the dependence of the fixation probability on dominance coefficient can differ from that expected in the static environment depending on the rate of environmental change, the time of appearance of the mutant and its fitness in the time-averaged environment. However, when recurrent mutations occur, our results for the average allele frequency and population fitness suggest that dominance does not have a strong influence on evolutionary dynamics.

2.2 Model

We consider a finite, randomly mating diploid population of size N with a single biallelic locus under selection. The (Wrightian) fitness of the three genotypes denoted by aa , aA , AA is $1 + s$, $1 + hs$, 1 , respectively, where the dominance coefficient $0 < h \leq 1$. The population evolves in a periodically changing environment that is modeled by a time-dependent selection coefficient $s(t) = \bar{s} + \sigma \sin(\omega t)$ where \bar{s} is the selection coefficient averaged over a period $2\pi/\omega$; in the following, we assume that \bar{s} is arbitrary but $\sigma > 0$. We ignore random fluctuations in the environment so that selection changes in a predictable fashion. Although dominance can evolve with time [17], for simplicity, here we assume the dominance coefficient to be constant in time. We also allow mutations to occur with a constant, symmetric probability μ between the two alleles.

The population dynamics are described by a continuous time birth-death model. Although in a finite population with overlapping generations, Hardy-Weinberg equilibrium

(HWE) does not strictly hold, it is a good approximation when selection and mutation are weak and population size is large [18]. In the following, we therefore work in these parameter regimes and assume that the population is in HWE immediately after mating (see also Sec. A.1). If the birth rate of an individual is given by its genotypic fitness and the death rate by one, the number of allele a (A) increases by one if it is chosen to give birth at rate equal to its marginal fitness, w_a (w_A) and an allele A (a) is chosen to die. Taking the effect of mutations on these birth and death processes into account, we find that the rate r_b and r_d at which the number i of allele a increases or decreases, respectively, by one are given by

$$r_b(t) = \frac{(1 - \mu)iw_a + \mu(2N - i)w_A}{\bar{w}} \times \frac{2N - i}{2N} \quad (2.1)$$

$$r_d(t) = \frac{(1 - \mu)(2N - i)w_A + \mu iw_a}{\bar{w}} \times \frac{i}{2N} \quad (2.2)$$

where $w_a = (1 + s)x + (1 + hs)(1 - x)$, $w_A = (1 - x) + (1 + hs)x$, $\bar{w} = w_a x + w_A(1 - x)$ is the population-averaged fitness and $x = i/(2N)$ is the frequency of allele a .

We study the model described above analytically using an appropriate perturbation theory and numerically through stochastic simulations in which the time interval Δ between successive generations, t and $t + \Delta$ is treated as a random variable. We first choose Δ from an exponential distribution with rate $R(t) = \Delta^{-1} \int_t^{t+\Delta} dt' (r_b(t') + r_d(t')) \approx r_b(t) + r_d(t)$ (the latter approximation is justified for small cycling frequencies as the correction to it is of order ω). Then the number of allele a and A is changed with a probability proportional to the rate of the respective event given above [19, 10].

Below we first consider the weak mutation regime ($2N\mu \ll 1$) in which once a mutant has appeared in a clonal population, further mutations may be ignored until the mutant is fixed or lost; here, we are interested in understanding how the fixation probability of a rare mutant depends on various environmental and population factors such as the cycling frequency and dominance parameter. We also briefly explore the strong mutation regime ($2N\mu \gg 1$) in which recurrent mutations occur; our objective is to understand the effect of mutations and environmental fluctuations on population fitness and the dynamics of allele frequency.

2.3 Fixation probability of a rare mutant

In a static environment, the fixation probability of a mutant allele in a large population ($N \rightarrow \infty$) under weak selection and weak mutation ($s, \mu \rightarrow 0$) with finite $2Ns$, $2N\mu$ can

be described by a backward Kolmogorov equation [20]. For the model described in the last section, the probability P_{fix} that mutant allele a present in frequency x at time t fixes eventually is given by [10]

$$-\dot{P}_{\text{fix}}(x, t) = s(t)g(x)\frac{\partial P_{\text{fix}}(x, t)}{\partial x} + \frac{x(1-x)}{2N}\frac{\partial^2 P_{\text{fix}}(x, t)}{\partial x^2}, \quad (2.3)$$

where dot denotes a derivative with respect to time and $g(x) = x(1-x)(x + h(1-2x))$. On the right-hand side (RHS) of the above equation, the first term describes the deterministic rate of change in the allele frequency [20] and the second term captures the stochastic fluctuations due to finite population size. Since the left-hand side (LHS) of (2.3) is nonzero, it is *inhomogeneous* in time; that is, the eventual fixation probability depends on the time of appearance t_a (or phase $\theta_a = \omega t_a$) of the mutant [10, 11].

Equation (2.3) does not appear to be exactly solvable, and approximate methods such as perturbation theory require an exact solution of the unperturbed problem ($\sigma = 0$), which is not known in a closed form for nonzero \bar{s} [16, 21]. Therefore to obtain an analytical insight, we study the fixation probability using a branching process for positive \bar{s} and analyze the above diffusion equation for $\bar{s} = 0$ using a time-dependent perturbation theory. Some numerical results for negative \bar{s} are also given. Before proceeding to a quantitative analysis, we first give a qualitative picture of the process in the following section.

2.3.1 Qualitative features

In a static environment, a dominant beneficial (deleterious) mutant has a higher (lower) chance of fixation [16]. In a changing environment, we expect that this result continues to hold when the mutant is beneficial or deleterious at all times (that is, when $\sigma < |\bar{s}|$ for the periodically changing $s(t)$; see Sec. A.2). But it is not obvious how dominance influences the fixation probability when the mutant is transiently beneficial or deleterious. Our results for the fixation probability in such situations are shown in Fig. 2.1, Fig. 2.2 and Fig. 2.3 when the mutant arises in an environment which is beneficial, neutral and deleterious on average, respectively.

In all these cases, in a slowly changing environment, the effect of dominance is found to be the same as in the static environment (that is, a dominant mutant that starts out as a beneficial (deleterious) one has a higher (lower) chance of fixation). This is because when the environment changes infinitesimally slowly ($\omega \rightarrow 0$), as Fig. 2.4a illustrates for on average neutral mutation, fixation occurs rapidly compared to the fluctuations in

selection so that the sign of selection remains the same from origination to fixation of the mutant.

However, in rapidly changing environments ($\omega \rightarrow \infty$), as Fig. 2.1, Fig. 2.2 and Fig. 2.3 demonstrate, the impact of dominance on the fixation probability can be different from that in a static environment. For large cycling frequencies, although the fixation times are much longer than the time period of environmental change (see Fig. 2.4b), the time of appearance still plays an important role in determining the chance of fixation as the mutant must escape the stochastic loss at short times (in fact, Fig. 2.4b shows that the effect of random genetic drift is strongest in the first seasonal cycle). Then a mutant that arises in an, on average, neutral environment while selection is positive but the selection strength is decreasing, will soon encounter an environment with negative fitness effects that affect a dominant mutant more adversely than the recessive one leading to a lower chance of fixation of the dominant mutant. In an environment that is beneficial on average, if a mutant arises while selection is negative, it will spend relatively less time in the negative cycle and therefore will effectively behave like a beneficial mutant resulting in the behavior of the fixation probability different from that in the static environment; a similar argument holds when $\bar{s} < 0$.

2.3.2 On average beneficial mutant in a large population

When the mutant is beneficial on average ($\bar{s} > 0$) and the population is large enough ($2N\bar{s} \gg 1$), one can use a branching approximation to find the fixation probability of a rare mutant. The basic idea is that a beneficial mutant will get fixed once it is present in finite frequency in the population, but it must survive the loss due to random genetic drift when it is initially present in small number compared to the population size. Then, the probability that $i \ll 2N$ number of a alleles are present at time t is governed by $\dot{P}(i, t) = r_-(i+1)P(i+1, t) + r_+(i-1)P(i-1, t) - (r_+ + r_-)iP(i, t)$, along with boundary condition $P(i, t) = 0, i < 0$, where $r_-(t) = \lim_{N \rightarrow \infty} r_d/i$ and $r_+(t) = \lim_{N \rightarrow \infty} r_b/i$ are, respectively, per capita birth rate and death rate of the mutant in a large population. The probability of eventual fixation, $P_{\text{fix}} = 1 - \lim_{t \rightarrow \infty} P(0, t)$ is given by [22]

$$P_{\text{fix}} = \left[1 + \int_0^\infty d\tau r_-(\tau) e^{\int_0^\tau dt' (r_-(t') - r_+(t'))} \right]^{-1}. \quad (2.4)$$

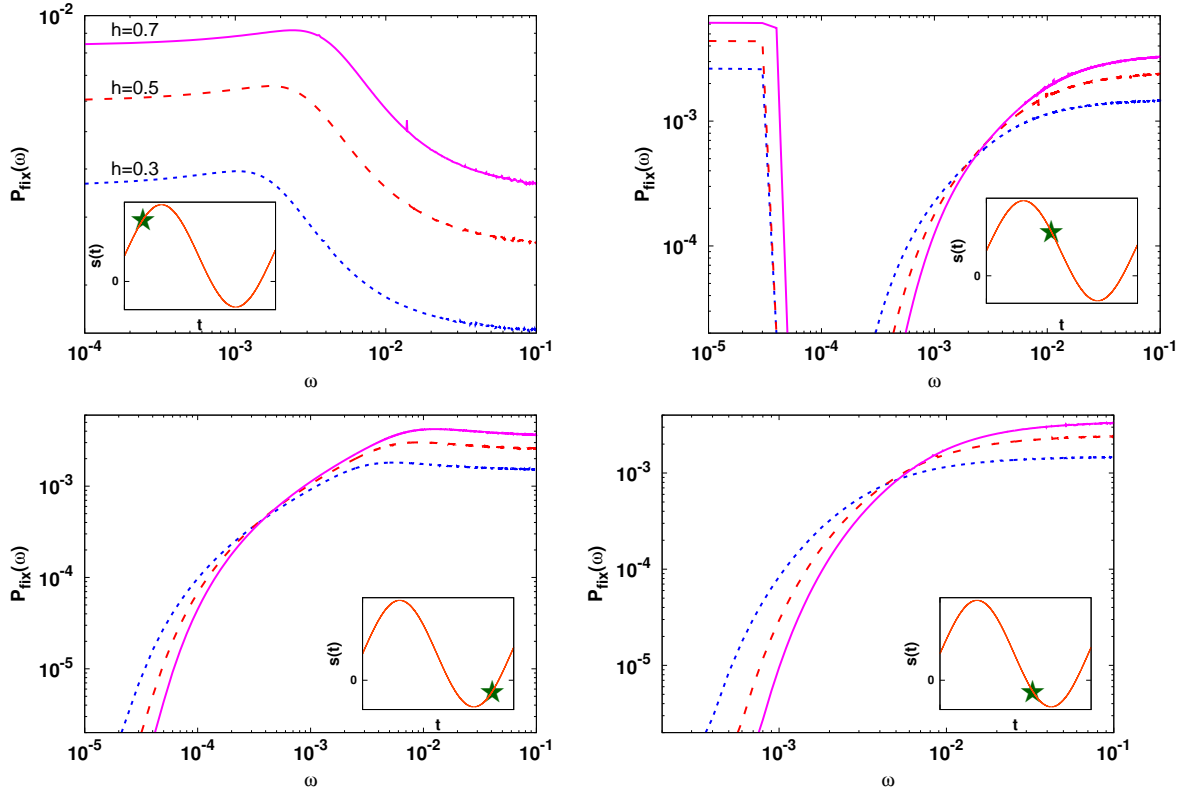


Fig. 2.1 Fixation probability (2.5) obtained using branching process approximation for a mutant that is beneficial on average ($\bar{s} = 0.005$, $\sigma = 2\bar{s}$) for $\theta_a = \pi/4, 7\pi/8, 5\pi/4, 7\pi/4$ (clockwise from top left as shown in insets) for $h = 0.3$ (dotted), 0.5 (dashed), 0.7 (solid). Note that the h -dependence of the fixation probability is different at small and large cycling frequencies when the mutant is deleterious at the time of appearance.

From (2.1) and (2.2), we obtain $r_- = 1, r_+ = 1 + hs$; using these in (2.4), we find that

$$P_{\text{fix}} = \left[1 + \int_0^\infty e^{-h\bar{s}t + \frac{h\sigma}{\omega} (\cos(\omega t + \theta_a) - \cos(\theta_a))} dt \right]^{-1}, \quad (2.5)$$

which reduces to (29) of Uecker and Hermisson (2011) for $\xi = 1$ when $h = 1/2$ and $s(t) \rightarrow 2s(t)$ (note that their expression contains a typographical error). Numerical studies of (2.5) have shown that the fixation probability is, in general, a nonmonotonic function of cycling frequency ω and strongly depends on the phase, $\theta_a = \omega t_a$ [10, 12].

Equation (2.5) is analyzed in Appendix B.1 for $h\bar{s}, h\sigma \ll 1$, and we find that

$$P_{\text{fix}} = \begin{cases} hs(t_a) + \frac{\omega\sigma \cos(\theta_a)}{s(t_a)} & , \omega \ll h\bar{s}, h\sigma \text{ and } s(t_a) > 0 & (2.6a) \\ 0 & , \omega \ll h\bar{s}, h\sigma \text{ and } s(t_a) < 0 & (2.6b) \\ h\bar{s} + \frac{h^2\bar{s}\sigma \cos(\theta_a)}{\omega} & , \omega \gg h\bar{s}, h\sigma, \text{ any } s(t_a) & (2.6c) \end{cases}$$

where $s(t_a) = \bar{s} + \sigma \sin(\theta_a)$. Since the fixation probability of a beneficial mutant with constant selection coefficient s_0 is given by hs_0 (Haldane, 1927), the above expressions show that, for slowly changing environments, the fixation probability is determined by the selection coefficient of the mutant at the instant it arose, while for rapidly changing environments, it depends on the time-averaged selection coefficient \bar{s} [7, 9].

For $\sigma < \bar{s}$, the mutant is beneficial at all times; in this case, the effect of a slowly changing environment is captured by the deviation from $hs(t_a)$ in (2.6a) which changes linearly with the cycling frequency and is *independent* of the dominance parameter. In contrast, for rapidly changing environments, the fixation probability (2.6c) is sensitive to dominance as the deviation from the asymptotic result $h\bar{s}$ depends on h (also, see Fig. A.2). The inset of Fig. A.2 as also (2.6a) and (2.6c) show that the dominant mutant has higher fixation probability than the recessive one at *all* cycling frequencies. In other words, Haldane's sieve [15] that favors the establishment of beneficial dominant mutations in static environments continues to operate in changing environments in which the mutant is beneficial at all times. Equations (2.6a) and (2.6c) also emphasize the important role of the time of appearance of the mutant. If the beneficial mutant arises while the selection coefficient is increasing (decreasing) with time, the fixation probability at small cycling frequencies increases (decreases) with ω and approaches the asymptotic value $h\bar{s}$ from above (below) at high cycling frequencies.

As explained in Appendix B.1, on equating the expressions (2.6a) and (2.6c), the fixation probability is found to have an extremum at a *resonance frequency*,

$$\omega_r \approx h\bar{s} \left(\frac{\sqrt{4 + \tan^2(\theta_a)} - \tan(\theta_a)}{2} \right). \quad (2.7)$$

The above expression shows that a minimum or a maximum in the fixation probability occurs when the environment changes at a rate proportional to the average growth rate (Malthusian fitness), $h\bar{s}$ of the population. As already mentioned above, this extremum is a minimum if the mutant appears while selection is decreasing ($\pi/2 < \theta_a < 3\pi/2$)

and a maximum otherwise. For the two special values, $\theta_a = \frac{\pi}{2}$ and $\frac{3\pi}{2}$, the fixation probability decreases and increases monotonically, respectively, with ω .

For $0 < \bar{s} < \sigma$ the mutant is not beneficial at all times; in this case, the expression (2.6a) for small cycling frequencies holds if $s(t_a) > 0$ (see Appendix B.1). Otherwise as the mutant is initially deleterious and arises in an infinitely large population, the fixation probability is essentially zero. As shown in Fig. 2.1, the dominant mutant has a higher fixation probability than the recessive one at large cycling frequencies, irrespective of the time at which the mutant appeared (see also (2.6c)). But at small cycling frequencies, the effect of dominance depends on whether the mutant is beneficial or deleterious when it originated: for positive (negative) $s(t_a)$, the dominant (recessive) mutant is favored. For an initially beneficial mutant, as discussed above, the fixation probability changes nonmonotonically with cycling frequency, and the resonance frequency is given by (2.7). But it can exhibit an extremum for initially deleterious mutant also (see Fig. 2.1 for $\theta_a = 7\pi/4$). Note that the fixation probability curves intersect for different dominance curves which can be estimated for large cycling frequencies as discussed in Appendix B.1.

To summarize, in an environment that is beneficial on average, the impact of dominance on fixation probability is different in slowly and rapidly varying environments if the mutant is deleterious when it appears in the population.

2.3.3 On average neutral mutant in a finite population

We now calculate the fixation probability of an on average neutral mutant using the backward diffusion equation (2.3).

Small population

We first consider a small population of size $N \ll \sigma^{-1}$ and analyze the $\omega \ll \sigma$ and $\omega \gg \sigma$ regimes in Appendix B.2 and Appendix B.3, respectively. On using (B.2.8) and (B.3.2), we find that the fixation probability of allele a present in a single copy at time $t_a = \theta_a/\omega$ is given by

$$2NP_{\text{fix}} = \begin{cases} \left(1 + \frac{(1+h)N\sigma \sin(\theta_a)}{3}\right) + \left(\frac{4+h}{9}\right) N^2\sigma \cos(\theta_a)\omega & , \omega \ll \sigma \quad (2.8a) \\ 1 + \frac{\sigma}{2\omega} \left(\frac{\cos(\theta_a - \tan^{-1} \ell)}{\sqrt{1+\ell^2}} + \frac{(2h-1) \cos(\theta_a - \tan^{-1} 3\ell)}{\sqrt{1+9\ell^2}}\right) & , \omega \gg \sigma \quad (2.8b) \end{cases}$$

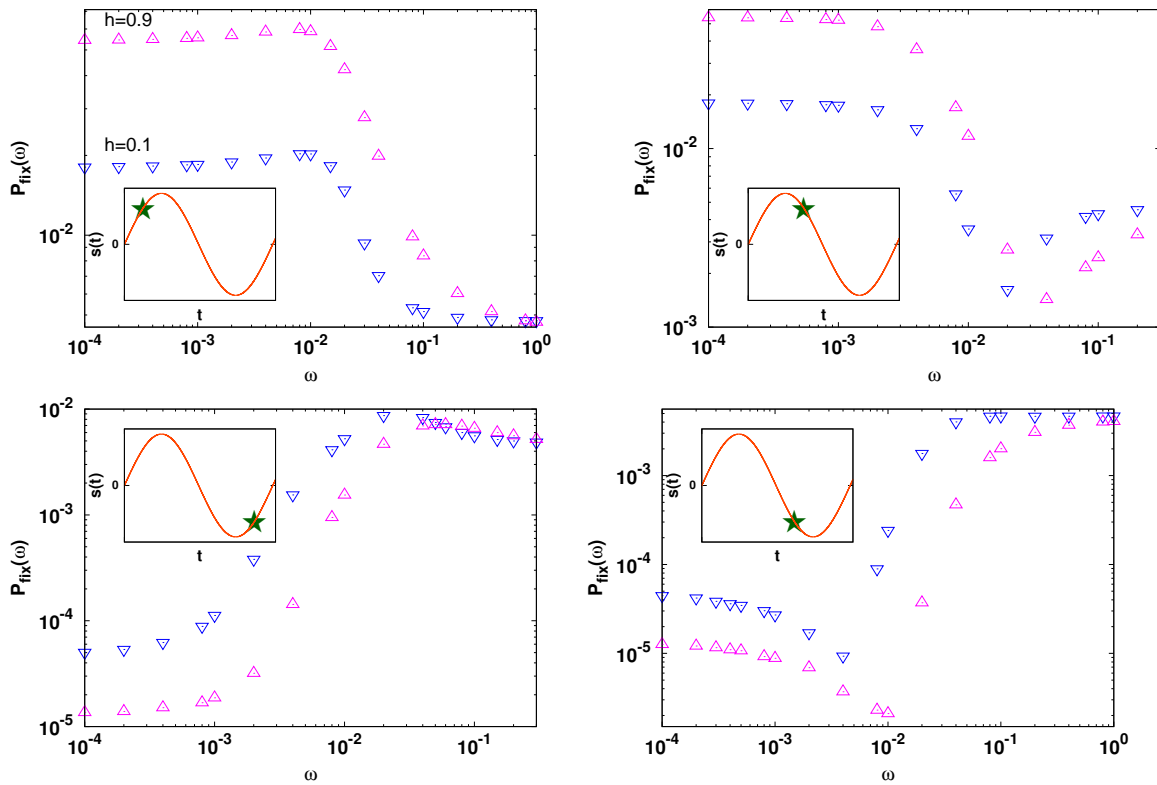


Fig. 2.2 Fixation probability as a function of cycling frequency for a mutation that is neutral on average and arises in a large population of size $N \gg \sigma^{-1}$ for $h = 0.1(\nabla)$ and $0.9(\Delta)$, and $\theta_a = \pi/4, 3\pi/4, 5\pi/4, 7\pi/4$ (clockwise from top left). The other parameters are $N = 100$ and $\sigma = 0.1$. The simulation data are obtained by averaging over 10^7 independent runs. A dominant (recessive) mutant that is beneficial (deleterious) when it appears in the population can be disfavored at large cycling frequencies.

where $\ell = (N\omega)^{-1}$. The expression (2.8b) holds for any $\omega \gg \sigma$ but for $\omega \gg N^{-1}$, it simplifies to

$$2NP_{\text{fix}} \approx 1 + \frac{h\sigma \cos(\theta_a)}{\omega}, \quad \omega \gg N^{-1} \quad (2.9)$$

which monotonically approaches the fixation probability of a neutral mutant in a static environment. The above results show that the change in the fixation probability depends weakly on the dominance parameter when the environment changes slowly, but has a strong dependence on h in rapidly changing environments. The top panel of Fig. 2.5 shows that the expressions (2.8a) and (2.8b) are in very good agreement with the simulation results, and suggests that the resonance frequency where the fixation probability has an extremum does not depend on the dominance coefficient. As detailed in Appendix B.3, we find that

$$\omega_r \propto N^{-1} \quad (2.10)$$

and depends weakly on the dominance coefficient.

Large population

We now consider large populations with size $N \gg \sigma^{-1}$. For $\omega \ll N^{-1} \ll \sigma$, as discussed in Appendix B.2, we find that in slowly varying environments,

$$2NP_{\text{fix}} = \begin{cases} 1 + \frac{(4+h)N^2\sigma \cos(\theta_a)\omega}{9} & , \theta_a = 0, \pi \quad (2.11a) \\ 2Nh\sigma \sin(\theta_a) + 2N \cot(\theta_a)\omega & , 0 < \theta_a < \pi \quad (2.11b) \\ 2(1-h)|N\sigma \sin(\theta_a)|e^{-|N\sigma \sin(\theta_a)|} \left(1 - \frac{N \cot(\theta_a) \ln(2h|N\sigma \sin(\theta_a)|)\omega}{h}\right) & , \pi < \theta_a < 2\pi \quad (2.11c) \end{cases}$$

The above equations show that the fixation probability increases linearly with cycling frequency if the mutant arises while selection is increasing but decreases otherwise. For positive $s(t_a)$, the magnitude of the slope is independent of h and σ but varies with these parameters for $s(t_a) \leq 0$. For large cycling frequencies ($\omega \gg N^{-1}, \sigma$), the fixation probability is given by (2.9) for any $s(t_a)$, and approaches the asymptotic neutral behavior from above (below) when $\dot{s}(t_a) = ds/dt|_{t=t_a}$ is positive (negative) with the fixation probability increasing (decreasing) with increasing h . Thus, as shown in Fig. 2.2, in an, on average neutral environment, the impact of dominance depends on both $s(t_a)$ and $\dot{s}(t_a)$. Figure 2.5 shows a comparison between our analytical and numerical results when the mutant appears at $\theta_a = 0$ (for other values of θ_a , see Fig. A.3), and we find a good agreement.

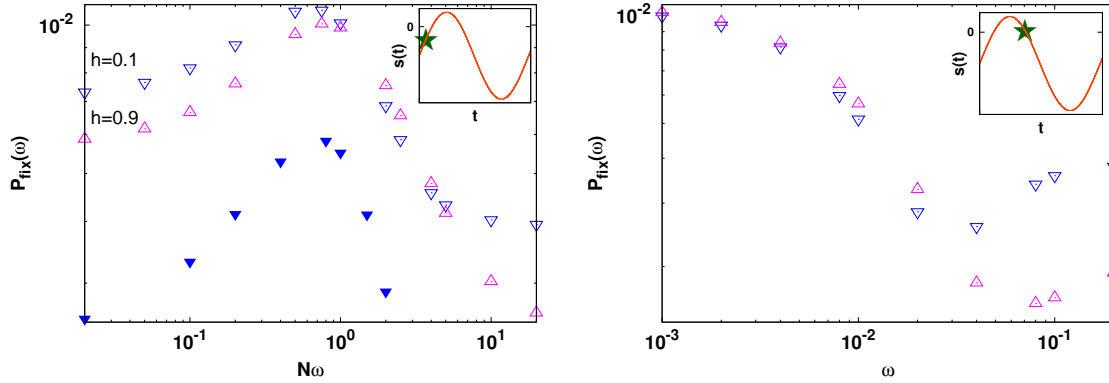


Fig. 2.3 Fixation probability of a mutant which is deleterious on average for $\bar{s} = -0.04$, $\sigma = 0.06$, and $\theta_a = \pi/8$ (left panel) and $3\pi/4$ (right panel). The simulation data are averaged over 10^7 runs. The other parameters are $N = 50$, $h = 0.1$ (∇), 0.9 (Δ). In the left panel, the data for $h = 0.1$, $N = 100$ (\blacktriangledown) is shown to support the claim that the resonance frequency scales as N^{-1} . Note that the recessive mutant that is beneficial when it appears in the population is favored at large cycling frequencies.

Our perturbation expansions in Appendix B.2 and Appendix B.3 are not valid for intermediate cycling frequencies ($N^{-1} \ll \omega \ll \sigma$). However, our numerical simulations suggest that as for small populations, the resonance frequency scales as N^{-1} here also.

2.3.4 On average deleterious mutant in a finite population

When a mutant is deleterious at all times ($\bar{s} < 0$, $|\bar{s}| > \sigma$), its fixation probability is lower than that of a neutral mutant in both static and time-dependent environments, and the dominant mutant has a lower chance of fixation than the recessive one. But, when $\bar{s} < 0$ and $|\bar{s}| < \sigma$, the mutant can be beneficial for some time in a periodically changing environment and its fixation probability can exceed the neutral value depending on the time of appearance. In the left panel of Fig. 2.3, the selection coefficient $s(t_a) < 0$ and therefore the recessive mutant is favored at small cycling frequencies, while in the right panel of Fig. 2.3, since $s(t_a) > 0$, the dominant mutant has a higher chance of fixation in slowly changing environments. In either case, at high cycling frequencies, the fixation probability of a recessive mutant is higher than that for a dominant mutant since the time-averaged selection coefficient is negative. Thus, when $\bar{s} < 0$, the effect of dominance is different in slowly and rapidly changing environments when $s(t_a) > 0$. We also note that in Fig. 2.3a, there is a regime where the dominant mutant's fixation probability exceeds that of the recessive one; however, the difference is quite small and a more detailed investigation is needed to evaluate the importance of this effect.

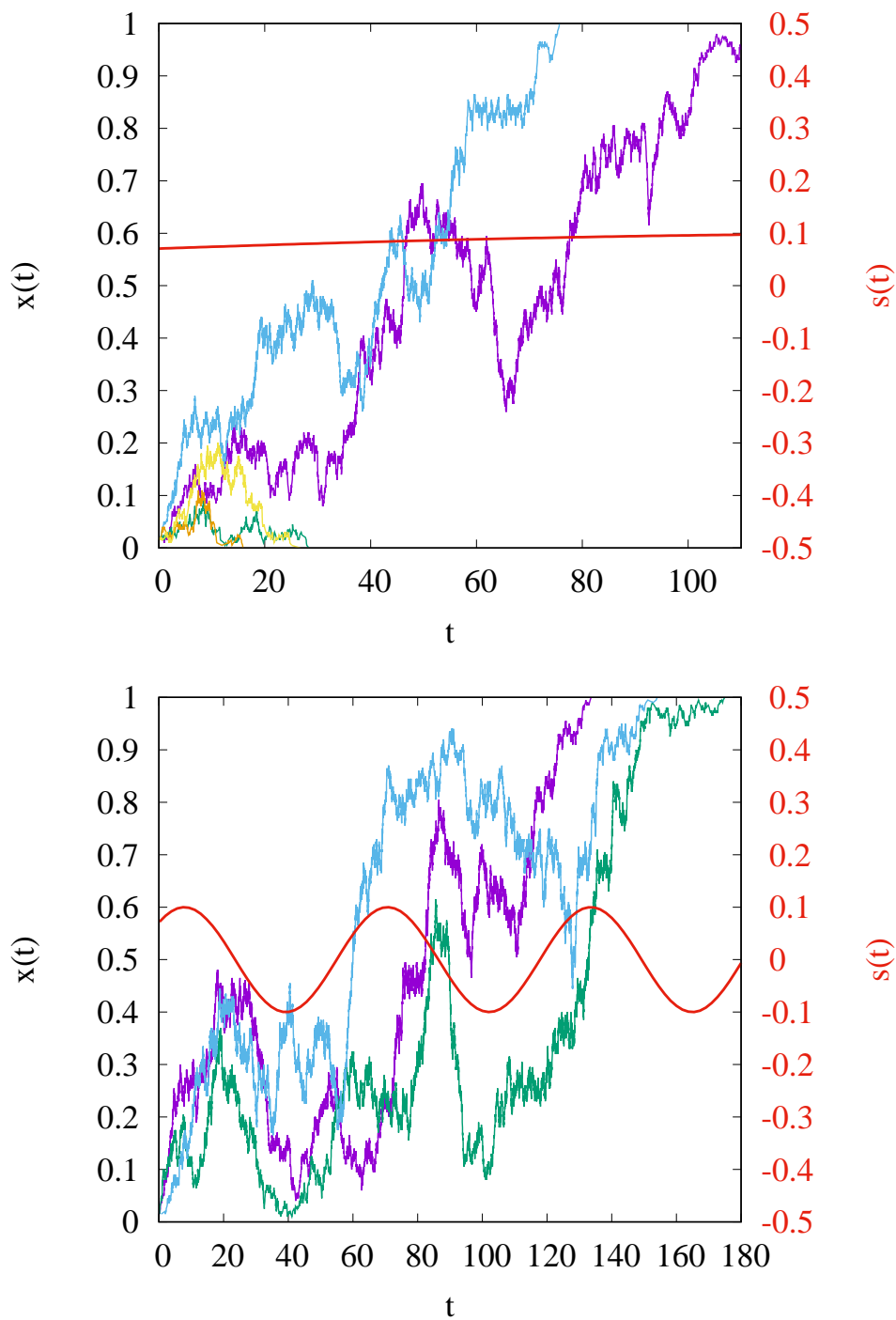


Fig. 2.4 Stochastic trajectories of allele frequency for an on average neutral mutant, starting with a single mutant for $N = 200$, $\bar{s} = 0$, $\sigma = 0.1$, $h = 0.5$, $\theta_a = \pi/4$ for $\omega = 0.005$ (top) and 0.1 (bottom). The successful mutant passes through several cycles of selection before fixing in a rapidly changing environment.

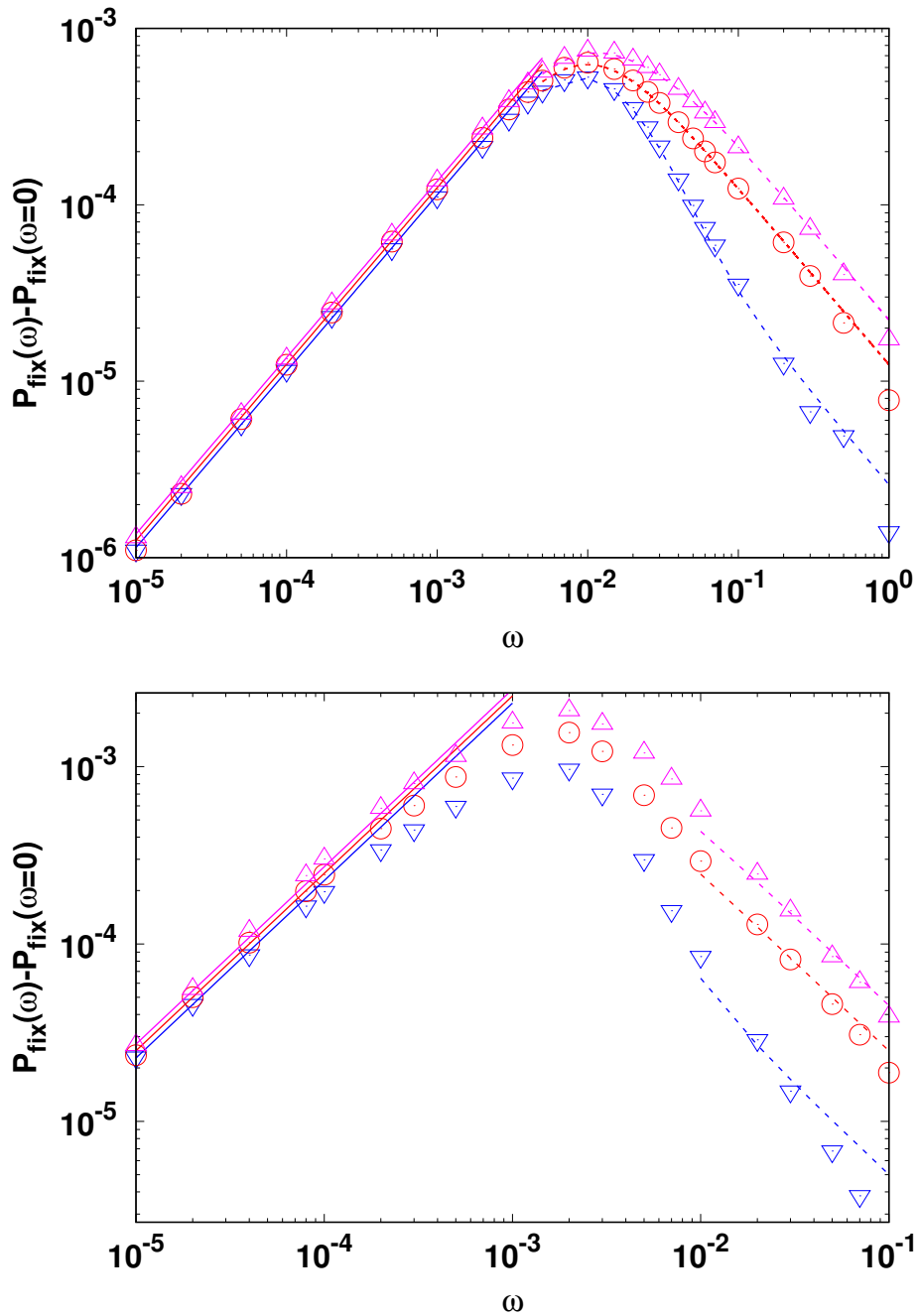


Fig. 2.5 Effect of a changing environment on the fixation probability of a mutant that is neutral on average and arises in a small population ($N \ll \sigma^{-1}$, top) and large population ($N \gg \sigma^{-1}$, bottom). The points show the simulation data obtained by averaging over 10^7 independent runs. The analytical results obtained using the diffusion theory are shown by lines; the solid lines show the expression (2.8a) for small cycling frequencies and the dashed lines represent (2.8b) for large cycling frequencies. Here $N = 100, \sigma = 0.005$ (top) and $N = 1000, \sigma = 0.01$ (bottom), $\theta_a = 0$, and $h = 0.1(\nabla), 0.5(\circ), 0.9(\Delta)$. The value $P_{\text{fix}}(\omega = 0)$ subtracted on the y -axis was obtained numerically.

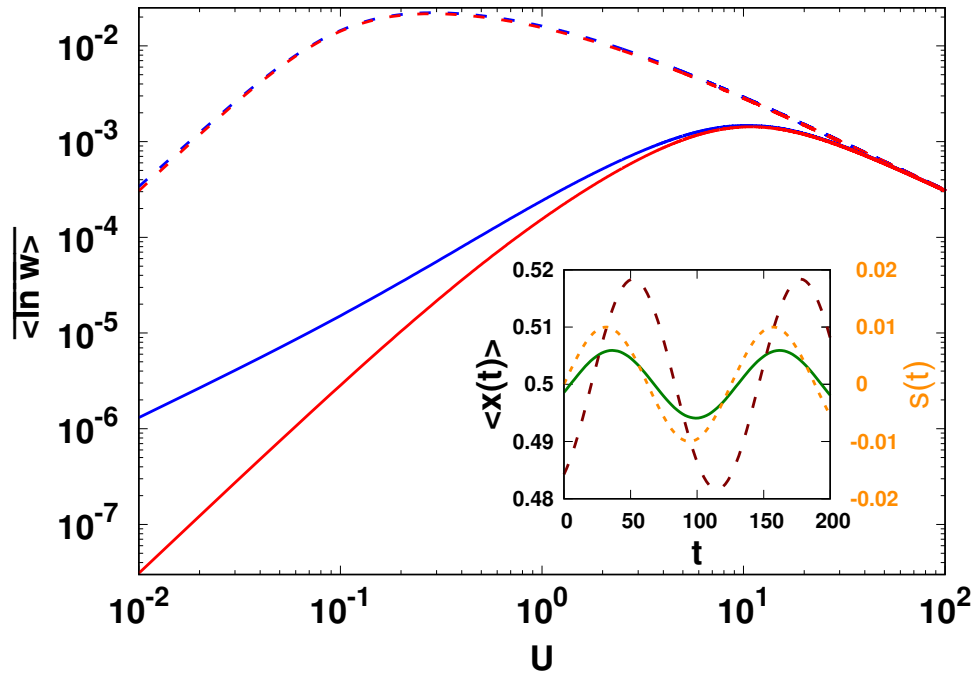


Fig. 2.6 Main: Average log fitness (2.16) in a periodically changing environment as a function of scaled mutation rate $U = 4N\mu$ for scaled selection $S = 4N\sigma = 20$, scaled cycling frequency $\Omega = 2N\omega = 0.1$ (dashed lines), 10 (solid lines) and dominance parameter $h = 0.1$ (blue), 0.5 (red). The effect of dominance is apparent only for small cycling frequency in the weak mutation regime. Inset: Dynamics of population-averaged allele frequency (2.14) for $U = 6$ (dashed), 40 (solid). The mutations decrease the phase lag between the average allele frequency and selection (dotted). Note that $\langle x(t) \rangle$ is independent of dominance coefficient. In the inset plots, $N = 100$, $\sigma = 0.01$, and $\omega = 0.05$.

2.4 Average allele frequency and population fitness

We now turn to the strong mutation regime where $2N\mu \gg 1$ and briefly study the dynamics of the allele frequency in changing environments. For $\bar{s} = 0$, the frequency distribution $\Phi(x, t)$ of allele a under changing selection, mutation, and random genetic drift obeys the following forward Kolmogorov equation [20],

$$\dot{\Phi}(x, t) = -\frac{\partial}{\partial x} \left[(s(t)g(x) + m(x))\Phi(x, t) \right] + \frac{1}{2N} \frac{\partial^2}{\partial x^2} \left[x(1-x)\Phi(x, t) \right], \quad (2.12)$$

where the mutation term $m(x) = \mu(1 - 2x)$ and, as before, $s(t) = \sigma \sin(\omega t)$, $g(x) = x(1-x)(x + h(1 - 2x))$. The above equation is analyzed in Appendix B.4 for small selection amplitude σ , and at large times, the allele frequency distribution $\Phi(x, t)$ is given by (B.4.5).

To get an insight into how the allele frequency changes in changing environments, we find the population-averaged allele frequency,

$$\langle x(t) \rangle = \int_0^1 dx x \Phi(x, t) \quad (2.13)$$

$$= \frac{1}{2} + \frac{S}{16} \frac{U \sin(\omega t - \phi)}{(U + 1)\sqrt{U^2 + \Omega^2}}, \quad S \ll U, \quad (2.14)$$

where $U = 4N\mu$, $S = 4N\sigma$, $\Omega = 2N\omega$, $\phi = \tan^{-1}\left(\frac{\Omega}{U}\right)$. The above equation shows that $\langle x(t) \rangle$ oscillates around one half with the same cycling frequency as $s(t)$ but a different phase. As depicted in Fig. 2.6, the phase difference ϕ decreases with increasing mutation rate so that the allele frequency changes almost in-phase with the environment for $U \gg \Omega$ but lags behind by a phase $\pi/2$ for $U \ll \Omega$. The latter behavior for rare mutations is already illustrated in Fig. 2.4 where the mutant's allele frequency keeps increasing as long as the selection is positive and decreases when $s(t)$ becomes negative. In contrast, for $U \gg \Omega$, the population keeps up with the environment as mutations occur faster than the time scale of environmental change.

Equation (2.14) also shows that the allele frequency amplitude remains close to the time-averaged amplitude when the environment changes rapidly. But it is significantly different from one half in slowly changing environments and varies nonmonotonically with the mutation rate with a maximum at the scaled mutation rate $\hat{U} = \Omega^{2/3}$. We also find that although the distribution $\Phi(x, t)$ depends on the dominance coefficient (see Appendix B.4), the average allele frequency (for small σ) is independent of h .

The above described behavior of allele frequency has implications for the average fitness of the population. When the mutant allele is present in frequency x at time t , the population fitness $w(x, t) = (1 + s)x^2 + 2x(1 - x)(1 + hs) + (1 - x)^2 = 1 + \sigma \sin(\omega t)f(x)$ where $f(x) = (1 - 2h)x^2 + 2hx$ (see MODEL section). The population-averaged log fitness $\langle \ln w \rangle$ oscillates around a constant which is obtained on averaging over a period of the oscillation and is given by

$$4N \overline{\langle \ln w \rangle} = \frac{4N}{T} \int_0^T dt \langle \ln w(x, t) \rangle \quad (2.15)$$

$$= \frac{S^2}{16} \frac{U}{1 + U} \left[\frac{U}{2(U^2 + \Omega^2)} + \frac{(1 - 2h)^2(1 + U)}{(3 + U)(4(1 + U)^2 + \Omega^2)} \right]. \quad (2.16)$$

We thus find that although the selection is zero on average, the population fitness is nonzero.

Equation (2.16) shows that, for a given mutation rate, the average log fitness decreases towards zero with increasing cycling frequency; this behavior is expected as the time-averaged environment governs the dynamics in a rapidly changing environment. However, it is a nonmonotonic function of the scaled mutation rate U : for $1 \ll U \ll \Omega$, the average log fitness is close to zero because the phase difference ϕ between the allele frequency and selection is large (see (2.14)). But for high mutation rate ($U \gg \Omega$), although the phase lag is small, the allele frequency does not deviate substantially from one half, resulting in low fitness. From (2.16), we find that the average fitness has a peak at an optimal mutation rate,

$$U^* = \begin{cases} \left(\frac{12}{6 - (1 - 2h)^2} \right)^{1/3} \Omega^{2/3} & , \Omega \ll 1 \\ \Omega & , \Omega \gg 1 \end{cases} \quad (2.17a)$$

$$(2.17b)$$

which increases with the rate of environmental change. Finally, equation (2.16) also shows that the fitness is a symmetric function of dominance coefficient but the h -dependence is quite weak (see Fig. 2.6), and is apparent only at small mutation rates and for fast environmental changes; we thus conclude that dominance does not have an appreciable effect when recurrent mutations occur.

2.5 Discussion

In this Chapter, we studied the evolutionary dynamics of a finite, diploid population in a varying environment for both weak and strong mutations. The fixation probability of a mutant has been studied in infinitely large populations when selection changes gradually in both magnitude and direction [10, 12] and in finite populations that are subjected to abrupt changes in the direction of selection [6, 9, 13, 14]. Here we modeled a situation in which the mutant allele is beneficial during a part of the seasonal cycle and deleterious in another, and hence its selection coefficient $s(t)$ varies periodically with time. In contrast to previous work, here we focused on the impact of dominance on evolutionary dynamics in changing environments, and obtained simple analytical expressions for the fixation probability in both infinite and finite populations.

Rate of environmental change and time of appearance: In a slowly changing environment, the fixation probability of a mutant is expected to depend on the time it appears in the population. But it is perhaps not obvious if the dependence on the initial condition remains in fast changing environments as the fixation probability in an infinitely fast changing environment is given by the corresponding result in a static environment with the time-averaged selection coefficient \bar{s} . However, as shown in Fig. 2.4, a mutant must escape the stochastic loss at short times in order to fix in the population, and therefore, the eventual fate of the rare mutant depends on its time of appearance at any finite rate of environmental change.

Using branching process and diffusion theory [10, 11], here we have obtained simple expressions for the fixation probability when the frequency of the environmental change is smaller or larger than the resonance frequency ω_r of the population which is given by the average growth rate of the population when the time-averaged selection strength $\bar{s} > 0$ and inverse population size for $\bar{s} \leq 0$. The fixation probability exhibits an extremum when the environment changes at a rate equal to the resonance frequency; whether this extremum is a minimum or a maximum also depends on the time of appearance, t_a , of the mutant.

As an illustration of the above discussion, for arbitrary \bar{s} , consider a beneficial mutant that arises when its selection strength is decreasing with time. In a slowly changing environment, as $\dot{s}(t_a) < 0$, its fixation probability is expected to be smaller than that in the static environment; for the same reason, it approaches the corresponding result in the time-averaged environment from below thus resulting in a minimum at the resonance frequency. It then follows that, in a periodically varying environment with zero or

negative time-averaged selection coefficient, if the environment changes at a rate faster than the resonance frequency, a mutant that is beneficial in a static environment will have a fixation probability lower than $(2N)^{-1}$. Similarly, a deleterious mutant that arises while selection strength is increasing can have enhanced chance of fixation compared to $(2N)^{-1}$ in changing environments that are neutral or beneficial on average.

The above discussion assumes that the mutations are rare. When recurrent mutations occur, we find that, in the on average neutral environment, the population can gain fitness which is, however, appreciable when the mutation rate is as high as the rate of environmental change.

Role of dominance in slowly changing environments: In a static environment, a dominant beneficial mutant enjoys a higher chance of fixation than a recessive one because the (marginal) fitness of the mutant allele (relative to the wild type allele) is higher in the former case [15]. This behavior is reversed for deleterious mutants where the fixation of recessives is favored [16]. In a slowly changing environment ($\omega \ll \omega_r$), if the mutant starts out as a beneficial mutant (that is, its selection coefficient at time of appearance $s(t_a) > 0$), Haldane's sieve operates. Similarly, if the mutant is deleterious to begin with, its chances of fixation are reduced if it is dominant. This result is attested by Figs. 2.1 and A.2 for $\bar{s} > 0$, Fig. 2.2 for $\bar{s} = 0$ and Fig. 2.3 for $\bar{s} < 0$.

Equations (2.6a) and (2.11b) for the fixation probability of a mutant in an environment that is, respectively, beneficial and neutral on average suggest that the change in fixation probability due to a slow change in the environment is simply equal to the change in the mutant's initial fitness relative to its initial fitness, that is, $\dot{s}(t_a)/s(t_a)$ which is *independent* of the dominance coefficient. This can be argued as follows: when the selection coefficient changes very slowly ($\omega \rightarrow 0$), it is reasonable to assume that the fixation probability has the same functional form as that in the static environment. Then, for an initially beneficial mutant, $P_{\text{fix}} \approx hs(t_a + \hat{t}) \approx hs(t_a) + h\hat{t}\dot{s}(t_a)$ where $\hat{t} \propto (hs(t_a))^{-1}$ is the time at which the mutant escapes stochastic loss, as estimated from a deterministic argument.

Role of dominance in fast changing environments: As already mentioned above, an initially beneficial mutant arising when the selection is declining can behave effectively as a deleterious mutant in a rapidly changing environment that is neutral or deleterious on average. This has the immediate consequence that the dominant mutant is less likely to fix than the recessive one, as supported by Fig. 2.2 for $\bar{s} = 0$ and Fig. 2.3 for $\bar{s} < 0$. This result can be relevant to understanding adaptation in environments that change fast and for a short period of time. In Sec. A.4, we construct such examples and find

that the fixation probability of an initially beneficial mutant in transiently changing environments exhibits the same dependence on dominance coefficient as discussed above for periodically changing environments.

Equations (2.6c) and (2.9) show that in fast changing environments, the fixation probability is proportional to $h\bar{s}$ and $(2N)^{-1}$, respectively, which are the results for the fixation probability of a single mutant in an infinitely fast changing environment. If genetic drift is ignored, the dynamics of the mutant frequency are described by $\dot{x} \approx h\sigma \sin(\omega t)x$, so that, at large times, the average number of mutants, $n = 1 + h\sigma \cos(\theta_a)/\omega$ for large ω , and therefore, the fixation probability in rapidly changing environments can be interpreted as simply that of n mutants in infinitely fast changing environments (also, see Sec. A.4).

Limitations and open questions: Our analytical results that provide an understanding of conditions under which the effect of dominance on the fixation probability is different in static and changing environments, are applicable to cycling frequencies that are much smaller or larger than the resonance frequency. As our analysis is not valid for intermediate cycling frequencies, we can not rule out if such differences occur at cycling frequencies around resonance frequency (see, Fig. 2.1 for $\theta_a = 7\pi/8$ and Fig. 2.3a).

Here we have mainly focused on the fixation probability and did not discuss how substitution rate and adaptation rate behave in changing environments. However, our preliminary simulations show that the substitution rate varies nonmonotonically with cycling frequency (also see [23]). A detailed understanding of these quantities requires the knowledge of fixation time which shows interesting dependence on dominance coefficient in static environments [24]; extending such results to temporally varying environments is desirable and will be discussed elsewhere.

When adaptation occurs due to standing genetic variation, the fixation probability of a beneficial mutant is known to be independent of dominance in static environments [25]; here, we have studied the fixation probability of a *de novo* mutation and a detailed understanding of how standing variation affects the results obtained here is a problem for the future.

Many empirical and theoretical studies show faster evolution of X-linked genes than autosomal ones, and it has been argued that the fixations of recessive beneficial alleles can cause the faster X effect [26]. This hypothesis is based on the evolution in a static environment where the ratio of the substitution rate of the X chromosomal genes to that of autosomal genes is greater than one for recessive beneficial alleles if the mutations are unbiased or male-biased. On the other hand, if the allele is deleterious, the ratio is less

than one for recessive alleles. The empirical evidence of the faster X effect strengthens the hypothesis of the fixations of recessive beneficial alleles. However, our study shows that an initially beneficial allele can behave as a deleterious allele when the environment changes and can have a lower fixation probability than a neutral mutant depending upon its time of appearance and rate of environmental change. Therefore, slower evolution of X-linked gene is expected when the recessive allele behaves as deleterious in changing environment, which suggests that the faster X effect may not be seen in changing environment even though the allele appears as a recessive beneficial allele. However, if the faster X effect is a common phenomenon irrespective of the environmental change, we expect the cause of faster X evolution may be something else than due to the recessive beneficial alleles. Our work, therefore, suggests to consider the effect of changing environments on the adaptation rate of X-chromosome.

Bibliography

- [1] J. H. Gillespie. *The Causes of Molecular Evolution*. Oxford University Press, Oxford, 1991.
- [2] P. W. Messer, S. P. Ellner, and N. G. Hairston Jr. Can population genetics adapt to rapid evolution? *Trends Genet.*, **32**: 408-418, 2016.
- [3] C. Bleuven and C. R. Landry. Molecular and cellular bases of adaptation to a changing environment in microorganisms. *Proc. R. Soc. B*, **283**: 20161458, 2016.
- [4] J. Salignon, M. Richard, E. Fulcrand, H. Duplus-Bottin, and G. Yvert. Genomics of cellular proliferation in periodic environmental fluctuations. *Mol. Syst. Biol.*, **14**: e7823, 2018.
- [5] S. Boyer, L. Hérissant, and G. Sherlock. Adaptation is influenced by the complexity of environmental change during evolution in a dynamic environment. *PLoS Genet.*, **17**: e1009314, 2021.
- [6] N. Takahata, K. Ishii, and H. Matsuda. Effect of temporal fluctuation of selection coefficient on gene frequency in a population. *Proc. Natl. Acad. Sci. USA*, **72**: 4541-4545, 1975.
- [7] J. H. Gillespie. Substitution processes in molecular evolution. I. Uniform and clustered substitutions in a haploid model. *Genetics*, **134**: 971-981, 1993.
- [8] M. Assaf, A. Kamenev, and B. Meerson. Population extinction in a time-modulated environment. *Phys. Rev. E*, **78**: 041123, 2008.
- [9] V. Mustonen and M. Lässig. Molecular evolution under fitness fluctuations. *Phys. Rev. Lett.*, **100**: 108101, 2008.
- [10] H. Uecker and J. Hermisson. On the fixation process of a beneficial mutation in a variable environment. *Genetics*, **188**: 915-930, 2011.

-
- [11] D. Waxman. A unified treatment of the probability of fixation when population size and the strength of selection change over time. *Genetics*, **188**: 907-913.
- [12] S. Peischl and M. Kirkpatrick. Establishment of new mutations in changing environments. *Genetics*, **191**: 895-906, 2012.
- [13] I. Cvijović, B. H. Good, E. R. Jerison, and M. M. Desai. Fate of a mutation in a fluctuating environment. *Proc. Natl. Acad. Sci. USA*, **112**: E5021-E5028, 2015.
- [14] A. M. Dean, C. Lehman, and X. Yi. Fluctuating selection in the Moran. *Genetics*, **205**: 1271-1283, 2017.
- [15] J. B. S. Haldane. A mathematical theory of natural and artificial selection, part v: selection and mutation. *Proc. Camb. Philos. Soc.*, **23**: 838-844, 1927.
- [16] M. Kimura. Some problems of stochastic processes in genetics. *Ann. Math. Statist.*, **28**: 882-901, 1957.
- [17] O. Mayo and R. Bürger. The evolution of dominance: a theory whose time has passed? *Biol. Rev. Camb. Philos. Soc.*, **72**: 97-110, 1997.
- [18] T. Nagylaki. *Introduction to Theoretical Population Genetics*. Springer-Verlag, Berlin, 1992.
- [19] M. M. Desai and D. S. Fisher. Beneficial mutation-selection balance and the effect of linkage on positive selection. *Genetics*, **176**: 1759-1798, 2007.
- [20] W. J. Ewens. *Mathematical Population Genetics*. Springer, Berlin, 2004.
- [21] K. Jain and A. Devi. Evolutionary dynamics and eigenspectrum of confluent Heun equation. *J. Phys. A: Math. Theor.*, **53**: 395602, 2020.
- [22] D. G. Kendall. On the generalized “birth-and-death” process. *Ann. Math. Statist.*, **19**: 1-15, 1948.
- [23] V. Mustonen and M. Lässig. Adaptations to fluctuating selection in *Drosophila*. *Proc. Natl. Acad. Sci. USA* **104**: 2277-2282, 2007.
- [24] F. Mafessoni and M. Lachmann. Selective strolls: fixation and extinction in diploids are slower for weakly selected mutations than for neutral ones. *Genetics*, **201**: 1581-1589, 2015.

-
- [25] H. A. Orr and A. J. Betancourt. Haldane's sieve and adaptation from the standing genetic variation. *Genetics*, **157**: 875-884, 2001.
- [26] B. Charlesworth, J. L. Campos, and B. C. Jackson. Faster-X evolution: Theory and evidence from *Drosophila*. *Molecular Ecology*, **27**: 3753-3771, 2018.

Chapter 3

Polygenic adaptation in changing environments

3.1 Introduction

In the previous Chapter, we investigated the evolution of a monogenic trait in a finite population due to a continually changing environment. Although many phenotypic traits are determined by a large number of genetic variants, how a polygenic trait adapts in response to the changes in the environment is still poorly understood. In the present Chapter, we study the adaptation dynamics of a polygenic trait that is determined by a finite number of genetic loci in an infinitely large population which is evolving under stabilizing selection and recurrent mutations.

Understanding phenotypic variation in terms of the underlying genetic variation is one of the central problems in biological evolution [1]. During the last decade, genome-wide association studies (GWAS) [2] have provided valuable insights into the genetic architecture of phenotypic traits, and the information about the number of genetic variants that affect a phenotype, the size of their effects and their relative frequency is becoming increasingly available [3]. In some cases such as industrial melanism in peppered moth [4], a phenotypic trait is determined by one or few genes. But many phenotypic traits ranging from crop yield and human height to complex diseases are polygenic as they are influenced by a large number of genetic variants. It has been suggested that such quantitative traits may even be omnigenic, determined by all the genes due to the interconnectedness of gene networks [5, 6]. The effect sizes of these genetic variants may be large or small, and the proportions in which they occur in a trait is governed by evolutionary forces such as selection [3].

For several decades, the infinitesimal model [7, 8] has served as workhorse for describing polygenic adaptation [9]. In this model, an infinite number of genetic loci each with an infinitesimal effect underlie a phenotypic trait. More precisely, the effect size is assumed to decrease with increasing number of loci which results in a genetic variance that remains constant in time in accordance with some phenotypic data [10] and renders the problem analytically tractable. However, the effect sizes can be finite, and genetic variance can change, at least, over some time scales.

Recently a model of polygenic adaptation was introduced [11] in which the phenotypic trait evolves under the action of stabilizing selection and mutations. A large but finite number of loci contribute to the trait, and the effect sizes which may be large or small are different at different loci. It is important to note that in [11], an effect size is large or small relative to a scaled mutation rate (defined later) and, unlike in the infinitesimal model, does not depend on the number of loci under selection.

In this Chapter, we study the adaptation dynamics within the framework of the model in [11] when the phenotypic optimum moves due to a change in the environment. The scenario in which the phenotypic optimum shifts suddenly because of, say, a natural disaster was recently studied and an analytical method was developed to take the changes in the genetic variance into account [12, 13]; here we consider the case when the phenotypic optimum moves gradually as a result of, for example, climate or societal change [14]. Adaptation in the face of moving phenotypic optimum has been previously investigated within infinitesimal model ignoring mutations and changes in the genetic variance [15, 16]. Here we find that the adaptation dynamics are strongly affected by mutations and the number of loci under selection when the effect sizes are small, and mediated by large transient changes in the genetic variance when the effect sizes are large.

3.2 Models

We study the evolution of a single quantitative trait in an infinitely large population of diploids. The phenotypic trait value z is determined by ℓ diallelic genetic loci, each of which contributes to the phenotype in an additive fashion. If the \pm allele at the i th locus has an effect $\pm\gamma_i/2$ on the trait, the mean phenotypic trait averaged over the population can be written as

$$c_1 = 2 \sum_{i=1}^{\ell} \left(\frac{\gamma_i}{2} \right) p_i + \left(\frac{-\gamma_i}{2} \right) q_i , \quad (3.1)$$

where p_i and $q_i = 1 - p_i$, respectively, denote the frequency of + and - allele at the i th locus in the population. In the following, the effect sizes are chosen independently from an exponential distribution with mean $\bar{\gamma}$, as suggested by quantitative-genetic studies [17].

We consider the situation when the allele frequencies and phenotypic properties evolve due to stabilizing selection and recurrent mutations. The fitness of a phenotypic trait under stabilizing selection is maximum at an optimum phenotypic value z_f which, in general, may vary with time (see below); away from the optimum, the fitness decreases quadratically, $w(z) = 1 - (s/2)(z - z_f)^2$ where $0 < s < 1$ is the strength of selection. Mutations generate variation and here, the + and - alleles mutate to each other at rate μ . We also assume that recombination occurs faster than selection and therefore the inter-loci correlations can be ignored (linkage equilibrium) [18]. Then it can be shown that the allele frequency p_i evolves according to [11]

$$\dot{p}_i = -s\gamma_i(c_1 - z_f)p_iq_i - \frac{s\gamma_i^2}{2}p_iq_i(q_i - p_i) + \mu(q_i - p_i) , \quad (3.2)$$

where dot denotes the derivative with respect to time. In the above equation, the first term on the right-hand side (RHS) that depends on the frequency of *all* the loci acts to decrease the deviation between the mean trait and the phenotypic optimum, the second term tends to fix one of the alleles thus depleting the genetic variation while the third term compensates for the loss in diversity through mutations.

In the stationary state where $\dot{p}_i = 0$, if the deviation between the mean trait and phenotypic optimum is zero, the stable solutions for the equilibrium allele frequencies are given by [11]

$$p_i^* = \begin{cases} \frac{1}{2} & , \gamma_i < \hat{\gamma} \\ \frac{1}{2} \pm \frac{1}{2}\sqrt{1 - \frac{\hat{\gamma}^2}{\gamma_i^2}} & , \gamma_i > \hat{\gamma} , \end{cases} \quad (3.3)$$

where $\hat{\gamma} = \sqrt{8\mu/s}$. Thus when the effect size is smaller than the threshold effect $\hat{\gamma}$, both the alleles are present in the population whereas for larger effect sizes, one of the alleles is close to fixation. The steady state deviation in the mean trait from its optimum need not be zero and can be estimated by approximating the effect size of all the loci by the average effect $\bar{\gamma}$. From (3.2) in the steady state, we then find the mean equilibrium trait to be $c_1^*/z_f \approx [1 + 4\mu(s\bar{\gamma}^2)^{-1}]^{-1}$.

In this Chapter, we are interested in the dynamics of the mean trait when the phenotypic optimum moves to a new value. From (3.2) for the allele frequency, it can be

shown that the time evolution equation for the mean trait depends on the variance and skewness of the phenotypic trait and, in general, the dynamics of a trait cumulant depend on two higher cumulants [19]. This cumulant hierarchy makes it difficult to obtain analytical results for the dynamics. However, recent work [20, 12] has established that the bulk of the adaptation process is driven by the deviation between the mean trait and the phenotypic optimum. Thus, at short times, it is a good approximation to retain only the first term on the RHS of (3.2); this yields the *directional selection model* in which [12]

$$\dot{p}_i \approx -s\gamma_i(c_1 - z_f)p_iq_i, \quad i = 1, \dots, \ell. \quad (3.4)$$

The above equation shows that the mean trait evolves as

$$\dot{c}_1 = -sc_2(c_1 - z_f), \quad (3.5)$$

where the genetic variance $c_2 = 2\sum_{i=1}^{\ell}\gamma_i^2p_iq_i$. If the genetic variance in (3.5) remains constant in time, we arrive at the Lande's equation for the evolution of the mean trait [21] which is obviously solvable. But even for time-dependent c_2 and other trait cumulants, the directional selection model is analytically tractable as briefly described below [12]. We first note that for any two loci k and j ,

$$\frac{dp_j}{\gamma_j p_j q_j} = \frac{dp_k}{\gamma_k p_k q_k} = -s(c_1 - z_f)dt. \quad (3.6)$$

From the first equality, we find that the allele frequency at the j th locus can be expressed in terms of its initial frequency and that at the k th locus,

$$p_j(t) = 1 - \frac{1}{1 + \frac{p_j(0)}{q_j(0)} \left(\frac{p_k(t)q_k(0)}{p_k(0)q_k(t)} \right)^{\gamma_j/\gamma_k}}. \quad (3.7)$$

Using this in (3.1), one can write the mean phenotypic trait as

$$c_1 = \sum_{i=1}^{\ell}\gamma_i - \sum_{i=1}^{\ell} \frac{2\gamma_i}{1 + \frac{p_i(0)}{q_i(0)} e^{\beta\gamma_i/\bar{\gamma}}}, \quad (3.8)$$

where

$$\beta(t) = \frac{\bar{\gamma}}{\gamma_k} \ln \left(\frac{p_k(t)q_k(0)}{p_k(0)q_k(t)} \right) \quad (3.9)$$

is locus-independent and, due to (3.4), evolves as

$$\dot{\beta} = -s\bar{\gamma}(c_1 - z_f) . \quad (3.10)$$

Equations (3.8) and (3.10) together yield a closed equation for the mean trait.

3.3 Results

We start with a population equilibrated to the phenotypic optimum at z_0 . The phenotypic optimum moves linearly until a time τ when it reaches $z_\tau > z_0$ where it stays for later times. Thus the new phenotypic optimum $z_f(t) = z_0 + vt, t < \tau$ where the velocity $v = (z_\tau - z_0)/\tau$. Here, $|z_0|, |z_\tau| < \ell\bar{\gamma}$ as the mean trait is bounded for finite ℓ . Our goal is to understand how the population adapts while the environment is changing. In the following, all the numerical data are obtained for a single realisation of effects as the quantities of interest are expected to be self-averaging [12].

3.3.1 When most effects are small ($\bar{\gamma} \ll \hat{\gamma}$)

Figure 3.1 shows that for linearly moving phenotypic optimum, the mean trait also increases linearly with time at a speed that decreases as the number of loci determining a trait decrease. However, the genetic variance c_2 (shown in the inset) remains close to its stationary value $c_2^* \approx \ell\bar{\gamma}^2$ [11] until time τ and then decreases to the stationary genetic variance corresponding to the equilibrium mean trait c_1^* [12]. For the parameters in Fig. 3.1, we expect c_1^*/z_τ to be 0.24, 0.39, 0.56 (see the discussion following (3.3)) which is close to $c_1(\tau)/z_\tau = 0.33, 0.47, 0.62$ for $\ell = 50, 100$ and 200, respectively. For this reason, the mean trait does not change substantially when the phenotypic optimum stops moving.

For $t \ll \tau$ where the genetic variance is approximately constant, (3.5) for the evolution of mean trait simplifies to $\dot{c}_1(t) \approx sc_2^*(z_f(t) - c_1(t))$ which can be readily integrated to yield

$$c_1(t) = z_0 + vt - \frac{v}{sc_2^*}(1 - e^{-sc_2^*t}) , \quad t < \tau , \quad (3.11)$$

and shows that the mean trait always lags behind the moving phenotypic optimum. At short times ($\ll (sc_2^*)^{-1}$), the mean trait increases quadratically. But at longer times, c_1 increases linearly with speed v and the lag $z_f(t) - c_1(v, t)$ reaches a constant value $v/(sc_2^*)$. This result has also been obtained in infinitesimal model [15, 16] in which

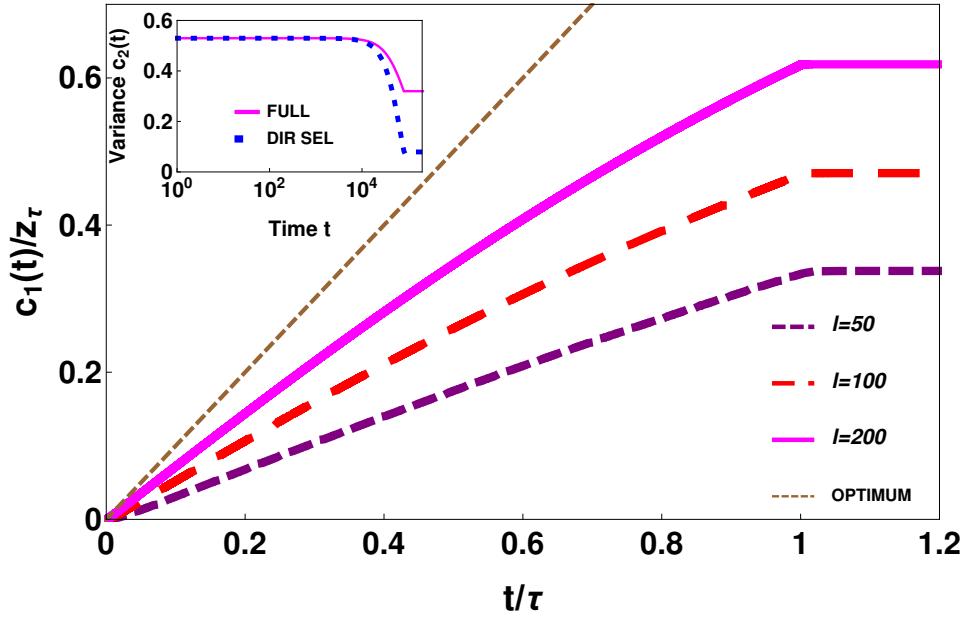


Fig. 3.1 Evolution of mean trait (main) in the full model when most effects are small ($\bar{\gamma} = 0.05 \ll \hat{\gamma} \approx 0.89$) and the phenotypic optimum moves with a constant speed $v = 10^{-4}$ for various ℓ . Here $s = 10^{-2}$, $\mu = 10^{-3}$, $z_0 = 0$ and $z_\tau = 0.8\ell\bar{\gamma}$. The phenotypic optimum $z_f(t)/z_\tau$ is also shown for comparison. The inset shows the evolution of genetic variance for $\ell = 200$.

an infinite number of loci, each with an infinitesimal effect ($\sim \ell^{-1/2}$), contribute to a phenotypic trait and the mean trait keeps increasing in an unbounded fashion; here, as a finite number of loci contribute to the trait, the linear behaviour of the mean trait sets in at a time $\sim \ell^{-1}$ and continues until the time τ .

Figure 3.2 shows that for $(sc_2^*)^{-1} \ll t \ll \tau$, the lag is constant in the directional selection model and matches the prediction (3.11) but it keeps increasing linearly with time in the full model. To understand this behavior, we note that at short times, by virtue of (3.3), the allele frequencies are close to one half, and therefore, the last two terms on the RHS of (3.2) can be ignored [12]. Indeed, as Fig. 3.2 shows, the full model and the directional model are in good agreement at short times. But at longer times, the allele frequencies are not in equilibrium and for $z_\tau > z_0$, as is assumed here, the frequency of the + allele increases towards one. Moreover, when the effects are small, the mutation rate is large ($\mu > s\gamma_i^2/8$). These considerations suggest to modify the directional selection model (3.4) by adding the mutation term to it when the phenotypic optimum is moving. The mean trait then evolves according to

$$\dot{c}_1(t) \approx sc_2^*(z_f(t) - c_1(t)) - 2\mu c_1(t), \quad (3.12)$$

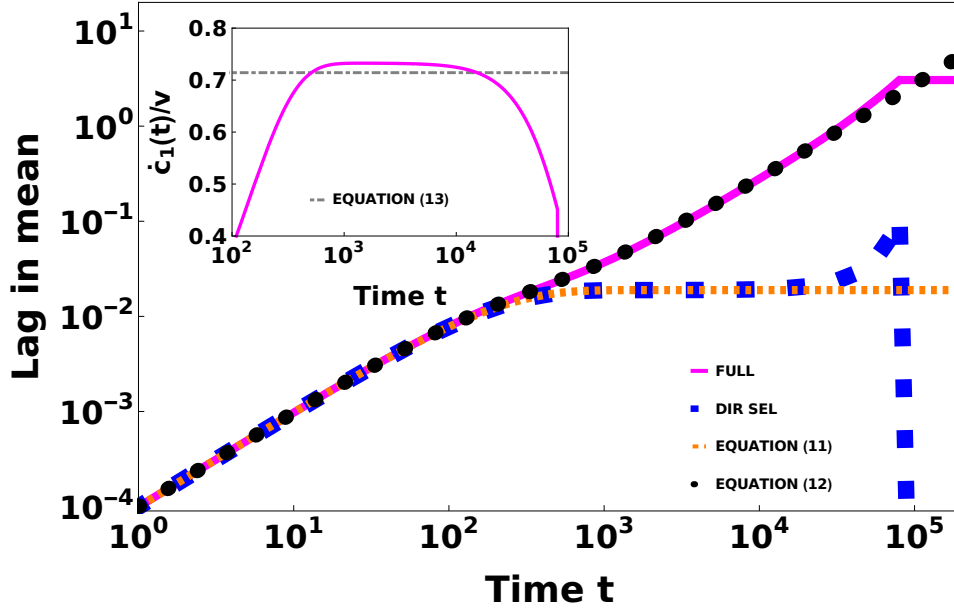


Fig. 3.2 Lag in mean when most effects are small (main). While the lag is constant in the directional selection model, it increases in the full model. This is because the mean trait moves slower than the phenotypic optimum (inset). Here $\ell = 200$ and rest of the parameters are the same as in Fig. 3.1.

which shows that at large times, the mean trait increases linearly as $c_1(t) = ut + \lambda$, $(sc_2^* + 2\mu)^{-1} < t < \tau$, where

$$u = \frac{v}{1 + 2\mu(sc_2^*)^{-1}} = \frac{v}{1 + \frac{1}{\ell} \left(\frac{\hat{\gamma}}{2\bar{\gamma}}\right)^2} \quad (3.13)$$

$$\lambda = \frac{z_0 - u(sc_2^*)^{-1}}{1 + 2\mu(sc_2^*)^{-1}}. \quad (3.14)$$

The inset of Fig. 3.2 shows that the rate of change of mean trait is in agreement with the speed u .

Equation (3.13) above makes two important points. First, the mean trait in the full model (3.2) increases *slower* than the phenotypic optimum with increasing mutation rates. At short times where the allele frequencies are close to their equilibrium value given by one half, mutations occurring at equal rate between the + and - allele do not affect the dynamics. But at larger times, as the + alleles become more abundant than the - alleles owing to selection, the net effect of the mutations is deleterious leading to an increased lag in the mean trait. Second, the speed of the mean trait increases with the number of loci under selection. When $\hat{\gamma}, \bar{\gamma}$ are of order one (as is the case here), the genetic variance is much larger than the mutations; this holds in the infinitesimal model

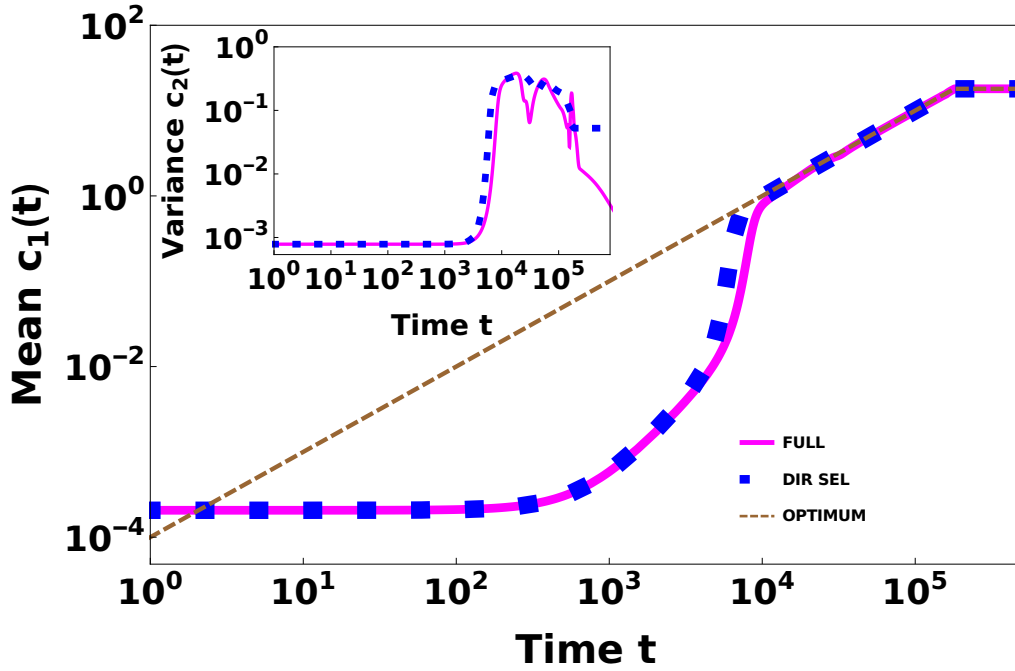


Fig. 3.3 Evolution of mean (main) and genetic variance (inset) when most effects are large ($\bar{\gamma} = 0.1 \gg \hat{\gamma} \approx 0.0028$) and the phenotypic optimum moves with a constant speed $v = 10^{-4}$. Here $\ell = 200$, $s = 10^{-2}$, $\mu = 10^{-8}$, $z_0 = 0$ and $z_\tau = 18$.

also where the mean effect decreases with ℓ keeping $\mu\ell$ finite. In either case, mutation is weaker than selection and may be neglected when $\ell \rightarrow \infty$. But for a finite number of loci, mutations also enter the picture and, as argued above, decrease the speed of the mean trait.

3.3.2 When most effects are large ($\bar{\gamma} \gg \hat{\gamma}$)

Since the mutations are unimportant when effect sizes are large, the directional selection model (3.4) describes the full model well (see Figs. 3.3 and 3.4). The inset of Fig. 3.3 shows that the genetic variance remains close to its equilibrium value $c_2^* = \ell\hat{\gamma}^2$ [11] for some time, rises quickly to $\tilde{c}_2 \sim 100c_2^*$ where it stays before finally dropping to c_2^* . As c_2^* is very small for the parameters in Fig. 3.3, due to (3.5), the mean trait remains close to z_0 initially and then increases before saturating to $c_1^* \approx z_\tau$. Since the genetic variance changes during the time intervals of interest, (3.5) for the mean trait evolution does not close, and therefore, we now work with (3.8) and (3.10).

As the equilibria are bistable for large effects (see (3.3)), a fraction f of the initial population carries + allele which is related to the initial phenotypic mean through $z_0 \approx$

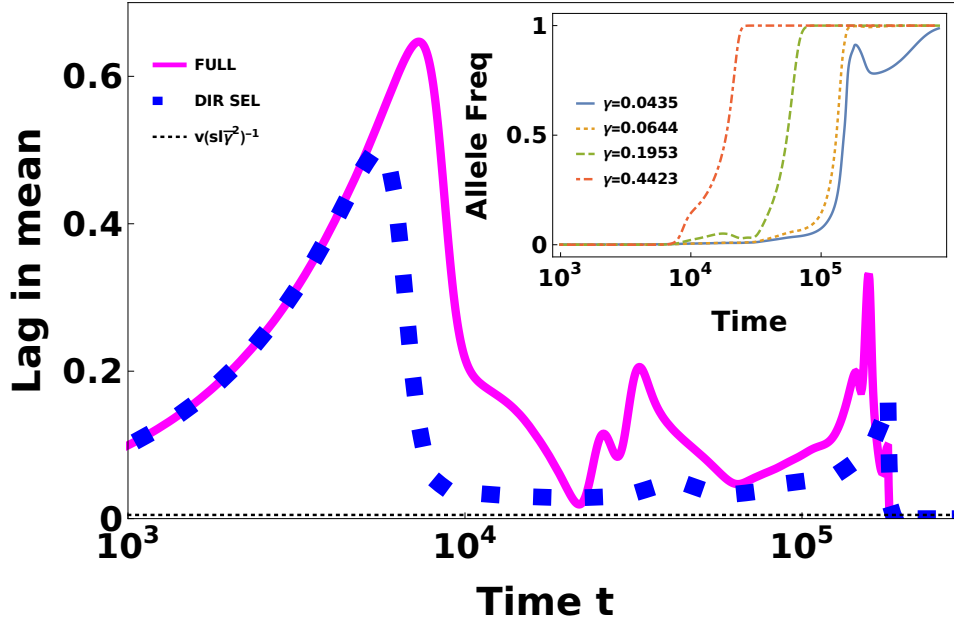


Fig. 3.4 Lag in mean (main) and allele frequency dynamics (inset) when most effects are large. All the parameters are the same as in Fig. 3.3.

$(2f - 1)\ell\bar{\gamma}$. We may therefore write the mean trait (3.8) as

$$c_1 = \sum_{i=1}^{\ell} \left(\gamma_i - \frac{2\gamma_i f}{1 + \frac{p_{i,+}^*}{q_{i,+}^*} e^{\beta\gamma_i/\bar{\gamma}}} - \frac{2\gamma_i(1-f)}{1 + \frac{p_{i,-}^*}{q_{i,-}^*} e^{\beta\gamma_i/\bar{\gamma}}} \right), \quad (3.15)$$

which, for large ℓ , simplifies to

$$\frac{c_1(t)}{\ell\bar{\gamma}} \approx 1 - \left(1 + \frac{z_0}{\ell\bar{\gamma}}\right) I_+(\beta) - \left(1 - \frac{z_0}{\ell\bar{\gamma}}\right) I_-(\beta), \quad (3.16)$$

where

$$I_{\pm}(\beta) = \int_{2/\alpha}^{\infty} dx \frac{x e^{-x}}{1 + (\alpha x)^{\pm 2} e^{\beta x}} \quad (3.17)$$

and $\alpha = 2\bar{\gamma}/\hat{\gamma} \gg 1$. Equation (3.16) generalises equation 24 of [12] where the initial phenotypic optimum is taken to be zero.

We first note that $\dot{\beta}, \beta \geq 0$ - the first assertion follows from the intuitive expectation that the lag must always be nonnegative and (3.10), and the second one on using $\beta(0) = 0$ (see (3.9)). Then it is easy to see that for large α , the integral $I_+ \rightarrow 0, I_- \rightarrow 1$. Neglecting I_+ in (3.16) and writing $I_- = \int_{2/\alpha}^{\infty} dx x e^{-x} - J_- \approx 1 - J_-$, we find that the parameter β evolves according to

$$\dot{\beta} \approx s\bar{\gamma}(\ell\bar{\gamma} - z_0) [\rho(t) - J_-(\beta)], \quad (3.18)$$

where

$$J_- = \int_{2/\alpha}^{\infty} dx \frac{x e^{-x}}{1 + (\alpha x)^2 e^{-\beta x}} \quad (3.19)$$

and $\rho(t) = vt/(\ell\bar{\gamma} - z_0)$. For $\beta \ll 1$, the integral $J_- \approx 0$ as it is heavily suppressed by the factor α^2 in the denominator of the integrand [12]. For $\beta \gg 1$, the integral J_- may be estimated by approximating the factor $(1 + (\alpha x)^2 e^{-\beta x})^{-1}$ in the integrand of J_- by a Heaviside theta function $\Theta(x - x_-)$ where $x_-(\beta)$ is a solution of $\alpha^2 x_-^2 e^{-\beta x_-} = 1$. We thus obtain $J_- \approx (1 + x_-)e^{-x_-}$, $\beta \gg 1$ [12].

We are now in a position to understand the behaviour of the mean trait given by

$$c_1(t) - z_0 = (\ell\bar{\gamma} - z_0)J_-(\beta) = vt - \frac{\dot{\beta}}{s\bar{\gamma}}, \quad (3.20)$$

where we have used (3.18) to express J_- in terms of $\dot{\beta}$. At short times ($t < \tau_0$), as the mean stays close to its initial value z_0 , the integral $J_- \approx 0$ and therefore $\beta(t) = (t/\tau_0)^2$ where $\tau_0 = \sqrt{2/(sv\bar{\gamma})}$. After time τ_0 , there is a large increase in the genetic variance and the mean trait starts evolving. Note that if the genetic variance was held constant at its initial value, as in the infinitesimal model, the mean trait will stay at z_0 and the population can not adapt.

When we consider the sudden shift with the same phenotypic optimum value as the maximum value z_τ in linearly moving optimum, the steady-state allele frequencies are same in both cases since the phenotypic distribution stabilizes to the same optimum. However, the dynamics of allele frequencies differ in these two models since the selection pressure changes differently with time. The initial selection pressure is high in a sudden shift in optimum, and therefore, the dynamics are faster in this case as compared to the slowly moving optimum. When the trait consists of mostly large effects loci, the adaptation mainly occurs through the sweeps, but many polymorphic loci contribute when the trait consists of mostly small effects loci irrespective of the sudden or moving optimum models. A criterion for short-time sweeps in the sudden shift model has been obtained by Jain and Stephan (2017) [12], whereas, loci with effect sizes larger than the average effect of loci sweep faster to reduce the lag between the mean and the optimum in moving optimum model. In the time interval $(s\tilde{c}_2)^{-1} < t < \tau$ where the mean trait increases linearly, the genetic variance $\tilde{c}_2 \gg c_2^*$ remains roughly constant. To estimate \tilde{c}_2 , we note from the inset of Fig. 3.4 that the allele frequencies at loci with effect size larger than $\bar{\gamma}$ sweep to fixation much earlier than at loci with smaller effect sizes. For the set of effects used in Fig. 3.4, the allele frequencies at 3 loci with effect size ≈ 0.4 swept

to fixation while nearly 30 selective sweeps occurred when the optimum was shifted suddenly to z_τ (data not shown). Large changes in allele frequency at many loci in the latter case are consistent with the fact that the population adapts exponentially fast over a short time scale (that decreases with ℓ) when the optimum shifts suddenly [12]; here the mean deviation changes slowly over a time of order ℓ and besides a few sweeps, many small frequency shifts (~ 0.1) also occur. While the selective sweep is in progress at loci with very large effects, the genetic variance rises to $\tilde{c}_2 \sim \ell \int_{\hat{\gamma}}^{\infty} d\gamma \gamma^2 p(\gamma) \sim \ell \bar{\gamma}^2$. Then replacing c_2^* by \tilde{c}_2 in (3.13) and using that $\hat{\gamma} \ll \bar{\gamma}$ when effects are large, it follows that, as in the infinitesimal model, the mean trait increases with speed v and lag $v/(s\tilde{c}_2)$.

We now perform a more careful analysis of the lag in the mean. The above discussion shows that the lag $\dot{\beta}/s\bar{\gamma}$ (second equality in (3.20)) is small for $\ell \gg 1$. Therefore, to a first approximation, we may write $\rho(t) \approx J_-(\beta)$ in (3.18) which yields

$$x_-(t) = -1 - W_{-1}\left(-\frac{\rho(t)}{e}\right), \quad (3.21)$$

where $W_{-1}(x)$ is the lower branch of the Lambert W function [22]. Using $\beta = (2/x_-) \ln(\alpha x_-)$, we find that

$$\dot{\beta} = \frac{2}{t} \frac{W_{-1}(-\rho/e)}{[1 + W_{-1}(-\rho/e)]^3} \ln\left(\frac{1 + W_{-1}(-\rho/e)}{-e/\alpha}\right). \quad (3.22)$$

For $t \ll \tau$ where $\rho/e \ll 1$, the function $W_{-1}(-\rho/e) \approx \ln(\rho/e) \sim \ln t$ [22] so that $\dot{\beta} \sim t^{-1}$. Thus when most effects are large, the mean trait moves with speed v but the lag between the mean trait and phenotypic optimum is not a constant. Although the lag $\sim (s\bar{\gamma}t)^{-1}$ decays rapidly with time, it is larger than that obtained within the infinitesimal model for a polymorphic population since the above discussion is valid for $t < \tau$, see Fig. 3.4. Furthermore, (3.5) and (3.10) show that the genetic variance $c_2(t) = (sv\bar{\gamma} - \ddot{\beta})/(s^2\bar{\gamma}z_0 + s\dot{\beta})$ which on using the above results for β yields $c_2(t) \sim v\bar{\gamma}t$. Thus, on time scales of order τ , we obtain the genetic variance to be \tilde{c}_2 in agreement with the argument above. Since the genetic variance increases from c_2^* to \tilde{c}_2 , for fixed $\hat{\gamma}, \bar{\gamma}$, a large change in variance occurs with increasing ℓ . But the change in variance is smaller if the mean effect and the threshold effect are not substantially different (see Fig. 3.5).

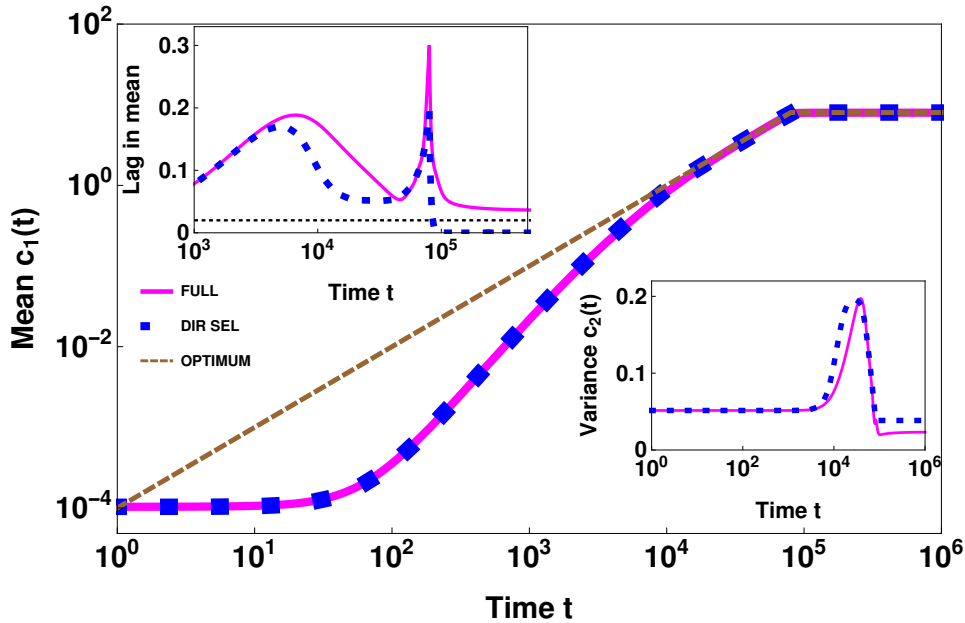


Fig. 3.5 Evolution of mean (main), lag in mean (top left inset) and genetic variance (bottom right inset) when equal number of effects are small and large ($\bar{\gamma} = 0.05$, $\hat{\gamma} \approx 0.028$) and the phenotypic optimum moves with a constant speed $v = 10^{-4}$. Here $\ell = 200$, $s = 10^{-2}$, $\mu = 10^{-6}$, $z_0 = 0$ and $z_\tau = 8$. The dotted line in the inset is the minimum lag $v(s\ell\bar{\gamma}^2)^{-1}$.

3.4 Summary and open questions

While stabilizing selection has the tendency to pull the population towards the phenotypic optimum, recurrent mutations create variants that push the population away from it. The behaviour of the mean trait in the large-effects case where selection is the dominant process resembles that in the infinitesimal model as the mean trait moves with the speed of the phenotypic optimum, while in the small-effects case where mutation rates are large, the mean trait moves slower than the phenotypic optimum. However, in the latter case, as the number of genetic loci affecting a trait increases, selection dominates over mutations and the speed of the mean trait approaches that of the phenotypic optimum (also, see the discussion after (3.14)).

In the large-effects case as the initial variance is small, the mean trait stays close to its initial value resulting in large deviation from the moving phenotypic optimum. But this causes the allele frequencies to change in a manner that increases the genetic variance thus paving the way for adaptation. On the other hand, when most effects are small, there is sufficient initial genetic variance for adaptation to proceed keeping genetic variance constant.

Equation (3.13) gives the formula of the speed of the mean trait and how the speed depends upon various genetic parameters. We believe that if experiments can be conducted to observe the lag between the mean trait and the phenotypic optimum, one can get an idea of the underlying genetics of the trait using our results.

In the last section, we studied two limiting cases of the genetic architecture, *viz.*, when $\bar{\gamma}/\hat{\gamma}$ is much smaller or larger than unity. Figure 3.5 shows that when both small and large effect sizes constitute a phenotypic trait, the behaviour of the mean trait is closer to the mostly large-effects case, possibly because the contribution of the small effect sizes to the mean trait increases slower than that of the large-effects loci. Thus, we conclude that, in general, the lag between mean trait and phenotypic optimum exceeds that predicted by the infinitesimal model for a polymorphic population [15, 16].

Although the study presented here goes beyond the standard quantitative-genetic theory [15, 16] by accounting for mutations and temporal changes in genetic variance, this work also has some limitations - we have neglected the effect of epistasis in the genotype-phenotype map, pleiotropic effects of other phenotypic traits and, perhaps most importantly, the finiteness of the population size. The effect of stochastic fluctuations on the speed of adaptation and extinction risk has been addressed in recent work [23, 24] when the genetic variance remains constant. Extending the results presented here to finite populations is desirable and we plan to address this in a future work.

Bibliography

- [1] N. H. Barton and P. D. Keightley. Understanding quantitative genetic variation. *Nat. Rev. Genet.*, **3**: 11-21, 2002.
- [2] P. M. Visscher, M. A. Brown, M. I. McCarthy, and J. Yang. Five years of GWAS discovery. *Am. J. Hum. Genet.*, **90**: 7-24, 2012.
- [3] N. J. Timpson, C. M. T. Greenwood, N. Soranzo, D. J. Lawson, and J. B. Richards. Genetic architecture: the shape of the genetic contribution to human traits and disease. *Nat. Rev. Genet.*, **19**: 110-124, 2018.
- [4] A. E. van't Hof, N. Edmonds, M. Dalíková, F. Marec, and I. J. Saccheri. Industrial melanism in British peppered moths has a singular and recent mutational origin. *Science*, **332**: 958-960, 2011.
- [5] E. A. Boyle, Y. I. Li, and J. K. Pritchard. An expanded view of complex traits: from polygenic to omnigenic. *Cell*, **169**: 1177-1186, 2017.
- [6] N. R. Wray, C. Wijmenga, P. F. Sullivan, J. Yang, P. M. Visscher. Common disease is more complex than implied by the core gene omnigenic model. *Cell*, **173**: 1573-1580, 2018.
- [7] R. A. Fisher. The correlation between relatives on the supposition of Mendelian inheritance. *Trans. R. Soc. Edinburgh*, **52**: 399-433, 1918.
- [8] M. G. Bulmer. *The Mathematical Theory of Quantitative Genetics*. Oxford University Press, Oxford, 1980.
- [9] M. Kopp and S. Matuszewski. Rapid evolution of quantitative traits: theoretical perspectives. *Evol. Appl.*, **7**: 169-191, 2014.
- [10] R. Lande. Natural selection and random genetic drift in phenotypic evolution. *Evolution*, **30**: 314-334, 1976.

-
- [11] H. P. de Vladar and N. H. Barton. Stability and response of polygenic traits to stabilizing selection and mutation. *Genetics*, **197**: 749-767, 2014.
- [12] K. Jain and W. Stephan. Rapid adaptation of a polygenic trait after a sudden environmental shift. *Genetics*, **206**: 389-406, 2017.
- [13] K. Jain and W. Stephan. Modes of rapid polygenic adaptation. *Mol. Biol. Evol.*, **34**: 3169-3175, 2017.
- [14] J. S. Sanjak, J. Sidorenko, M. R. Robinson, K. R. Thornton and P. M. Visscher. Evidence of directional and stabilizing selection in contemporary humans. *Proc. Natl. Acad. Sci. USA*, **115**: 151-156, 2018.
- [15] M. Lynch and R. Lande. in *Biotic Interactions and Global Change*, edited by P. M. Kareiva, J. G. Kingsolver, and R. B. Huey (Sinauer Associates, Sunderland, Mass.), pp. 234-250, 1993.
- [16] R. Bürger and M. Lynch. Evolution and extinction in a changing environment: a quantitative-genetic analysis. *Evolution*, **49**: 151-163, 1995.
- [17] T. F. C. Mackay. The genetic architecture of quantitative traits: lessons from *Drosophila*. *Curr. Opin. Genet. Dev.*, **14**: 253-257, 2004.
- [18] N. H. Barton and M. Turelli. Natural and sexual selection on many loci. *Genetics*, **127**: 229-255, 1991.
- [19] R. Bürger. *The Mathematical Theory of Selection, Recombination, and Mutation*. Wiley, Chichester, 2000.
- [20] K. Jain and W. Stephan. Response of polygenic traits under stabilizing selection and mutation when loci have unequal effects. *G3: Genes Genomes Genet.*, **5**: 1065-1076, 2015.
- [21] R. Lande. The response to selection on major and minor mutations affecting a metrical trait. *Heredity*, **50**: 47-65, 1983.
- [22] R. M. Corless, G. H. Gonnet, D. E. G. Hare, D. J. Jeffrey, and D. E. Knuth. On the LambertW function. *Adv. Comput. Math.*, **5**: 329-359, 1996.
- [23] A. G. Jones, S. J. Arnold, and R. Bürger. Evolution and stability of the G-Matrix on a landscape with a moving optimum. *Evolution*, **58**: 1639-1654.

-
- [24] S. Matuszewski, J. Hermisson, and M. Kopp. Catch me if you can: adaptation from Standing genetic variation to a moving phenotypic optimum. *Genetics*, **200**: 1255-1274, 2015.

Chapter 4

Evolutionary dynamics and eigenspectrum of confluent Heun equation

4.1 Introduction

In the last two Chapters, we studied the dynamics of adaptation of a trait in changing environments. Since the stochastic dynamics, even in a single sudden change in environment, are not well-studied, we focus on understanding the evolutionary process of a monogenic trait in a finite population under constant selection in the present Chapter.

Biological evolution has shaped the genetic diversity that we see today on earth [1, 2]. The basic processes that drive evolution include selection, mutation and random genetic drift. While selection decreases the genetic diversity, random mutations increase it. Besides these deterministic processes, stochasticity arising, for example, due to finite carrying capacity plays an important role in determining the evolutionary fate of a population. With growing interest in analyzing the time series data obtained from experiments or field studies [3, 4], and addressing fundamental questions about evolution in changing environments [5], it is important to understand the evolutionary dynamics of a population under the joint action of mutation, selection and genetic drift.

In the absence of selection, the dynamics are completely understood [6], as the Fokker-Planck equation for the distribution of allele frequency obeys the Gauss hypergeometric equation which has the nice property that its Frobenius series expansions lead to two-term recurrence relations for the expansion coefficients and for which the connection

formulae that connect its two local solutions are known [7]. But even in the simplest setting where only a single locus in a genome is under selection, the complete evolutionary dynamics are not explicitly known.

In this Chapter, we study the allele frequency distribution in a finite population in which a single, diallelic locus is under time-independent selection and mutations between the two alleles occur at equal rates. We find that the eigenfunctions of the Fokker-Planck equation for the frequency distribution obey the *confluent Heun equation* [8–10]. This equation has appeared in diverse physical contexts to describe the eigenspectrum of hydrogen molecule ion [11] and quantum Rabi model [12], quasi-normal modes of black holes [13, 14], relaxation dynamics of a polymer [15], etc. Heun equation and its confluent forms are an area of active interest in mathematics community also as the Heun functions generalize the well studied hypergeometric functions. The progress in understanding Heun functions has, however, been slow as Frobenius series or other orthogonal polynomial expansions of this class of equations lead to three-term recurrence relations for the expansion coefficients, and the connection formulae for the local solutions are not explicitly known [16].

For these reasons, here we study the eigenspectrum of the confluent Heun operator of interest, mainly, numerically. As the stationary state corresponding to the zero eigenvalue is exactly known [6], we will focus on the excited states and study them using an orthogonal polynomial expansion of the eigenfunctions. Such an expansion has previously been carried out in [17]; however, these authors obtained a five-term recurrence relation for the expansion coefficients and did not provide any insights into the solution. Here, we obtain a three-term recurrence equation and find that for strong selection, there is a *dynamic transition* as the relaxation time - which is inversely proportional to the eigenvalue for the first excited state - initially decreases with mutation rate and then becomes a constant at a finite mutation rate. We also show that the expansion coefficients have a scaling form which allows us to estimate the number of terms that contribute significantly to the orthogonal series for the eigenfunctions.

4.2 Model

We consider a haploid population of N individuals that evolves in time according to the standard Moran process [18]. In generation t , an individual is chosen to give birth with a probability equal to its fitness relative to that of the population while any individual (including the parent) can die with an equal probability. Thus, if the wild type individual

has a fitness 1 and the mutant's fitness is $1 + s$, the mutant produces a copy of itself with a probability $(1 + s)i/\bar{w}$ when i mutants are present in the population at time t , where $\bar{w}(t) = (1 + s)i + (N - i)$ is the average fitness of the population; similarly, the wild type individual replicates with a probability $(N - i)/\bar{w}$. After selection and reproduction, an offspring mutates to the other type with a probability u . Thus, the population evolves under the joint action of selection, mutation and random genetic drift.

We are interested in understanding the dynamics of the probability distribution of the mutant allele frequency, $p = i/N$ in the scaling limit of weak selection, weak mutation ($s, u \rightarrow 0$) and large population size ($N \rightarrow \infty$) with finite Ns, Nu . Using the mean and the variance of the change in the mutant frequency in the above scaling limits, one can show that the frequency distribution $\psi(p, \tau)$ obeys the following forward Fokker-Planck equation [6, 19],

$$\frac{\partial \psi}{\partial \tau} = -\frac{\partial J}{\partial p} = -\frac{\partial}{\partial p} \left[\sigma pq\psi + \mu(q - p)\psi - \frac{\partial}{\partial p} (pq\psi) \right], \quad (4.1)$$

where $q = 1 - p$ is the wild type frequency, $J(p, \tau)$ is the probability current, and $\tau = t/N, \mu = Nu, \sigma = Ns$ are the scaled time, mutation rate and selection rate, respectively. Below we will study the dynamics of the allele frequency distribution subject to the reflecting boundary conditions,

$$J(0, \tau) = J(1, \tau) = 0, \quad (4.2)$$

at all times.

Some comments are in order: in the following, we will assume that $s \geq 0$ since for $s < 0$, equation (4.1) is obeyed by the allele frequency q . While the Moran process described above assumes overlapping generations, the Wright-Fisher process for non-overlapping generation also obeys (4.1) when N is replaced by $2N$. Instead of the forward equation (4.1), one may study the corresponding backward equation [17]; however, the eigenspectrum of both equations is same [19]. For these reasons, it is sufficient to focus on the above forward equation (4.1).

We first write $\psi(p, \tau) = \sum_{\ell=0}^{\infty} A_{\ell} e^{-\lambda_{\ell} \tau} \phi_{\ell}(p)$ where the coefficient A_{ℓ} is determined by the initial condition $\psi(p, 0)$. From (4.1), we find that the time-independent eigenfunction $\phi_{\ell}(p)$ obeys the following eigenvalue equation,

$$-(\sigma pq\phi_{\ell} + \mu(q - p)\phi_{\ell})' + (pq\phi_{\ell})'' = -\lambda_{\ell}\phi_{\ell}, \quad (4.3)$$

where a prime denotes a derivative with respect to p . As the differential operator in (4.3) is of Sturm-Liouville form [20], we are guaranteed to have real eigenvalues and a complete set of orthonormal eigenfunctions for which

$$\int_0^1 dp \rho(p) \phi_\ell(p) \phi_{\ell'}(p) \propto \delta_{\ell, \ell'}, \quad (4.4)$$

where the weight function, $\rho(p) \propto \phi_0^{-1}$ (see below).

In equilibrium where the probability current J vanishes for all p , the probability distribution is given by [21, 6]

$$\phi_0(p) \propto (pq)^{\mu-1} e^{\sigma p}, \quad (4.5)$$

where the proportionality constant determined by (4.4) reduces to the normalization condition $\int_0^1 dp \phi_0(p) = 1$. For $\sigma = 0$, the above equilibrium distribution is U-shaped for $\mu < 1$ and bell-shaped for $\mu > 1$; however, for large σ , the stationary distribution $\phi_0(p)$ for the favored allele peaks close to $p = 1$.

4.3 Confluent Heun equation for the eigenfunctions

We will now focus on (4.3) which can be rewritten in the standard form as

$$\phi_\ell''(p) + \left(\frac{2-\mu}{p-1} + \frac{2-\mu}{p} - \sigma \right) \phi_\ell'(p) + \left(\frac{\nu_\ell}{p} + \frac{-2\sigma - \nu_\ell}{p-1} \right) \phi_\ell(p) = 0, \quad (4.6)$$

where $\nu_\ell = 2\mu - \sigma - 2 + \lambda_\ell$. Equation (4.6) is a (singly) confluent Heun equation which has regular singular points at $p = 0, 1$ and an irregular singularity of rank 1 at infinite p [8, 22, 10]. The following special cases of (4.6) are known [6]: for $\sigma = 0$ (no selection), (4.6) reduces to the Gauss hypergeometric equation which has regular singular points at zero, one and infinity, and for $\sigma = \mu = 0$ (only genetic drift), the eigenfunction ϕ_ℓ obeys the Gegenbauer equation. For nonzero selection but zero mutation rate, $V_\ell(z) = e^{-\sigma p/2} \phi_\ell(p)$ with $p = (1-z)/2$ obeys the oblate spheroidal equation [23]. However, except for the stationary state (4.5) corresponding to eigenvalue zero, neither the eigenvalue spectrum nor the eigenfunctions are known for the above confluent Heun differential operator.

The general solution of (4.6) can be expanded as a Frobenius series about $p = 0$ [24] which, on imposing the reflecting boundary condition (4.2) at $p = 0$ gives $\phi_\ell(p) =$

$p^{\mu-1}F_\ell(p)$ for $|p| < 1, \mu > 0$ where F_ℓ is an analytic function (see Appendix C.1). Due to the self-adjoint nature of the Heun operator, we can expand F_ℓ as a linear combination of suitable orthogonal functions [20]; a power series expansion of F_ℓ is given in Appendix C.1.

An orthogonal expansion of (4.6) with boundary conditions (4.2) has been carried out in [17] by writing the distribution function, $\phi_\ell(p) = \sum_n \hat{a}_n^{(\ell)} \hat{G}_n(p)$ where $\hat{G}_n = (pq)^{\mu-1} e^{\sigma p/2} P_n^{(\mu-1, \mu-1)}(1-2p)$ and $P_n^{(\alpha, \beta)}(x)$ denotes Jacobi polynomial of order n that obey the following orthogonality relation [25],

$$\int_{-1}^1 dx (1-x)^\alpha (1+x)^\beta P_n^{(\alpha, \beta)}(x) P_{n'}^{(\alpha, \beta)}(x) = h_n \delta_{n, n'}. \quad (4.7)$$

where h_n are given by 22.2.1 of [25]. The above \hat{G}_n has the property that they are orthogonal with respect to the same weight function as that for ϕ_ℓ , namely, ρ . But this choice leads to a five-term recursion relation for the coefficients $\hat{a}_n^{(\ell)}$ that are not amenable to analytical calculations.

Here, we write $\phi_\ell(p) = \sum_n a_n^{(\ell)} G_n$ with $G_n = (pq)^{\mu-1} P_n^{(\mu-1, \mu-1)}(1-2p)$ that, as can be verified using (4.7), are orthogonal with respect to the weight function $(pq)^{1-\mu}$. As detailed in Appendix C.2, our choice of the orthogonal basis leads to three-term recursion relations for $a_n^{(\ell)}$ (see also [15]), and we can write

$$\phi_\ell(p) = (pq)^{\mu-1} \sum_{n=1}^{\infty} c_n^{(\ell)} \frac{\Gamma(n)}{\Gamma(n+\mu-1)} P_{n-1}^{(\mu-1, \mu-1)}(1-2p), \quad (4.8)$$

which satisfies the boundary condition (4.2) at $p = 1$ also. The expansion coefficients $c_n^{(\ell)}$'s are determined recursively through the following equations,

$$\lambda_\ell c_1^{(\ell)} = 0, \quad (4.9)$$

$$T_-(n)c_{n-1}^{(\ell)} + T_0(n)c_n^{(\ell)} + T_+(n)c_{n+1}^{(\ell)} = -\lambda_\ell c_n^{(\ell)}, \quad n \geq 2, \quad (4.10)$$

where

$$T_-(n) = \frac{\sigma(2\mu+n-2)(2\mu+n-3)}{10-4\mu-4n} < 0, \quad (4.11)$$

$$T_+(n) = \frac{\sigma n(1-n)}{2-4\mu-4n} > 0, \quad (4.12)$$

$$T_0(n) = (1-n)(2\mu+n-2) < 0. \quad (4.13)$$

As already stated, the stationary state corresponding to $\lambda_0 = 0$ is given by (4.5) and it can be used to find the expansion coefficients $c_n^{(0)}$, as described in Appendix C.3. In the following, we are interested in excited states with nonzero eigenvalues; due to (4.9), this means that $c_1^{(\ell)} = 0$ for $\ell = 1, 2, \dots$. Furthermore, for large n , the ratio $r_n = c_{n+1}/c_n$ has following linearly independent solutions,

$$r_n^+ \sim \frac{4n}{\sigma}, \quad r_n^- \sim -\frac{\sigma}{4n} \quad (4.14)$$

for any ℓ . As the (minimal) solution r_n^- ensures the convergence of the continued fraction method for evaluating eigenvalues [26] (see also Sec. 4.4), we have the boundary condition that the expansion coefficients vanish at large n .

In summary, (4.10) along with boundary conditions $c_1^{(\ell)}, c_{K+2 \rightarrow \infty}^{(\ell)} = 0$ defines an eigenvalue problem, $\mathbf{T}\vec{c}^{(\ell)} = -\lambda_\ell \vec{c}^{(\ell)}$, $\ell \geq 1$ for eigenvector $\vec{c}^{(\ell)}$ and eigenvalue $-\lambda_\ell$ where \mathbf{T} is K -dimensional square matrix.

4.4 Eigenvalue problem: numerical analysis

For the ratio $r_n^{(\ell)}$, the recursion equation (4.10) can be written as

$$r_{n-1}^{(\ell)} = \frac{j_n}{k_n + r_n^{(\ell)}} = \frac{j_n}{k_n + \frac{j_{n+1}}{k_{n+1} + r_{n+1}^{(\ell)}}}, \quad (4.15)$$

where $j_n = -T_-(n)/T_+(n)$ and $k_n^{(\ell)} = (T_0(n) + \lambda_\ell)/T_+(n)$. Continuing in this manner, we have

$$r_2^{(\ell)} = \frac{j_3}{k_3^{(\ell)} + \frac{j_4}{k_4^{(\ell)} + \frac{j_5}{k_5^{(\ell)} + \dots}} = -k_2^{(\ell)}, \quad (4.16)$$

where we have used the boundary condition $c_1^{(\ell)} = 0$, $\ell > 0$. Starting from r_n^- in (4.14), the above continued fraction was used to calculate λ_ℓ and $r_n^{(\ell)}$ numerically [26], and we found the ratio $r_n^{(\ell)}$ to be negative for all n . From these ratios of expansion coefficients, the eigenfunction $\phi_\ell(p)$ was obtained by carrying out the sum over $K + 1$ terms in (4.8). One can also diagonalize matrix \mathbf{T} to find eigenvalues and eigenfunctions. To obtain numerical results, both these methods were applied to finite-dimensional matrix \mathbf{T} of large size K .

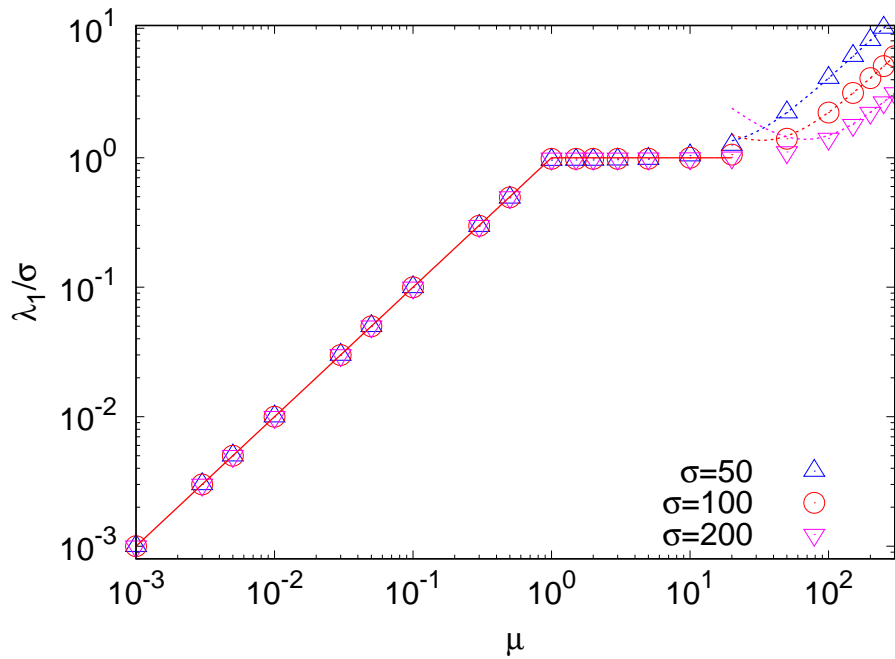


Fig. 4.1 Variation of eigenvalue λ_1 with mutation rate μ for various values of selection parameter σ and $K = 1000$. The points are obtained numerically using (4.10), and the solid and dotted lines show the conjecture (4.17) for strong selection and analytical expression (4.19) for weak selection, respectively.

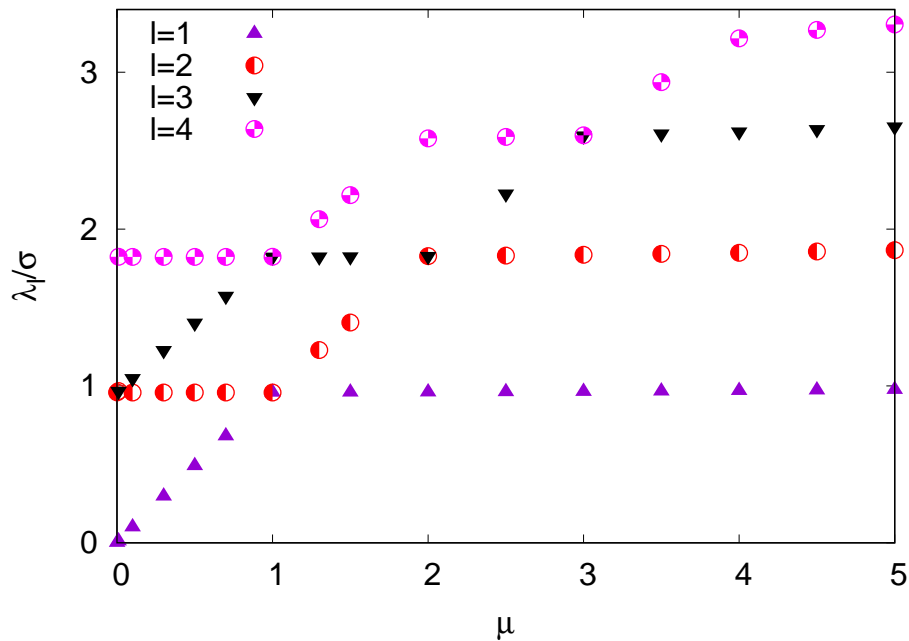


Fig. 4.2 Eigenvalue spectrum for strong selection obtained numerically using (4.10) for $\sigma = 50$ and $K = 1000$.

4.4.1 Eigenvalues

Figure 4.1 shows the numerical results for the eigenvalue λ_1 as a function of the mutation rate μ and large selection strengths. For $\mu \gg \sigma$ where selection is weak relative to mutation, the eigenvalue varies with μ essentially the same way as that in the absence of selection since, as discussed in Sec. 4.5, the correction to λ_1 due to selection is quadratic in σ/μ . But for $\mu \ll \sigma$, the eigenvalue increases linearly with σ (see Sec. 4.6), and our numerical results in Fig. 4.1 suggest that

$$\frac{\lambda_1}{\sigma} \xrightarrow{\sigma \rightarrow \infty} \begin{cases} \mu, & \mu \leq 1 \\ 1, & \mu > 1 \end{cases}. \quad (4.17)$$

We have also studied the corrections to the above conjectured eigenvalue, and find that they approach the asymptotic values as $1/\sigma$ (data not shown). The higher eigenvalues shown in Fig. 4.2 exhibit a more complex behavior. The eigenvalue λ_2 remains a constant for $\mu < 1$, increases linearly for $1 < \mu < 2$ and is a constant for $\mu \geq 2$; a similar pattern is seen for λ_3 and λ_4 .

4.4.2 Eigenfunctions

Figure 4.3 shows the numerical results for the eigenfunctions $\phi_1(p)$ and $\phi_2(p)$ for various values of σ and large K . As expected, the ℓ th excited state has ℓ nodes whose location depends on μ and σ . Other than this feature, the distribution is qualitatively similar to that in the stationary state given by (4.5). When selection is absent, the eigenfunctions are symmetric about $p = 1/2$ [6]; for this reason, the first excited state for small $\sigma \lesssim 1$ has a node close to one half. But for stronger selection, the eigenstate is highly asymmetric and as in the stationary state, the excited states also peak close to the allele frequency equal to one.

4.5 Weak selection limit

As the eigenvalues are known exactly for $\sigma = 0$ [6], we can use a perturbation theory to determine λ_ℓ 's for $\sigma \ll \mu$. On expanding the coefficient $c_n^{(\ell)}$ and eigenvalue λ_ℓ in a power series to quadratic orders in σ and substituting them in (4.10), we find that the zeroth order term in σ yields $\lambda_\ell(\sigma = 0) = \ell(2\mu + \ell - 1)$, $\ell = 0, 1, \dots$ [6]. The first order

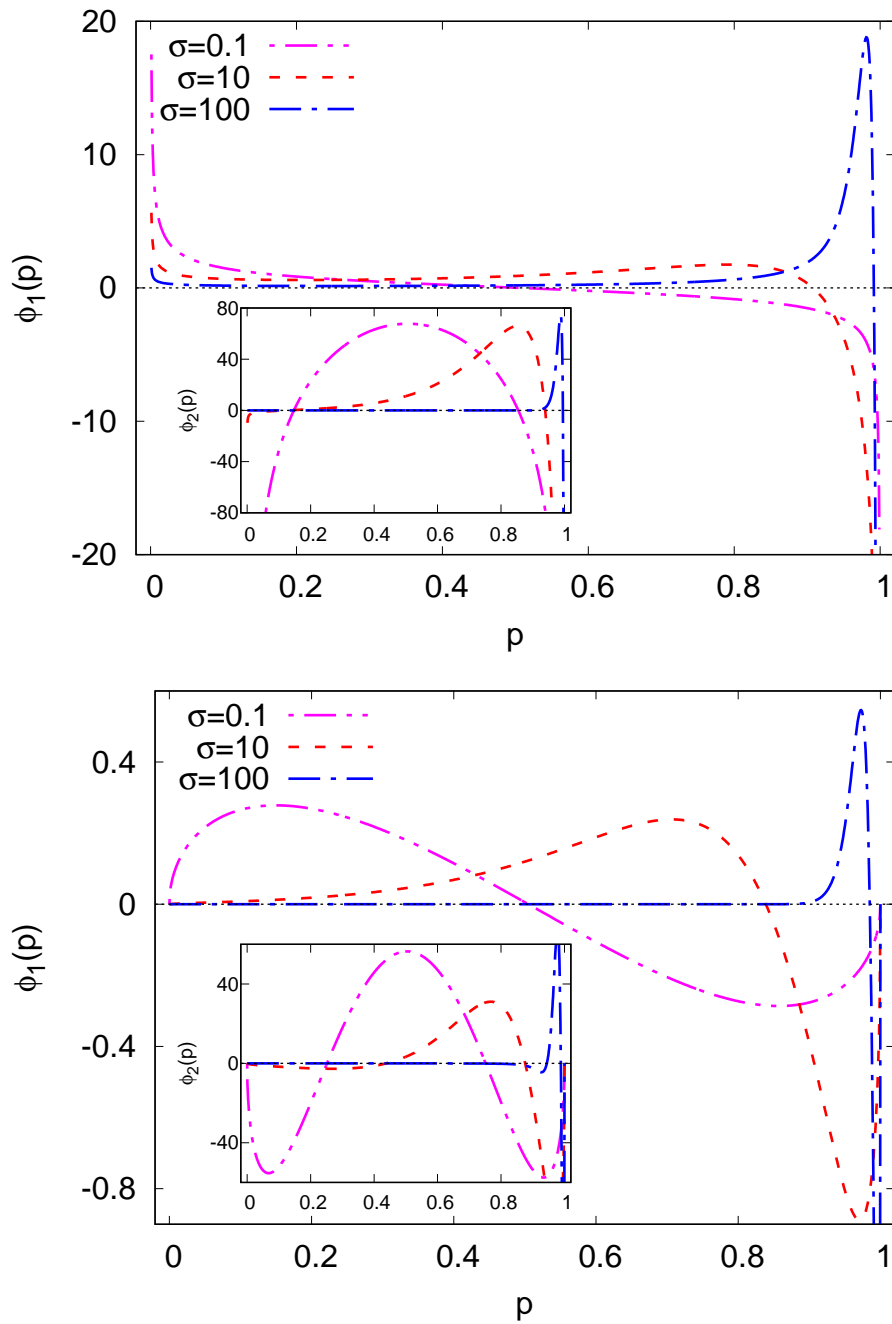


Fig. 4.3 First two excited states, $\phi_1(p)$ (main) and $\phi_2(p)$ (inset) obtained numerically using (4.8) and (4.10) for $\mu = 1/2$ (top panel) and $3/2$ (bottom panel), and $K = 1000$ for various selection strengths.

correction to the eigenvalue is found to be zero and the quadratic term in σ leads to

$$\lambda_\ell(\sigma) \approx \lambda_\ell(\sigma = 0) + \frac{T_+(\ell+1)T_-(\ell+2)}{T_0(\ell+2) - T_0(\ell+1)} + \frac{T_+(\ell)T_-(\ell+1)}{T_0(\ell) - T_0(\ell+1)}. \quad (4.18)$$

From the above expression, we obtain the eigenvalue for the first excited state to be

$$\lambda_1 \approx 2\mu + \frac{\sigma^2\mu}{(2\mu+2)(2\mu+3)}, \quad (4.19)$$

which is in good agreement with the numerical data in Fig. 4.1. Equation (4.18) also shows that as for $\sigma = 0$, the gap between the consecutive eigenvalues increases with index ℓ .

4.6 Strong selection limit

We now turn to the strong selection regime where $\sigma \gg \mu$. The coefficient $(T_0(n) + \lambda_\ell)/\sigma$ of $c_n^{(\ell)}$ in (4.10) shows that for $\sigma \rightarrow \infty$, a nontrivial eigenvalue for the excited states is obtained if λ_ℓ scales linearly with σ , in accordance with the numerical results shown in Fig. 4.1. One is then tempted to ignore the T_0 term altogether; however, as explained in Appendix C.4, this results in imaginary eigenvalues for any K . The correct limit procedure for strong selection is therefore to take $K \rightarrow \infty$ followed by $\sigma \rightarrow \infty$. In Sec. 4.6.1 and Sec. 4.6.2, we find the expansion coefficients for large and small n , respectively, for large, finite σ when $K \rightarrow \infty$. Our analysis, however, does not yield eigenvalues that were studied in Sec. 4.4 numerically.

4.6.1 Scaling form for the expansion coefficients

Although we have not been able to obtain the eigenvalues analytically, a simple but accurate approximation for the coefficients $c_n^{(\ell)}$, $n \gg 1$ for large σ can be obtained as follows. We again consider the coefficient $T_0(n) + \lambda_\ell$ of $c_n^{(\ell)}$: for large σ , $T_0 \sim n^2$ can be neglected in comparison to $\lambda_\ell \sim \sigma$ when $n \ll \sqrt{\sigma}$, and as a consequence, the expansion coefficient $c_n^{(\ell)}$ is independent of σ for small n . But the eigenvalue can be ignored for $n \gg \sqrt{\sigma}$ and we may expect a σ -dependence for $c_n^{(\ell)}$ when n is large. These observations suggest that for $\sigma \gg 1$, the coefficient $|c_n^{(\ell)}|$ is of a scaling form,

$$\frac{|c_n^{(\ell)}|}{|c_2^{(\ell)}|} = C_{\sigma,\mu} f_\ell \left(\frac{n}{\sqrt{\sigma}} \right), \quad (4.20)$$

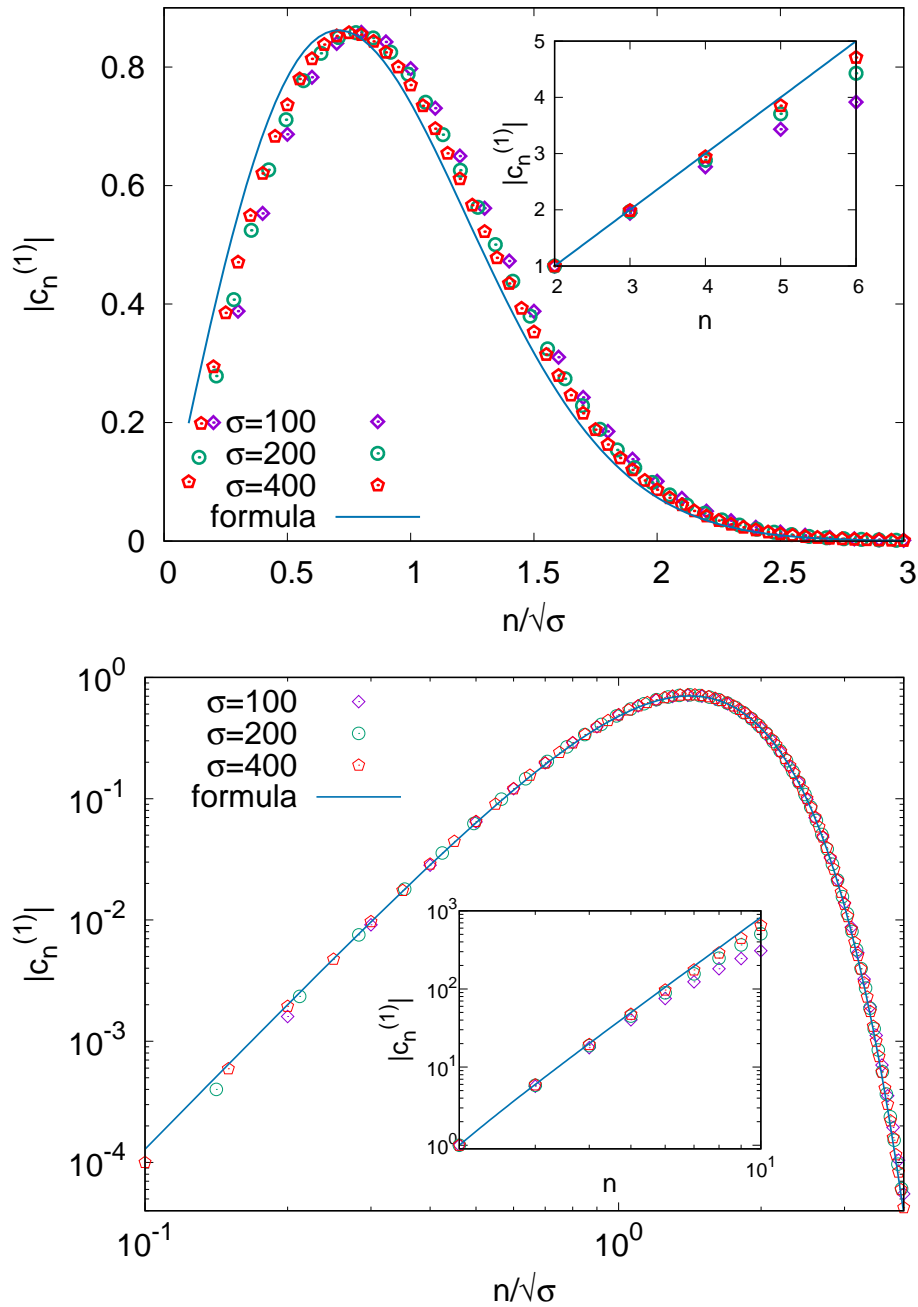


Fig. 4.4 Main: Expansion coefficient $|c_n^{(1)}|$ obtained numerically (points) for various σ and analytical expression (4.23) in scaling limit for $\mu = 1/2$ (top) and $3/2$ (bottom), and $K = 1000$. The inset shows the expansion coefficient for small n and is compared with (4.26).

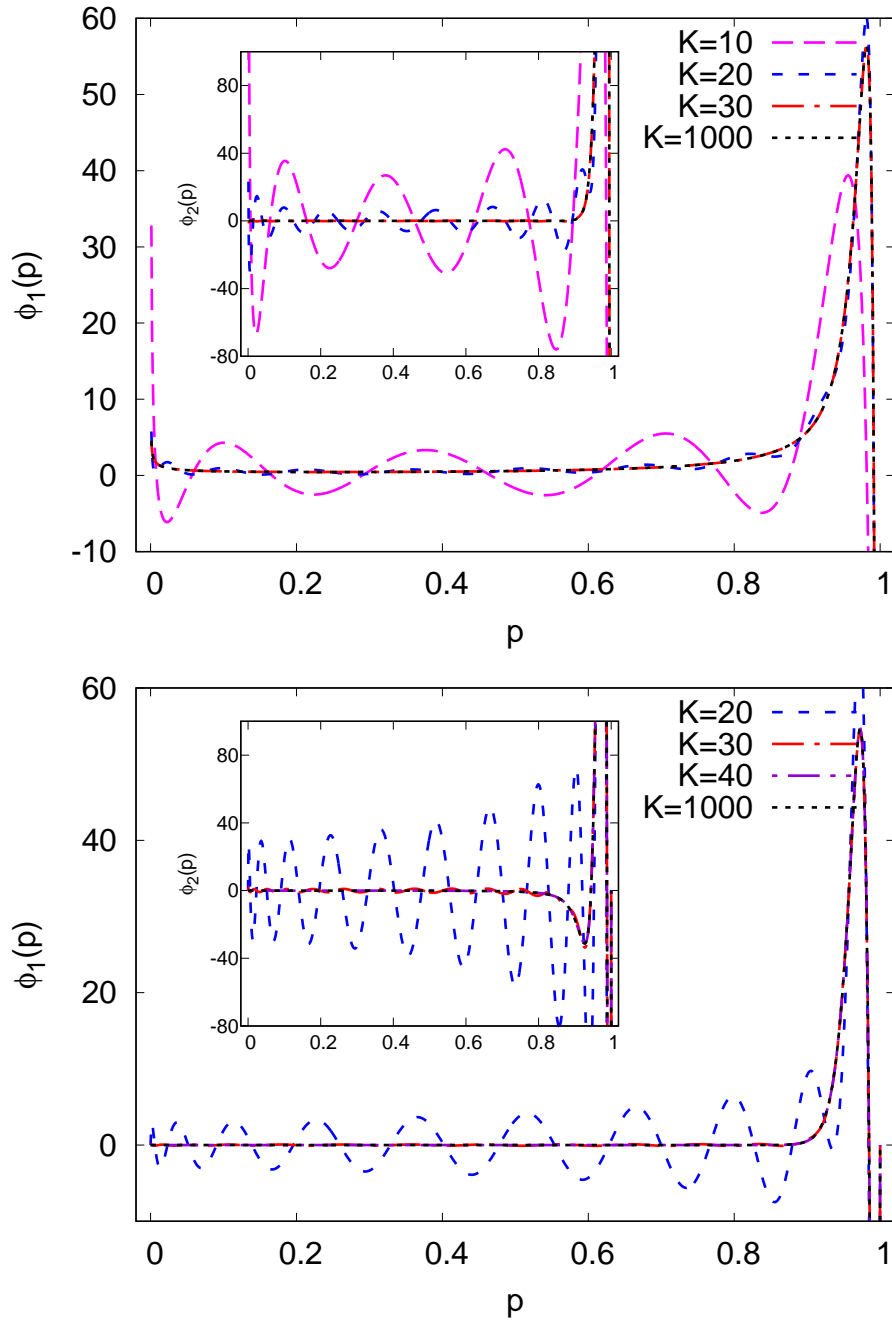


Fig. 4.5 First two excited states, $\phi_1(p)$ (main) and $\phi_2(p)$ (inset) obtained numerically when the orthogonal expansion series (4.8) is terminated at $n = K + 1$ for strong selection ($\sigma = 100$) and mutation rate, $\mu = 1/2$ (top panel) and $3/2$ (bottom panel).

where the σ -dependence of C is fixed using that the $|c_n^{(\ell)}|$ must be independent of σ for small n .

Since the $c_n^{(\ell)}$'s have alternating signs, (4.10) gives

$$T_-(n)|c_{n-1}^{(\ell)}| + T_+(n)|c_{n+1}^{(\ell)}| = (T_0(n) + \lambda_\ell)|c_n^{(\ell)}|, \quad n \geq 2. \quad (4.21)$$

Using the scaling form (4.20) in the above equation and collecting terms to order σ , we arrive at a *first order* linear differential equation for the scaling function $f_\ell(u)$ given by (see also Appendix C.4)

$$\frac{u}{2}f'_\ell(u) + \left(u^2 - \mu - \kappa_\ell + \frac{1}{2}\right)f_\ell(u) = 0, \quad (4.22)$$

where $\kappa_\ell = \lim_{\sigma \rightarrow \infty} \lambda_\ell/\sigma$. On solving the above differential equation, we find that

$$|c_n^{(\ell)}| \approx C_\mu n^{2\mu+2\kappa_\ell-1} e^{-n^2/\sigma}. \quad (4.23)$$

In Fig. 4.4, the numerically obtained expansion coefficients $|c_n^{(1)}|$ and the above expression along with the conjectured eigenvalue (4.17) for the first excited state are compared and we find a very good agreement, except for small n where the scaling limit is not valid. Equation (4.22) also shows that the scaling function $f_\ell(u)$ has a turning point at $u_\ell^* = \sqrt{\mu + \kappa_\ell - \frac{1}{2}}$; for the first excited state, using the conjecture (4.17), we find that $|c_n^{(1)}|$ is a nonmonotonic function for $\mu > 1/4$ and decreases monotonically otherwise. We have numerically verified that (4.23) works well for higher excited states also (data not shown).

Equation (4.23) suggests that as the expansion coefficients decay fast for large n , it may be sufficient to keep terms up to $n \lesssim \sqrt{\sigma}$ for the evaluation of sum (4.8) for the eigenfunction. This expectation is tested in Fig. 4.5 for two eigenfunctions, and we find that when the sum is terminated at small $K \sim \sqrt{\sigma}$, the result matches well with those obtained with $K \gg \sigma$. We remark that at small K , the eigenfunction is seen to have several nodes. But, as already shown in Fig. 4.3, the eigenfunction $\phi_\ell(p)$ has ℓ nodes for large enough K .

4.6.2 Expansion coefficients for infinite selection

As shown in Fig. 4.4, the expansion coefficients in (4.23) do not match with the numerical results for small n . Here, we show that these can be found exactly for special values of

μ . For this purpose, it is useful to define

$$d_n^{(\ell)} = \left| \frac{c_n^{(\ell)}}{6 - 4\mu - 4n} \right|, \quad n \geq 2. \quad (4.24)$$

As shown in Appendix C.4, the generating function $\mathcal{D}_\ell(z) = \sum_{n=2}^{\infty} d_n^{(\ell)} z^n$ obeys a third order differential equation given by (C.4.2); however, for $\sigma \rightarrow \infty$, we obtain

$$\mathcal{D}_\ell(z) = \begin{cases} \frac{z}{4\kappa_\ell} \left(\left(\frac{1+z}{1-z} \right)^{2\kappa_\ell} - 1 \right) & (\mu = 1/2) \\ \left(\frac{z}{1-z^2} \right)^2 \left(\frac{1+z}{1-z} \right)^{2\kappa_\ell} & (\mu = 3/2) \end{cases} \quad (4.25)$$

on choosing $d_2^{(\ell)} = 1$. Using the conjecture (4.17), we get

$$\frac{|c_n^{(1)}|}{|c_2^{(1)}|} \xrightarrow{\sigma \rightarrow \infty} \begin{cases} n - 1 & (\mu = 1/2) \\ \frac{n^2(n^2-1)}{12} & (\mu = 3/2) \end{cases}, \quad (4.26)$$

which are consistent with the power law scaling in (4.23) and the numerical data in the inset of Fig. 4.4 for small n .

4.7 Discussion

For a quite general class of stochastic processes, the eigenvalue problem for the corresponding Fokker-Planck equation can be described by Heun equation [30]. Here, we have elucidated a connection between the confluent Heun equation and the Fokker-Planck equation for the allele frequency distribution in a standard population-genetics model. This relationship is useful, especially for biologists [27, 28, 3], as one can simply use the standard packages (such as Maple and latest version of Mathematica) to solve the partial differential equation (4.1) numerically. However, in [17] and here, an orthogonal series expansion is used to recast the problem as an eigenvalue problem (4.10) which can also be easily implemented numerically and is, perhaps, more amenable to analysis (see, for e.g., [13]).

Here we have studied the eigenvalues and eigenfunctions of the confluent Heun operator in some detail. Our main result for the first eigenvalue λ_1 which is inversely proportional to the relaxation time is summarized in Fig. 4.1. For strong selection ($\sigma \gg \mu$), we find that there is a transition at mutation rate $\mu = 1$ and the eigenvalue λ_1

is independent of mutation rate for $1 < \mu \ll \sigma$. In contrast, in the absence of selection, the relaxation time decreases monotonically as $1/\mu$ [6].

Although we have produced strong numerical evidence for the behavior of the eigenvalues with model parameters, for the reasons described in Sec. 4.1, it seems very difficult to make analytical progress. However, in the limit of strong selection, an analytical understanding of (4.17), perhaps using a WKB approximation [29], may be possible. Factorization methods [30, 31], such as supersymmetric quantum mechanics [32], may also be a fruitful approach to tackle 4.6, and although our preliminary investigation in this direction is encouraging, more work is required to fully understand the eigenvalue problem studied here.

Bibliography

- [1] J. F. Crow and M. Kimura. *An Introduction to Population Genetics Theory*. Harper and Row, New York, 1970.
- [2] B. Charlesworth and D. Charlesworth. *Elements of Evolutionary Genetics*. Ben Roberts, Colorado, 2010.
- [3] R. N. Gutenkunst, R. D. Hernandez, S. H. Williamson, and C. D. Bustamante. Inferring the joint demographic history of multiple populations from multidimensional SNP frequency data. *PLoS Genet.*, **5**: e1000695, 2009.
- [4] T. Taus, A. Futschik and C. Schlötterer. Quantifying selection with pool-seq time series data. *Mol. Biol. Evol.*, **34**: 3023-3034, 2017.
- [5] A. Devi and K. Jain. The impact of dominance on adaptation in changing environments. *Genetics*, **216**: 227-240, 2020.
- [6] M. Kimura. Diffusion models in population genetics. *J. Appl. Probab.*, **1**: 177-232, 1964.
- [7] A. Erdélyi, W. Magnus, F. Oberhettinger, and F. G. Tricomi. *Higher Transcendental Functions*, vol 1. New York: McGraw-Hill, 1953.
- [8] P. P. Fiziev and D. Staicova. The Heun project: Heun functions, their generalizations and applications. <https://theheunproject.org>, 2012.
- [9] A. Ronveaux. *Heun's Differential Equation*. Oxford University Press, Oxford, 1995.
- [10] M. Hortaçsu. Heun functions and some of their applications in physics. *Adv. High Energy Phys.*, 2018.
- [11] G. Jaffé. Zur theorie des wasserstoffmolekülions. *Z. Phys.*, **87**: 535-544, 1934.

-
- [12] Q. Xie, H. Zhong, M. T. Batchelor and C. Lee. The quantum Rabi model: solution and dynamics. *J. Phys. A: Math. Theor.*, **50**: 113001, 2017.
- [13] E. W. Leaver. An Analytic representation for the quasi normal modes of Kerr black holes. *Proc. R. Soc. Lond. A*, **402**: 285-298, 1985.
- [14] P. P. Fiziev and D. Staicova. Application of the confluent Heun functions for finding the quasinormal modes of nonrotating black holes. *Phys. Rev. D*, **84**: 127502, 2011.
- [15] D. Vincenzi and E. Bodenschatz. Single polymer dynamics in elongational flow and the confluent Heun equation. *J. Phys. A: Math. Gen.*, **39**: 10691-10701, 2006.
- [16] W. Lay, K. Bay, and S. Y. Slavyanov. Asymptotic and numeric study of eigenvalues of the double confluent Heun equation. *J. Phys. A: Math. Gen.*, **31**: 8521, 1998.
- [17] Y. S. Song and M. Steinrücken. A simple method for finding explicit analytic transition densities of diffusion processes with general diploid selection. *Genetics*, **190**: 1117-1129, 2012.
- [18] W. J. Ewens. *Mathematical Population Genetics*. Springer, Berlin, 2004.
- [19] H. Risken. *The Fokker-Planck Equation, Methods of Solution and Applications*. Springer-Verlag, Berlin, 1996.
- [20] J. Mathews and R. L. Walker. *Mathematical Methods of Physics*. Benjamin, New York, 1970.
- [21] S. Wright. The distribution of gene frequencies in populations. *Proc. Natl Acad. Sci. USA*, **23**: 307-320, 1937.
- [22] P. P. Fiziev. Novel relations and new properties of confluent Heun's functions and their derivatives of arbitrary order. *J. Phys. A: Math. Theor.*, **43**: 035203, 2010.
- [23] L. J. Chu and J. A. Stratton. Elliptic and spheroidal wave functions. *J. Math. Phys.*, **20**: 259-309, 1941.
- [24] E. W. Leaver. Solutions to a generalized spheroidal wave equation: Teukolsky's equations in general relativity, and the two-center problem in molecular quantum mechanics. *J. Math. Phys.*, **27**: 1238, 1986.
- [25] M. Abramowitz and I. A. Stegun. *Handbook of Mathematical Functions with Formulas, Graphs, and Mathematical Tables*, Dover, 1964.

-
- [26] W. Gautschi. Computational aspects of three-term recurrence relations. *SIAM Rev.*, **9**: 24-82, 1967.
- [27] Y. Wang and B. Rannala. A novel solution for the time-dependent probability of gene fixation or loss under natural selection. *Genetics*, **168**: 1081–1084, 2004.
- [28] J. P. Bollback, T. L. York and R. Nielsen. Estimation of $2Nes$ from temporal allele frequency data. *Genetics*, **179**: 497-502, 2008.
- [29] V. Ferrari and B. Mashhoon. New approach to the quasinormal modes of a black hole. *Phys. Rev. D*, **30**: 295-304, 1984.
- [30] A. Debosscher. Unification of one-dimensional Fokker-Planck equations beyond hypergeometrics: Factorizer solution method and eigenvalue schemes. *Phys. Rev. E*, **57**: 252-275, 1998.
- [31] A. A. Stahlhofen. Susy, Gauss, Heun and physics: a magic square? *J. Phys. A: Math. Gen.*, **37**: 10129-10138, 2004.
- [32] F. Cooper, A. Khare, and U. Sukhatme. Supersymmetry and quantum mechanics. *Phys. Rep.*, **251**: 267-385, 1995.

Chapter 5

Conclusions and open questions

In this Chapter, we summarise the important results obtained in the thesis and discuss some open problems that can be addressed by extending our work. Although natural environments are never truly static, the effect of the time-varying environment on the adaptation process is not well-studied. The primary focus of this thesis is to understand the evolution of a population under continually changing environments in the presence of evolutionary forces of natural selection, mutation, recombination, and random genetic drift. Since the stochastic dynamics of adaptation, even under constant selection, are not well-studied, we also investigated the evolutionary dynamics of a monogenic trait in a constant environment.

In Chapter 2, we studied the evolution of a monogenic trait in a periodically changing environment where the selection pressure changes its sign with time, and the mutant, which is favorable for certain times, can become unfavorable at other times. We considered a finite, diploid population with intermediate dominance and found that:

- (i) In a slowly changing environment, the fixation probability of a mutant is determined by the selection coefficient of the mutant at the instant it arose.
- (ii) The fixation probability depends on both the time-averaged selection and the time of appearance in a rapidly changing environment.
- (iii) An initially beneficial (deleterious) mutant can have a fixation probability lower (higher) than that for a neutral mutant depending on its time of appearance and rate of environmental change.
- (iv) Haldane's sieve does not always hold in a time-varying environment.

(v) Depending upon the rate of environmental change, there is an optimal mutation rate at which the average fitness of the population is maximum.

In Chapter 3, we analyzed the adaptation of a polygenic trait where selection acts on a large number of genes to maintain an optimum phenotype. Evolution of an infinitely large, diploid population in a linearly changing environment is considered in this Chapter. The important findings are:

- (i) Stabilizing selection pulls the population towards the new phenotypic optimum, and recurrent mutations push the population away from it.
- (ii) The mean trait evolves with the speed of the phenotypic optimum and there is a constant lag between them when the mutation rate is low as compared to the selection pressure.
- (iii) When the mutation rate is high, the mean trait evolves with a speed lower than that of the optimum, which increases the lag between the mean trait and the optimum.

Although the bulk of the thesis describes the evolution of a trait in a changing environment, we also studied the evolution of a single, biallelic locus in a finite, haploid population in a constant environment in Chapter 4, using an eigenfunction expansion method. We found that:

- (i) The eigenfunctions obey a confluent Heun equation which is a generalization of the hypergeometric equation.
- (ii) The first eigenvalue that determines the dynamics exhibits a sharp transition: for mutation rate below one, the eigenvalue increases linearly with increasing mutation rate and then remains a constant.

We conclude this Chapter with a brief discussion of some open questions.

- (i) In Chapter 3, that is devoted to the evolution of a polygenic trait, we have neglected the effect of random genetic drift. As the natural population is finite, it is crucial to understand the stochastic dynamics of the trait. The stochastic dynamics are not well-understood even under a single sudden change in environment. Therefore, it would be interesting to investigate the stochastic evolution of the trait under both sudden and continual changes in the environment.
- (ii) We have ignored the linkage disequilibrium in the evolutionary process in this thesis,

which is important to be considered when the loci are close to each other since the recombination rate depends on the physical distance between the loci. An extension of the analyses in this thesis is desirable.

Our thesis mainly focuses on the evolution of a trait in changing environments and suggests that the results in the time-varying environment can be very different than in a static environment. Since natural environments are seldom static, our studies put forward the importance of consideration of fluctuations in the environment to get any inference from the empirical studies.

Appendix A

A.1 Discrete and continuous time models for diploids

Consider a randomly mating population of N diploids with discrete generations in which the selection acts on the viability of an individual. Then the life cycle consists of a juvenile phase during which mutation, selection and random genetic drift act, and determine the chance of survival of an individual to the adult phase in which reproduction occurs. For a large population, immediately after random mating, the frequency of the genotypes can be approximated by the corresponding Hardy-Weinberg proportions as the deviations from it are of order $1/N$ [1]. The dynamics in the juvenile phase can be modeled by a discrete time Wright-Fisher process [2].

In contrast to the discrete time model described above, we work with a continuous time model when the environment changes gradually. In overlapping generations, a model that incorporates details of the life cycle is necessarily complex as the age-structure of the population must be carefully taken into account. Moreover, besides large N , additional assumptions, viz., small selection coefficient, s and mutation probability, μ are required for Hardy-Weinberg equilibrium to hold in such continuous time models [1].

However, in the diffusion approximation where $s \rightarrow 0, \mu \rightarrow 0, N \rightarrow \infty$ with finite $2Ns, 2N\mu$ in the continuous time model and $4Ns, 4N\mu$ in the discrete time model, we obtain essentially the same Kolmogorov equations for both models [2]. In Chapter 2, we studied the dynamics of adaptation in the framework of diffusion theory when the mutant is on average neutral as the $\bar{s} \neq 0$ case does not seem to be analytically tractable.

However, for positive \bar{s} , it is possible to make analytical progress by modeling the fixation process as a branching process [3, 4]. The branching approximation applies as long as the mutants are rare, that is, a finite number of mutants are present in an infinitely large population. In this approximation, the transition rate matrix for the discrete time model discussed above is not a continuant matrix [2]. However, as the

number of mutants is small, it is reasonable to assume that the transition rates are significantly different from zero only when the number of mutant allele changes by one in a generation; in other words, we arrive at a birth-death model. The above discussion thus provides a justification for the birth-death model for diploids and in the main text, we have used it for all parameter regimes.

A.2 Fixation probability of a mutant that is beneficial at all times

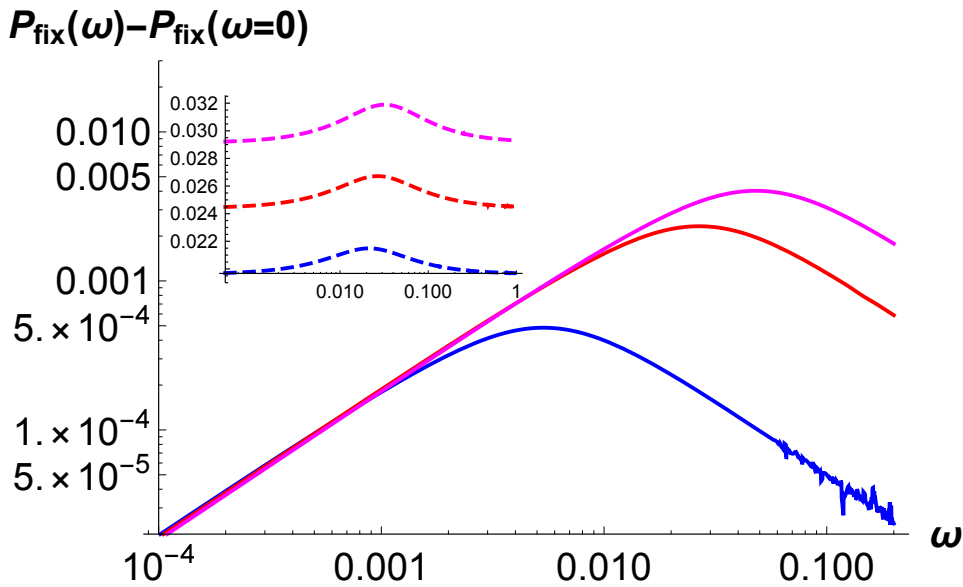


Fig. A.2 The inset shows the fixation probability $P_{\text{fix}}(\omega)$ given by (2.5) for a mutant that is beneficial on average for dominance coefficient $h = 0.4, 0.5, 0.6$ (bottom to top). In the main figure, the effect of a changing environment is shown by subtracting the fixation probability $P_{\text{fix}}(\omega = 0) = hs(t_a)/[1 + hs(t_a)]$ with $s(t_a) = \bar{s} + \sigma \sin(\theta_a)$ for $h = 0.1, 0.5, 0.9$ (bottom to top). In both plots, $\bar{s} = 0.05, \sigma = 0.2\bar{s}, \theta_a = 0$.

A.3 Fixation probability of an on average neutral mutant

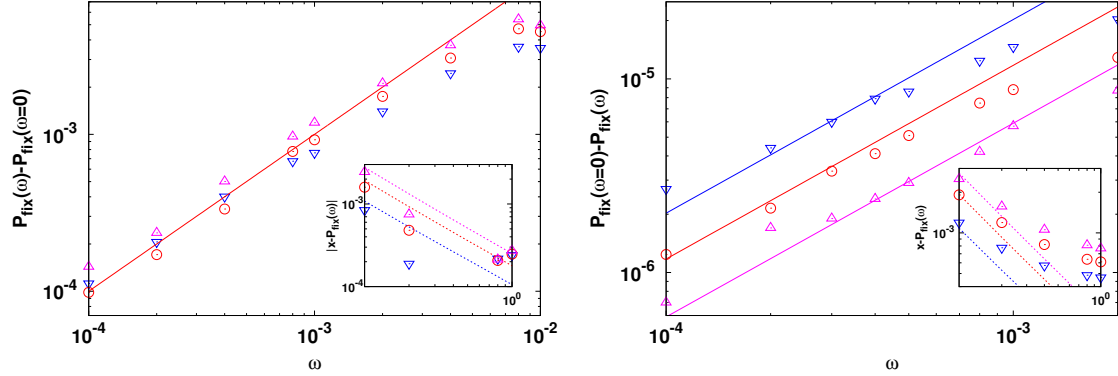


Fig. A.3 Fixation probability of a mutant that is neutral on average for $N\sigma \gg 1$ when the mutant appeared at $\theta_a = \pi/4$ (left panel) and $5\pi/4$ (right panel). The solid line shows the expression (2.11b) (left panel) and (2.11c) (right panel) for small cycling frequencies and the dashed lines represent (2.8b) for large cycling frequencies. Here $N = 100$, $\sigma = 0.1$ and $h = 0.3(\nabla)$, $0.5(\circ)$, $0.7(\Delta)$. The numerically obtained value $P_{\text{fix}}(\omega = 0) = 2.53 \times 10^{-2}$, 3.40×10^{-2} , 4.38×10^{-2} for $h = 0.3, 0.5, 0.7$, respectively, for the left panel. For the right panel, $P_{\text{fix}}(\omega = 0) = 3.55 \times 10^{-5}$, 2.58×10^{-5} , 1.98×10^{-5} for $h = 0.3, 0.5, 0.7$, respectively. The simulation results are averaged over 10^7 runs.

A.4 Fixation probability of a mutant in transiently varying selection

Here we consider a situation in which the time-averaged selection coefficient is nonzero and changes over a finite time T_e ,

$$s(t) = \begin{cases} \sigma \sin(\omega t) & , t < T_e \\ 0 & , t > T_e . \end{cases} \quad (\text{A.4.1})$$

$$(\text{A.4.2})$$

Waxman (2011) [5] has shown that in such a case, the fixation probability is simply given by the mean allele frequency at the end of selection. Here we estimate this allele frequency using the deterministic evolution equation,

$$\dot{x} = s(t)x(1-x)(x+h(1-2x)) \stackrel{x \rightarrow 0}{\approx} hs(t)x . \quad (\text{A.4.3})$$

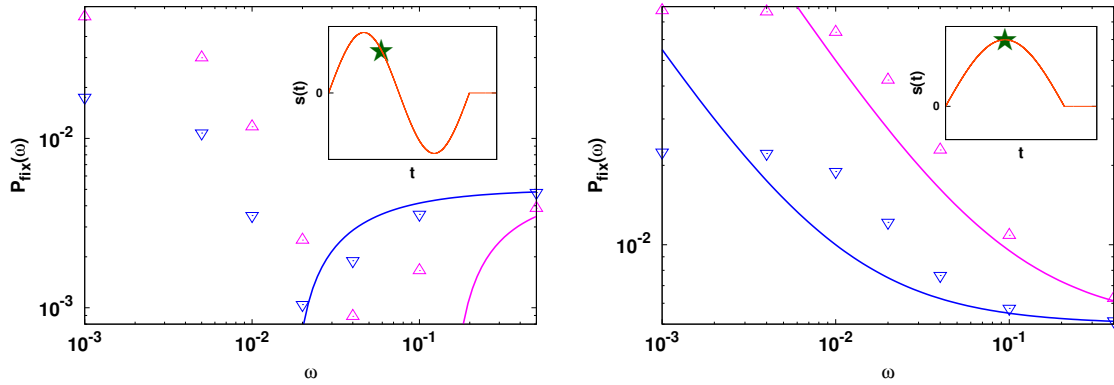


Fig. A.4 Fixation probability of a mutant in transiently varying environments defined by (A.4.1) and (A.4.2) and illustrated in the inset. The lines show the expression (A.4.4) and the points show the simulation data obtained by averaging over 10^7 independent runs for $\theta_a = 3\pi/4, T_e = 2\pi/\omega$ (left panel) and $\theta_a = \pi/2, T_e = \pi/\omega$ (right panel). In all the plots, $N = 100$, $\sigma = 0.1$ and $h = 0.1(\nabla), 0.9(\Delta)$.

For large ω , starting from a single mutant, the number of mutants at time T_e is then given by

$$2Nx(T_e) = n(T_e) = 1 + \frac{h\sigma}{\omega} (\cos(\theta_a) - \cos(\omega T_e)) . \quad (\text{A.4.4})$$

For large cycling frequencies, this prediction matches qualitatively with the numerical results in Fig. A.4, and therefore captures the effect of dominance when the environment changes fast over a short interval of time.

Bibliography

- [1] T. Nagylaki. *Introduction to Theoretical Population Genetics*. Springer-Verlag, Berlin, 1992.
- [2] W. J. Ewens. *Mathematical Population Genetics*. Springer, Berlin, 2004.
- [3] M. M. Desai and D. S. Fisher. Beneficial mutation-selection balance and the effect of linkage on positive selection. *Genetics*, **176**: 1759-1798, 2007.
- [4] H. Uecker and J. Hermisson. On the fixation process of a beneficial mutation in a variable environment. *Genetics*, **188**: 915-930, 2011.
- [5] D. Waxman. A unified treatment of the probability of fixation when population size and the strength of selection change over time. *Genetics*, **188**: 907-913, 2011.

Appendix B

B.1 Branching process approximation

The fixation probability of a mutant that arises in a large wild type population and is beneficial on average, is given by (2.5). For $\omega \rightarrow \infty$, the fixation probability is given by $h\bar{s}/(1+h\bar{s})$ while for $\omega = 0$, it is equal to $hs(t_a)/(1+hs(t_a))$ for $s(t_a) > 0$, and zero otherwise.

Away from these extreme limits, the integral appearing in (2.5) can be analyzed for small $h\bar{s}, h\sigma$ as follows. For small cycling frequencies $\omega \ll h\bar{s}, h\sigma$, by first expanding the integrand in powers of ω and then carrying out the resulting integrals, we obtain

$$\frac{P_{\text{fix}}}{hs(t_a)} = 1 + \frac{h\sigma \cos(\theta_a)\omega}{(hs(t_a))^2} - \left(\frac{\sigma^2(1 + \cos^2(\theta_a))}{s^2(t_a)} + \frac{\bar{s}\sigma \sin(\theta_a)}{s^2(t_a)} \right) \left(\frac{\omega}{hs(t_a)} \right)^2, \quad (\text{B.1.1})$$

provided $s(t_a) > 0$, and zero otherwise. Similarly, for large cycling frequencies, the fixation probability can be found by first expanding the integrand in powers of $h\sigma/\omega$; for $\omega \gg h\bar{s}, h\sigma$, this finally results in

$$\frac{P_{\text{fix}}}{h\bar{s}} = 1 + \frac{h\sigma}{\omega} \cos(\theta_a) + \frac{h\bar{s}h\sigma}{\omega^2} \sin(\theta_a) - \frac{1}{4} \left(\frac{h\sigma}{\omega} \right)^2 \cos(2\theta_a). \quad (\text{B.1.2})$$

Note that the first order corrections in (B.1.1) and (B.1.2) vanish for $\theta_a = \pi/2$ and $3\pi/2$.

As discussed in the main text, an extremum in the fixation probability occurs at the resonance frequency ω_r . Ignoring terms of order ω^2 and $1/\omega^2$ in (B.1.1) and (B.1.2), respectively, and equating the resulting expressions, we arrive at a quadratic equation for ω_r whose positive root is given by (2.7). Furthermore, in Fig. 2.1, for $\pi/2 < \theta_a < 3\pi/2$, the fixation probability curves for dominance coefficient h and h' coincide at a

cycling frequency higher than ω_r , which can be estimated using (B.1.2), and found to be $-(h + h')\sigma \cos(\theta_a)$.

B.2 Diffusion approximation for small cycling frequencies

Here we study (2.3) for $\bar{s} = 0$ and small cycling frequencies within a perturbation theory by writing $P_{\text{fix}} = P_0 + N\omega P_1$. It is useful to rewrite (2.3) as

$$-\frac{\partial P_{\text{fix}}(x, \tau)}{\partial \tau} = \frac{\sigma \sin(\tau)g(x)}{\omega} \frac{\partial P_{\text{fix}}(x, \tau)}{\partial x} + \frac{x(1-x)}{2N\omega} \frac{\partial^2 P_{\text{fix}}(x, \tau)}{\partial x^2}, \quad (\text{B.2.1})$$

where $\tau = \omega t + \theta_a, t \geq 0$.

In a static environment, if the mutant arises at time $t_a = \theta_a/\omega$ and has fraction x in the population, its fixation probability is given by $P_0(x, \theta_a) = \int_0^x dy I(y, \theta_a) / \int_0^1 dy I(y, \theta_a)$, where

$$I(y, \theta_a) = e^{-Ns(t_a)y(y+2h(1-y))} \quad (\text{B.2.2})$$

and $s(t_a) = \sigma \sin(\theta_a)$ [1]. For a strongly beneficial mutation ($Ns(t_a) \gg 1$), the fixation probability P_0 increases with dominance coefficient and given by $hs(t_a)$, while, for a deleterious mutation, it decreases with h . The chance of fixation also decreases with population size for $h \leq 1/2$, but the variation with N is non-monotonic for $h > 1/2$.

The effect of a slowly changing environment on the fixation probability is captured by P_1 that, by virtue of (B.2.1), obeys the following ordinary differential equation,

$$-\frac{\partial P_0(x, \tau)}{\partial \tau} = N\sigma \sin(\tau)g(x) \frac{\partial P_1(x, \tau)}{\partial x} + \frac{x(1-x)}{2} \frac{\partial^2 P_1(x, \tau)}{\partial x^2}. \quad (\text{B.2.3})$$

Equation (B.2.3) subject to boundary conditions $P_1(0, \tau) = P_1(1, \tau) = 0$ has the solution

$$P_1(x, \tau) = \frac{\int_0^x dx' I(x')}{\int_0^1 dx' I(x')} \int_0^1 dx'' I(x'') \int_0^{x''} dx' \frac{2}{x'(1-x')I(x')} \frac{\partial P_0}{\partial \tau} - \int_0^x dx'' I(x'') \int_0^{x''} dx' \frac{2}{x'(1-x')I(x')} \frac{\partial P_0}{\partial \tau}, \quad (\text{B.2.4})$$

which, for small initial frequency ($\tau = \theta_a, x \rightarrow 0$) can be approximated by

$$P_1(x, \theta_a) \approx x \frac{\int_0^1 dx'' I(x'') \int_0^{x''} dx' \frac{2}{x'(1-x')I(x')} \frac{\partial P_0(x', \tau)}{\partial \tau} \Big|_{\tau=\theta_a}}{\int_0^1 dx' I(x')} . \quad (\text{B.2.5})$$

The following cases need to be considered separately:

(i) $-1 \ll Ns(t_a) \ll 1$: For small $N\sigma$ and arbitrary θ_a , we first expand $I(x, \tau)$ to linear order in $N\sigma$ and carry out the integrals in the expression for P_0 given above to obtain

$$P_0(x, \tau) = x \left[1 + N\sigma \sin(\tau)(1-x) \left(\frac{(1-2h)(1+x) + 3h}{3} \right) \right], \quad (\text{B.2.6})$$

$$\left. \frac{\partial P_0}{\partial \tau} \right|_{\tau=\theta_a} = \frac{N\sigma \cos(\theta_a)x(1-x)(1+x+h(1-2x))}{3}. \quad (\text{B.2.7})$$

Using these approximations in (B.2.5), to leading order in $N\sigma$, we get

$$P_{\text{fix}}(x, \theta_a) = P_0(x, \theta_a) + \left(\frac{4+h}{9} \right) N^2 \omega \sigma \cos(\theta_a)x. \quad (\text{B.2.8})$$

For $Ns(t_a) = 0$ (that is, $\theta_a = 0$ or π , arbitrary $N\sigma$), it can be easily seen that the function $I(x, \theta_a) = 1$ and the derivative $\frac{\partial P_0}{\partial \tau}$ is given by (B.2.7) thus leading to (B.2.8).

(ii) $Ns(t_a) \gg 1$: For large $|Ns(t_a)|$, using the asymptotic expansion of the error function $\text{erf}(x)$ [2], the fixation probability $P_0(x, \tau)$ can be approximated as

$$P_0(x, \tau) = \frac{1 - \frac{he^{-N\sigma \sin(\tau)x(x+2h(1-x))}}{h+(1-2h)x}}{1 - \frac{he^{-N\sigma \sin(\tau)}}{h+(1-2h)}} \quad (\text{B.2.9})$$

(more precisely, the above expression holds for $|\frac{h^2 N\sigma \sin(\tau)}{1-2h}| \gg 1$). For large, positive $Ns(t_a)$, the denominator in (B.2.9) can be approximated by one leading to

$$\left. \frac{\partial P_0}{\partial \tau} \right|_{\tau=\theta_a} = \frac{Nh\sigma \cos(\theta_a)x(x+2h(1-x))}{h+x(1-2h)} I(x, \theta_a). \quad (\text{B.2.10})$$

Using the above expression in (B.2.5), and performing the integrals for $Ns(t_a) \gg 1$, we finally obtain the following simple result,

$$P_{\text{fix}}(x, \theta_a) = P_0(x, \theta_a) + 2N\omega \cot(\theta_a)x. \quad (\text{B.2.11})$$

(iii) $Ns(t_a) \ll -1$: Taking the derivative of P_0 in (B.2.9) with respect to τ and keeping factors proportional to $e^{-N\sigma \sin(\tau)}$ only, we obtain

$$\left. \frac{\partial P_0}{\partial \tau} \right|_{\tau=\theta_a} = \left(\frac{h-1}{h} \right) N\sigma \cos(\theta_a) e^{N\sigma \sin(\theta_a)} \left[1 + \frac{h(1-x)(1+x-2hx)}{(2h-1)x-h} I(x, \theta_a) \right]. \quad (\text{B.2.12})$$

Noting that the dominant contribution to the inner integral in the numerator of (B.2.5) comes from $x' \rightarrow 0$, we finally get

$$P_1(x, \theta_a) \approx \frac{2(1-h)N\sigma \cos(\theta_a) x e^{N\sigma \sin(\theta_a)}}{h \int_0^1 dx' I(x')} \int_0^1 dx'' I(x'') \int_0^{x''} dx' \frac{e^{2hN\sigma \sin(\theta_a)x'} - 1}{x'} \quad (\text{B.2.13})$$

$$\approx \frac{2(1-h)N\sigma \cos(\theta_a) x \ln(2h|N\sigma \sin(\theta_a)|)}{h} e^{-|N\sigma \sin(\theta_a)|} . \quad (\text{B.2.14})$$

B.3 Diffusion approximation for large cycling frequencies

Here we calculate the fixation probability of a neutral mutant ($\bar{s} = 0$) when the cycling frequency is larger than the amplitude of selection ($\omega > \sigma$). On writing $P_{\text{fix}} = P_0 + \frac{\sigma}{\omega} P_1$ in (B.2.1) and collecting terms to zeroth and first order in σ/ω , we find that $P_0 = x$, as expected. The correction P_1 obeys an inhomogeneous partial differential equation,

$$\frac{\partial P_1(x, \tau)}{\partial \tau} + \frac{x(1-x)}{2N\omega} \frac{\partial^2 P_1(x, \tau)}{\partial x^2} = -\sin(\tau)g(x). \quad (\text{B.3.1})$$

with boundary conditions $P_1(0, \tau) = P_1(1, \tau) = 0$.

The homogeneous equation can be solved using standard eigenfunction expansion method [3, 4], and we find that $P_1^{\text{homo}}(x, \tau) = \sum_{n=0}^{\infty} c_n e^{-\lambda_n \tau} X_n(x)$ with the eigenvalue $\lambda_n = -\frac{(n+1)(n+2)}{2N\omega}$ and eigenfunction $X_n(x) \propto x(1-x)\mathcal{P}_n^{(1,1)}(1-2x)$ where $\mathcal{P}_n^{(\alpha,\beta)}(x)$ is the Jacobi polynomial [2]. However, as this homogeneous solution is not periodic in τ , it does not contribute to the full solution. But since the eigenfunctions $X_n(x)$ form a complete set of basis, we can write $P_1(x, \tau) = \sum_{n=0}^{\infty} a_n X_n(x)$ and $g(x) = \sum_{n=0}^{\infty} b_n X_n(x)$ where b_n are obtained using the orthogonality property of $X_n(x)$. Using these in (B.3.1), we obtain

$$P_1(x, \tau) = \frac{x(1-x)}{2} \left[\frac{\cos(\tau + \tan^{-1} \lambda_0)}{\sqrt{1 + \lambda_0^2}} + \frac{(2h-1)(1-2x) \cos(\tau + \tan^{-1} \lambda_1)}{\sqrt{1 + \lambda_1^2}} \right]. \quad (\text{B.3.2})$$

When a single mutant with frequency $x = (2N)^{-1}$ appears at time t_a , the above expression reduces to (2.8b) and can be used to find the resonance frequency at which the probability of fixation has an extremum. For $h = 1/2$, we find that

$$N\omega_r = \frac{1}{\tan(\theta_a) + \text{sgn}(\cos(\theta_a)) \sec(\theta_a)} . \quad (\text{B.3.3})$$

For arbitrary h , we are unable to find a simple closed expression for ω_r as it is a solution of a 6th order algebraic equation. But a numerical study of this equation shows that ω_r depends weakly on dominance coefficient. For $\theta_a = 0$, we find $N\omega_r \approx 0.88, 1.0, 1.14$ for $h = 0.1, 0.5, 0.9$, respectively; the corresponding values for $\theta_a = 3\pi/4$ are given by 1.73, 2.41, 3.84.

B.4 Allele frequency distribution for strong mutation

The forward time dynamics of the population under mutation and selection are described by (2.12) for the allele frequency distribution $\Phi(x, t)$. The distribution Φ_0 for the population subject to mutation and random genetic drift is given by $\Phi_0(x, t) = \sum_{n=0} a_n e^{-\lambda_n t} X_n(x)$ with eigenvalues $\lambda_n = n \left(\frac{n-1}{2N} + 2\mu \right)$ and eigenfunctions $X_n(x) \propto (x(1-x))^{2N\mu-1} \mathcal{P}_n^{(2N\mu-1, 2N\mu-1)}(1-2x)$ where, $\mathcal{P}_n^{(\alpha, \beta)}(z)$ is the Jacobi polynomial [5]. These eigenfunctions are orthogonal with respect to the weight function $\rho(x) = [x(1-x)]^{1-2N\mu}$.

For weak selection ($\sigma < \mu$), we can expand $\Phi(x, t)$ as a power series in σ/μ to write $\Phi = \Phi_0 + (\sigma/\mu)\Phi_1$. Using this in (2.12), we find that Φ_1 obeys the following differential equation,

$$\begin{aligned} & \dot{\Phi}_1(x, t) + \frac{\partial}{\partial x} [m(x)\Phi_1(x, t)] - \frac{1}{2N} \frac{\partial^2}{\partial x^2} [x(1-x)\Phi_1(x, t)] \\ &= -\mu \sin(\omega t) \frac{\partial}{\partial x} [g(x)\Phi_0(x, t)] . \end{aligned} \quad (\text{B.4.1})$$

To find the distribution $\Phi_1(x, t)$, we expand it and the RHS of above equation as a linear combination of $X_n(x)$. Writing $\Phi_1(x, t) = \sum_{n=1}^{\infty} b_n(t) X_n(x)$ in (B.4.1), we find that at large times,

$$b_n(t) \xrightarrow{t \gg 1} \int_0^{\infty} dt' e^{-\lambda_n t'} c_n(t-t') \quad (\text{B.4.2})$$

where

$$c_n(t) = \frac{-\mu \sin(\omega t)}{\int_0^1 dx \rho(x) X_n^2(x)} \int_0^1 dx \rho(x) X_n(x) \frac{\partial}{\partial x} [g(x)\Phi_0(x, t)] . \quad (\text{B.4.3})$$

As $\Phi_0(x, t) \xrightarrow{t \rightarrow \infty} X_0(x)$, from (B.4.2), we obtain

$$b_n(t) = \frac{\mu \sin(\theta_n - \omega t)}{\sqrt{\lambda_n^2 + \omega^2}} \left(\frac{\delta_{n,1}}{2} + \frac{(2h-1)\delta_{n,2}}{1+2N\mu} \right) \frac{\Gamma(4N\mu)}{[\Gamma(2N\mu)]^2} \quad (\text{B.4.4})$$

where $\theta_n = \tan^{-1}(\omega/\lambda_n)$. We thus have

$$\Phi(x, t) = \Phi_0(x) + b_1(t)X_1(x) + b_2(t)X_2(x). \quad (\text{B.4.5})$$

Bibliography

- [1] M. Kimura. Some problems of stochastic processes in genetics. *Ann. Math. Stat.*, **28**: 882-901, 1957.
- [2] M. Abramowitz and I. A. Stegun. *Handbook of Mathematical Functions With Formulas, Graphs, and Mathematical Tables*, Dover, 1964.
- [3] M. Kimura. Solution of a process of random genetic drift with a continuous model. *Proc. Natl. Acad. Sci. USA*, **41**: 144-150, 1955.
- [4] W. J. Ewens. *Mathematical Population Genetics*. Springer, Berlin, 2004.
- [5] J. F. Crow and M. Kimura. Some genetic problems in natural populations. *In: Neyman J (ed) Proceedings of the Third Berkeley Symposium on Mathematical Statistics and Probability*, Vol. 4. University of California Press, Berkeley, pp. 1-22, 1956.

Appendix C

C.1 Frobenius series expansion

Since $p = 0$ is a regular singular point of the confluent Heun equation, we can expand the eigenfunction in a Frobenius series by writing $\phi_\ell(p) = p^a \sum_{n=0}^{\infty} f_n^{(\ell)} p^n$, $|p| < 1$ [1]. Substituting it in (4.6) and setting the coefficient of p^{a-1} to zero, we find the indicial exponents to be $a = 0$ and $\mu - 1$. For $\mu \neq 1$, the eigenfunction can be written as

$$\phi_\ell(p) = \tilde{a}_1 H_C(-\sigma, 1 - \mu, 1 - \mu, -\mu\sigma, \eta_\ell, p) + \tilde{a}_2 p^{\mu-1} H_C(-\sigma, \mu - 1, 1 - \mu, -\mu\sigma, \eta_\ell, p), \quad (\text{C.1.1})$$

where $\eta_\ell = (1 - 2\lambda_\ell + \mu(\sigma - \mu))/2$ and $H_C(\alpha, \beta, \gamma, \delta, \eta, p)$ is the confluent Heun function [2]. For $\mu = 1$, the first solution has a logarithmic singularity at $p = 0$. In either case, the vanishing current boundary condition (4.2) at $p = 0$ yields $\tilde{a}_1 = 0$.

The coefficients of terms of $\mathcal{O}(p^a)$ or higher in the Frobenius series lead to a three-term recursion relation for $f_n^{(\ell)}$'s given by

$$(n + \mu)(n + 1)f_{n+1}^{(\ell)} + [(n + \mu - 1)(\mu - \sigma - n - 2) + \nu_\ell]f_n^{(\ell)} + \sigma(n + \mu)f_{n-1}^{(\ell)} = 0, \quad n = 0, 1, \dots \quad (\text{C.1.2})$$

with $f_{-1}^{(\ell)} = 0$. The reflecting boundary condition at $p = 1$ imposes the condition $\sum_{n=0}^{\infty} f_n^{(\ell)} = 0$. Note that unlike in the expansion (4.10), here the parameter σ appears in the coefficient of $f_n^{(\ell)}$ and $f_{n-1}^{(\ell)}$.

C.2 Orthogonal polynomial expansion

We begin with the observation that in the absence of selection, the eigenfunctions are exactly given by [3]

$$\phi_\ell(p, \sigma = 0) \propto (pq)^{\mu-1} P_\ell^{(\mu-1, \mu-1)}(1-2p), \quad (\text{C.2.1})$$

with eigenvalue $\lambda_\ell(\sigma = 0) = \ell(2\mu + \ell - 1)$, $\ell = 0, 1, \dots$. For nonzero selection, we therefore write

$$\phi_\ell(p, \sigma) = (pq)^{\mu-1} \sum_{n=0}^{\infty} a_n^{(\ell)} P_n^{(\mu-1, \mu-1)}(1-2p). \quad (\text{C.2.2})$$

As this expansion is valid for $|p| < 1$, in order to impose the boundary condition (4.2) at $p = 1$, we used the relationship between Jacobi polynomials and Gauss hypergeometric function and the connection formulae for the latter [4], and verified that (4.2) is indeed satisfied.

Substituting the expansion (C.2.2) in the confluent Heun equation (4.6) and using the expression for the second derivative of Jacobi polynomial (see 22.6.2 of [4]), we obtain

$$-\sigma(pq\phi'_\ell(p) - 2p\phi_\ell) = \sum_{n=0}^{\infty} a_n^{(\ell)} [n(2\mu - 1 + n) - \lambda_\ell + \sigma](1-x^2)^{\mu-1} P_n^{(\mu-1, \mu-1)}(x), \quad (\text{C.2.3})$$

where $x = 1-2p$. It can be verified that the above equation reproduces the eigenspectrum in the absence of selection.

To proceed further, we need the following identities:

1. From 22.8.1 of [4], we get

$$(1-x^2) \frac{dP_n^{(\mu-1, \mu-1)}(x)}{dx} = -nxP_n^{(\mu-1, \mu-1)}(x) + (n+\mu-1)P_{n-1}^{(\mu-1, \mu-1)}(x). \quad (\text{C.2.4})$$

2. Furthermore, 22.7.15 and 22.7.18 of [4], gives

$$\begin{aligned} (1-x)P_n^{(\mu-1, \mu-1)}(x) &= P_n^{(\mu-1, \mu-1)}(x) - \frac{n+\mu-1}{2\mu+2n-1}P_{n-1}^{(\mu-1, \mu-1)}(x) \\ &\quad - \frac{(n+1)(2\mu+n-1)}{(\mu+n)(2\mu+2n-1)}P_{n+1}^{(\mu-1, \mu-1)}(x). \end{aligned} \quad (\text{C.2.5})$$

Using (C.2.4) and (C.2.5) in (C.2.3), we find that

$$\begin{aligned} & \frac{pq\phi'_\ell(p) - 2p\phi_\ell(p)}{(1-x^2)^{\mu-1}} + \sum_{n=0}^{\infty} a_n^{(\ell)} P_n^{(\mu-1, \mu-1)}(x) \\ &= \sum_{n=1}^{\infty} \left[\frac{n(2\mu+n-2)(2\mu+n-1)}{2(\mu+n-1)(2\mu+2n-3)} a_{n-1}^{(\ell)} - \frac{(\mu+n)n}{2(1+2\mu+2n)} a_{n+1}^{(\ell)} \right] P_n^{(\mu-1, \mu-1)}(x). \end{aligned} \quad (\text{C.2.6})$$

On matching the coefficient of $P_n^{(\mu-1, \mu-1)}(x)$ on both sides of the equation, we finally obtain (4.8)-(4.10).

C.3 Stationary state

For $\lambda_0 = 0$, we can find the coefficient $c_n^{(0)}$ using the known steady state distribution (4.5) and orthonormality property of Jacobi polynomials. From (4.8), we have

$$\frac{e^{\sigma p}}{Z} = \sum_{m=0}^{\infty} c_{m+1}^{(0)} \frac{\Gamma(m+1)}{\Gamma(m+\mu)} P_m^{(\mu-1, \mu-1)}(1-2p), \quad (\text{C.3.1})$$

where Z is the normalization constant. Using the orthonormality property (4.7) of Jacobi polynomials, we arrive at

$$c_{m+1}^{(0)} \frac{\Gamma(m+1)}{\Gamma(m+\mu)} h_m Z = \int_{-1}^1 dx (1-x^2)^{\mu-1} P_m^{(\mu-1, \mu-1)}(x) e^{\frac{\sigma(1-x)}{2}} \quad (\text{C.3.2})$$

$$= \frac{\sqrt{\pi} \Gamma(m+\mu) e^{\frac{\sigma}{2}}}{m! \Gamma(m+\mu+\frac{1}{2})} \left(\frac{-\sigma}{4} \right)^m {}_1F_1\left(1, m+\mu+\frac{1}{2}, \frac{\sigma^2}{16}\right) \quad (\text{C.3.3})$$

where ${}_1F_1(1; b; x)$ is confluent hypergeometric function [4]. It is straightforward to check that the expansion choice of [5] leads to essentially the same result as above.

C.4 Generating function for strong selection

The expansion coefficient d_n defined in (4.24) obeys the following recursion equation,

$$(2\mu+n-2)(2\mu+n-3)d_{n-1}^{(\ell)} + n(1-n)d_{n+1}^{(\ell)} = \left[\kappa_\ell + \frac{(1-n)(2\mu+n-2)}{\sigma} \right] (6-4\mu-4n)d_n^{(\ell)}. \quad (\text{C.4.1})$$

The above form allows one to write a differential equation for the generating function $\mathcal{D}(z) = \sum_{n=2}^{\infty} d_n z^n$ that obeys the following third order ordinary differential equation,

$$\begin{aligned} z(z^2 - 1)\mathcal{D}'' + 2(1 + (2\mu - 1)z^2)\mathcal{D}' + 2(z(1 - \mu)(2\mu - 1) - z^{-1})\mathcal{D} - \kappa[(6 - 4\mu)\mathcal{D} - 4z\mathcal{D}'] \\ = \frac{1}{\sigma} [4z^3\mathcal{D}''' + 6z^2(2\mu - 1)\mathcal{D}'' + 4z(\mu - 1)(2\mu - 3)\mathcal{D}' + 4(1 - \mu)(2\mu - 3)\mathcal{D}], \end{aligned} \quad (\text{C.4.2})$$

where we have dropped the eigenvalue label for brevity. The above equation does not appear to be solvable; however, in the scaling limit, $z \rightarrow 1, \sigma \rightarrow \infty$ such that $x = (1 - z)\sqrt{\sigma}$ is finite, we obtain

$$\frac{d^3\mathcal{D}}{dx^3} - \frac{x}{2} \frac{d^2\mathcal{D}}{dx^2} - (\eta + \mu) \frac{d\mathcal{D}}{dx} = 0, \quad (\text{C.4.3})$$

that yields

$$\mathcal{D}(x) = \tilde{c}_1 \frac{H_{1-2\eta-2\mu}(\frac{x}{2})}{1-2\eta-2\mu} + \tilde{c}_2 x {}_1F_1\left(\eta + \mu, \frac{3}{2}, \frac{x^2}{4}\right) + \tilde{c}_3, \quad (\text{C.4.4})$$

where $H_n(x)$ is the Hermite function and ${}_1F_1(a, b, z)$ is the Kummer confluent hypergeometric function [4]. As $n \geq 2$, the constant $\tilde{c}_3 = 0$; furthermore, we numerically found that the inverse Laplace transform of the second term on the RHS grows exponentially with n and therefore $\tilde{c}_2 = 0$. The asymptotic expansion of the Hermite function then yields (4.23).

For $\mu = 1/2$ and $3/2$, the recursion equation (C.4.1) for $d_n, n \geq 2$ simplifies and leads to following second order differential equation for \mathcal{D} :

$$(1 - z^2)\mathcal{D}' + (z - z^{-1})\mathcal{D} - d_2 z = 4[\kappa\mathcal{D} - \frac{1}{\sigma}(z^2\mathcal{D}'' - z\mathcal{D}' + \mathcal{D})] \quad (\mu = 1/2). \quad (\text{C.4.5})$$

$$(1 - z^2)\mathcal{D}' - 2(z + z^{-1})\mathcal{D} = 4[\kappa\mathcal{D} - \frac{1}{\sigma}(z^2\mathcal{D}'' + z\mathcal{D}' - \mathcal{D})] \quad (\mu = 3/2). \quad (\text{C.4.6})$$

Both of these equations have an irregular singularity at $z = 0$ and infinity, each of rank 1 which is the same as doubly-confluent Heun equation [6, 7]. Thus the generating function can not be reduced to simpler functions. However, for $\sigma \rightarrow \infty$, we obtain (4.25) in Chapter 4.

We note that the matrix \mathbf{T} in (4.10) is not normal (that is, it does not commute with its transpose), and therefore there is no guarantee that its eigenvalues would be real [1]. For finite σ , we found numerically that the first few eigenvalues are real and the rest are complex for finite K but the imaginary part of the eigenvalue decreases towards zero with increasing K . For infinite σ and finite K , the generating function

$\mathcal{D}(z) = \sum_{n=2}^K z^n d_n$ for $\mu = 1/2$ obeys the inhomogeneous equation,

$$(1 - z^2)\mathcal{D}' + (z - z^{-1})\mathcal{D} - d_2 z = 4\kappa\mathcal{D} - (K - 1)z^{K+1}d_K. \quad (\text{C.4.7})$$

On demanding that the solution of the above equation does not have terms of order z^{K+1} and higher, we find that one of the eigenvalues is zero (if K is odd) and the rest are complex for any K . This discussion thus reiterates the point that the eigenvalues of interest are obtained if the strong selection limit is taken after $K \rightarrow \infty$.

Bibliography

- [1] J. Mathews and R. L. Walker. *Mathematical Methods of Physics*. W A Benjamin, New York, 1970.
- [2] P. P. Fiziev. Novel relations and new properties of confluent Heun's functions and their derivatives of arbitrary order. *J. Phys. A: Math. Theor.*, **43**: 035203, 2010.
- [3] M. Kimura. Diffusion models in population genetics. *J. Appl. Probab.*, **1**: 177-232, 1964.
- [4] M. Abramowitz and I. A. Stegun. *Handbook of Mathematical Functions with Formulas, Graphs, and Mathematical Tables*, Dover, 1964.
- [5] Y. S. Song and M. Steinrücken. A simple method for finding explicit analytic transition densities of diffusion processes with general diploid selection. *Genetics*, **190**: 1117-1129, 2012.
- [6] P. P. Fiziev and D. Staicova. The Heun project: Heun functions, their generalizations and applications. <https://theheunproject.org>, 2012.
- [7] M. Hortaçsu. Heun functions and some of their applications in physics. *Adv. High Energy Phys.*, 2018.

